Imperial College London

Imperial College of Science, Technology and Medicine

Department of Physics

MSc Quantum Fields and Fundamental Forces

Discrete Gauging, Folding, and hyper-Kähler Quotients of Coulomb Branches of $3d$ $\mathcal{N} = 4$ Quiver Gauge Theories

Author:
Guhesh Kumaran

Supervisor:
Prof. Amihay Hanany

September 19, 2022

Acknowledgements

My first encounter with quivers was in my third year of undergraduate study where I did a UROP supervised by Prof. Hanany. Although at the time I was rather inexperienced with topics in theoretical physics, he encouraged my enthusiasm for the subject and helped me develop the confidence and ability to do theoretical physics research. More recently, during this year, his insights in both physics and mathematics have been inspiring during his SUSY lectures and discussions outside. I am extremely grateful for the guidance I have received from him and I am looking forward to the next few years.

A significant number of computations in this work would not have been possible if not for Rudolph Kalveks' `Mathematica` code. Not only this, but his weekly "helpdesk" of all things quiver and code related have tremendously helped me proceed and I thank him greatly for it.

I want to thank also Julius Grimminger and Kirsty Gledhill for answering my questions when I had them and for welcoming me to the quiver group. In addition, Deshuo Liu and Chunhao Li have been great colleagues.

A lot of the hardships this year have been softened by the company of the most excellent friends. I want to thank my QFFF classmates Lucas Fernandéz, with whom I started my quiver journey, and Sam Bennett, for discussing quivers this Summer and for the three years of friendship prior. The computer suite was always a fun place to work due to the presence of Akshay, Aparna, Ahad, Marcell, Urvi, and Simran (when she came to visit) and many others. Outside of College life I wish to thank my friends from school days who have reminded me to also relax this Summer.

Last but not least, I want to thank my family for their continued support of my academic endeavors. Appa for his practical advice, Amma for lifing the stresses of home life and Lahasthaa for keeping a smile on my face. There are insufficient words in the union of all human languages which can express how thankful I am to have them as family.

Abstract

We study the Coulomb branches of $3d$ $\mathcal{N} = 4$ quiver gauge theories. The Hilbert series of certain Coulomb branches are computed using the monopole formula which counts gauge invariant operators. The folding of Lie algebras also has a natural realisation to the folding of Coulomb branches and a few examples are computed to demonstrate this. The notion of discretely gauging Coulomb branches which are nilpotent orbits are reviewed and computed using the Burnside lemma on the highest weight generating function. The Kostant-Brylinski classification of discretely gauged nilpotent orbits is also realised in terms of discretely gauged Coulomb branches. Finally, hyper-Kähler quotients of Coulomb branches which are nilpotent orbits by $SU(n)$ are computed giving also, non-trivially, other nilpotent orbits. A quiver subtraction technique also reproduces some of these hyper-Kähler quotients.

Contents

1 Introduction

Noether's work on symmetries and conserved currents [1] changed how physicists viewed the Universe. Symmetry became a key idea in the formulation of new theories and an essential tool for physicists.

The Standard Model (SM) is one of the most successful theories of physics and champions the ideas of Noether. It is written using the language of gauge theory and quantum field theory; it is specified by a gauge group of $U(1)_Y \times SU(2) \times SU(3)$ (ignoring subtleties of a discrete quotient by its center) and a spacetime which is Poincaré invariant. Although the requirement of gauge symmetry and Poincaré invariance appear to be simple, their implications are quite dramatic. The forces of electromagnetism, the weak nuclear force, and the strong nuclear force have been unified and renormalised in the SM [2–5]. The idea of spontaneous symmetry breaking explains how leptons and other particles gain mass through the Higgs mechanism [6–9].

The Standard Model is not without fault, for example, a major shortcoming of the SM is that it does not incorporate Einstein's theory of gravity, General Relativity [10], and this is still one of the biggest problems in theoretical physics. Physicists have turned to other theories beyond the Standard Model to solve these issues. We will study one of these ideas, beyond the SM, not in the perspective of gravity but that of gauge theory.

Supersymmetry is an extension to the Poincaré algebra used in the Standard Model. There are features in supersymmetric theories which are not present in QFTs such as having a definite zero vacuum. The supersymmetry algebra is also the only Lie algebra of symmetries of the S-matrix which is compatible with QFT [11], which was shown by Haag, Sohnius, and Loposzanski [12] based off the Coleman-Mandula theorem [13]. For this reason, it is of interest to many physicists to study supersymmetry in the context of gauge theory. Furthermore, supersymmetry plays a crucial role in the development of string theories which have the potential to unify gravity and the other fundamental forces of nature.

Despite all of the results in experimental particle physics achieved in the last fifty years, progress has slowed down. The theoretical side of gauge theory and string theory has made significant advances in the meantime. In particular string theory has been used to prove the monstrous moonshine conjecture [14] and superstring theories were used to discover mirror symmetry and use it to solve problems in algebraic geometry [15, 16]. The understanding of physics in relation to mathematics is a motivation to study supersymmetric gauge theories for some physicists.

An important intellectual milestone in a theorists' career is to see the SM Lagrangian written down. Although short enough that it can be printed onto T-shirts or a coffee mug for example, it is still quite a lengthy expression. Matters are not any different when considering non-linear sigma models or other supersymmetric gauge theories. It would be nice to encode the information about the gauge theory in some more compact way. Quiver diagrams allow for the gauge symmetry, flavour symmetry, and the representations that hypermultiplets transform in, to be expressed in a simple diagram consisting of circles, squares, and lines [17]. Furthermore, some non-Lagrangian theories can also be expressed as a quiver. Not only this, but dynamics of brane systems for these theories can also be seen at the level of the quiver [18] through processes like quiver subtraction [19].

The particular class of supersymmetric gauge theories we will study are $3d$ $\mathcal{N}=4$ quiver gauge theories. The choice to study $3d$ theories is because we also wish to study theories with an additional conformal symmetry which has garnered interest due to the Ads/CFT correspondence [20] but also due to string theory in which $3d$ $\mathcal{N}=4$ quiver gauge theories are theories on the worldvolume of branes in various types of string theory. With this choice of dimension, we also want to study theories with enough supersymmetry that they are rich but not too much that they are restrictive. For this reason, we study $\mathcal{N}=4$ supersymmetry as there are $2^{\lfloor 3/2 \rfloor}\times 4 = 8$ supercharges which is a good balance. There is a duality symmetry between the Higgs and Coulomb branches of $3d$ $\mathcal{N}=4$ theories called *3d mirror symmetry* [21] which exchanges the Higgs and Coulomb branches and is a nice and useful symmetry to have.

Classically, the vacuum solutions to a theory may often be of little interest to physicists. Quantum mechanically the vacuum is deeply interesting, the fact that there is no well defined zero vacuum in QFT leads to the ideas of renormalisation [5]. In addition, Casimir showed that there is energy in the vacuum in QFT [22, 23]. As mentioned, we will not be considering phenomenological reasons to study the vacuum solutions of $3d$ $\mathcal{N}=4$ quiver gauge theories but instead the mathematics. The $3d$ $\mathcal{N}=4$ quiver gauge theories have interesting vacuum solutions when on the Higgs and Coulomb phases which form a moduli space of vacua. The name moduli space is in reference to the same ideas in algebraic geometry. For $3d$ $\mathcal{N}=4$ theories moduli space of vacua in the Higgs and Coulomb phase are hyper-Kähler quotients and for the theories we will study here, nilpotent orbits.

Results in the mathematics literature about nilpotent orbits [24, 25] have also been studied as $3d$ $\mathcal{N}=4$ quiver gauge theories in [26–29]. In particular, the discrete quotients of nilpotent orbits classified by Kostant and Brylinski in [24] were studied as Coulomb branches of $3d$ $\mathcal{N}=4$ quiver gauge theories in [26]. A natural extension would be to consider continuous groups by taking hyper-Kähler quotients of nilpotent orbits, this work attempts to find relationships between nilpotent orbits through hyper-Kähler quotients.

This dissertation is organised as follows:

- Section 2 introduces the necessary mathematical tools. Lie algebras and the representations as well as (affine) Dynkin diagrams are introduced. Nilpotent orbits, which is one of the central topics in this work, are introduced. The outline of their classification are also given following [30]. A brief introduction of the Hilbert series of algebraic varieties is also given. Finally, a review of hyper-Kähler geometry is given including the notion of hyper-Kähler quotients. Simple examples will be given to illustrate some of these ideas.

- Section 3 reviews aspects of $3d$ $\mathcal{N}=4$ gauge theories. The supersymmetry algebra is introduced and the content of hypermultiplets and vectormultiplets are constructed. A unique feature of $3d$ theories, the topological symmetry, is discussed and its relation to monopole operators. Finally, the geometry of the moduli space of vacua for the Higgs and Coulomb branch of $3d$ $\mathcal{N}=4$ gauge theories is discussed and their relation through $3d$ mirror symmetry.

- Section 4 introduces quivers, the monopole formula which is used to construct the Hilbert series of the Coulomb branch of a quiver gauge theory. Other useful objects such as the highest weight generating function are defined. Various techniques such as gluing, reading balance, Namikawa's theorem, and the Nilpotent Orbit Normalisation formula are mentioned to aid with computations.

- Section 5 introduces two types of discrete actions on Coulomb branches; discrete gauging and folding. The link to the mathematics in the Kostant-Brylinski classification of discretely gauged nilpotent orbits and the folding of Lie algebras are seen in the context of $3d$ $\mathcal{N}=4$ quiver gauge theories. This section will mainly follow the results in [26].

- Section 6 shows how one can compute hyper-Kähler quotients of nilpotent orbits by $SU(n)$ groups and these are also seen in terms of quiver subtractions for certain nilpotent orbits. Many of the results here are original contributions or have very recently appeared in the literature.

- Section 7 reviews the results found in the previous sections. In particular, future directions in light of the results of Section 6 and recent work are discussed.

2 Mathematical Preliminaries

The relevant mathematical concepts such as representation theory, nilpotent orbits, algebraic geometry, and hyper-Kähler geometry are covered. Proofs of results will not be provided but will be referenced. The approach to the mathematics will be in order to serve the physics in later sections, and so this section will not be extremely rigorous.

2.1 Lie Algebras and their Representations

Some definitions here will follow [31].

Definition 2.1 (Lie Algebra)**.** The Lie algebra $\mathfrak{g}$ of a Lie group G is a vector space of $\mathbb{R}$ with a Lie bracket $[\cdot,\cdot] : \mathfrak{g} \times \mathfrak{g} \to \mathfrak{g}$ which satisfies:

- Bilinearity. $[\cdot,\cdot]$ is a bilinear map.
- Anti-symmetry. $[X, Y] = -[Y, X], \forall X, Y \in \mathfrak{g}$.
- Jacobi Identity. $[X, [Y, Z]] + [Y, [Z, X]] + [Z, [X, Y]] = 0, \forall X, Y, Z \in \mathfrak{g}$.

Definition 2.2 (Lie Algebra Homomorphism)**.** A Lie algebra homomorphism between two Lie algebras $\mathfrak{g}$ and $\mathfrak{g}'$ is a linear map $\phi : \mathfrak{g} \to \mathfrak{g}'$ s.t.

$$\phi\big([X, Y]\big) = [\phi(X), \phi(Y)]. \tag{1}$$

If this map ϕ is an isomorphism we say that the Lie algebras are isomorphic.

Definition 2.3 (Lie Algebra Representation)**.** A complex finite-dimensional representation of a Lie algebra $\mathfrak{g}$ is a homomorphism $\hat{\rho} : \mathfrak{g} \to \mathfrak{gl}(n, \mathbb{C})$.

It is useful in physics to work with the complexified Lie algebra $\mathfrak{g}_{\mathbb{C}}$ of the Lie algebra $\mathfrak{g}$ of a simply connected group G for two reasons; finite dimensional irreps of G are in one-to-one correspondence with finite dimensional reps of $\mathfrak{g}_{\mathbb{C}}$, and secondly, if G is also simply connected, then finite dimensional irreps of G are in one-to-one with finite dimensional unitary irreps of $\mathfrak{g}_{\mathbb{C}}$.

Definition 2.4 (Complexified Lie Algebra)**.** Given a Lie algebra $\mathfrak{g}$, the complexified Lie algebra is

$$\mathfrak{g}_{\mathbb{C}} = \{X_1 + iX_2 | X_1, X_2 \in \mathfrak{g}\}. \tag{2}$$

Furthermore, we can extend a representation of $\mathfrak{g}$ to $\mathfrak{g}_{\mathbb{C}}$ by complexifying the representation in an analogous way to above. It is often useful to think about Lie algebra representations as a (left) $\mathfrak{g}$-module.

Definition 2.5 (Left $\mathfrak{g}$-module)**.** A left $\mathfrak{g}$-module is a vector space V over $\mathbb{C}$ with a product $\cdot : \mathfrak{g} \times V \to V$ such that :

- $[X, Y] \cdot v = X \cdot (Y \cdot v) - Y \cdot (X \cdot v)$
- $X \cdot (\lambda_1 v_1 + \lambda_2 v_2) = \lambda_1 X \cdot v_1 + \lambda_2 X \cdot v_2$

$\forall X, Y \in \mathfrak{g}, v \in V, \lambda_1, \lambda_2 \in \mathbb{C}$.

A special type of $\mathfrak{g}$-module we will use is the adjoint $\mathfrak{g}$-module.

Definition 2.6 (Adjoint $\mathfrak{g}$-module)**.** The idea behind the adjoint $\mathfrak{g}$-module is to take the Lie algebra as a vector space itself.

$$X \cdot v = [X, v] \in V, \tag{3}$$

if one fixes a basis T^i then we can write $X = X^i T_i$ and $v = v^j T_j$ and have

$$X \cdot v = [X, v] = X^i v^j [T_i, T_j] = X^i v^j f_{ij}{}^k T_k \tag{4}$$

where the $f_{ij}{}^k$ are the structure constant for $\mathfrak{g}$. Upon relabelling some indices we have

$$v^i \to X^k f_{kj}{}^i v^j = \hat{\rho}_{adj}(X)^i{}_j v^j \tag{5}$$

Using our definition of the adjoint representation we can define an inner product.

Definition 2.7 (Killing Form)**.** The Killing form for $\mathfrak{g}$ is a bilinear map $\langle ., . \rangle : \mathfrak{g} \times \mathfrak{g} \to \mathbb{R}$

$$\langle X, Y \rangle = tr(\hat{\rho}_{adj}(X) \cdot \hat{\rho}_{adj}(Y)), \forall X, Y \in \mathfrak{g}. \tag{6}$$

Definition 2.8 (Cartan Subalgebra)**.** The Cartan subalgebra $\mathfrak{h}$ of a Lie algebra $\mathfrak{g}$ is :

- Abelian. $[H_1, H_2] = 0 \forall H_1, H_2 \in \mathfrak{h}$.
- Maximal. If $[X, H] = 0 \forall H \in \mathfrak{h}$ then $X \in \mathfrak{h}$.

Definition 2.9 (Root)**.** A root of a Lie algebra $\mathfrak{g}$ is a map $\alpha : \mathfrak{h} \to \mathbb{C}$s.t. that there exists a non-zero $X \in \mathfrak{g}_{\mathbb{C}}$ (the complexified Lie algebra) s.t.

$$ad_H X = [H, X] = \alpha(H) \cdot X, \forall H \in \mathfrak{h}. \tag{7}$$

From this we can define the root space.

Definition 2.10 (Root Space)**.** The root space is a subspace $\mathfrak{g}_\alpha$ of $\mathfrak{g}_{\mathbb{C}}$ given by

$$\mathfrak{g}_\alpha = \{X \in \mathfrak{g}_{\mathbb{C}} | [H, X] = \alpha(H)X, \forall H \in \mathfrak{h}, \forall X \in \mathfrak{g}_{\mathbb{C}}\} \tag{8}$$

With this, one can decompose a complexified Lie algebra in the following way,

$$\mathfrak{g}_{\mathbb{C}} = \mathfrak{h}_{\mathbb{C}} \oplus \bigoplus_{\alpha \in \Delta} \mathfrak{g}_\alpha. \tag{9}$$

There is a symmetry acting on the roots which is given by the Weyl group.

Definition 2.11 (Weyl Group)**.** For a given root α consider the reflection in the plane perpendicular to α, $s_\alpha : \mathfrak{h}^* \to \mathfrak{h}^*$, this acts on another root λ as

$$s_\alpha(\lambda) = \lambda - \frac{2\langle \alpha, \lambda \rangle}{\langle \alpha, \alpha \rangle} \alpha \tag{10}$$

the set of all $s_\alpha \forall \alpha \in R$ is the Weyl group $\mathcal{W}$.

A similar object we can define are the co-roots.

Definition 2.12 (Co-root)**.** To a root α the co-root is

$$\alpha^\vee = \frac{2}{\langle \alpha, \alpha \rangle} \alpha \tag{11}$$

the co-roots also define a dual root space.

We need not work with all the roots since there is a Weyl group action which allows us to produce some roots from others. A set of *fundamental roots* can be chosen which can be used to construct all of the other roots using Weyl group reflections. The set of fundamental roots has the following properties:

- The set of fundamental roots $\Pi = \{\alpha_1, \cdots, \alpha_r\}$, where r is the rank of the algebra, forms a basis for $\mathfrak{h}^*$.

- Any root $\beta = k^i \alpha_i$ where $k^i \geq 0$ or $k^i \leq 0$.

The information about the lengths of the fundamental roots and the angles between the fundamental roots can be encapsulated in an $r \times r$ matrix called the Cartan matrix.

Definition 2.13 (Cartan Matrix)**.** The elements of the Cartan matrix are given by

$$A_{ij} = \frac{2\langle \alpha_i, \alpha_j \rangle}{\langle \alpha_i, \alpha_i \rangle}, \quad \alpha_i, \alpha_j \in \Pi. \tag{12}$$

Note that all diagonal entries of the Cartan matrix are trivially two and for semi-simple Lie algebras the off diagonal terms are non-positive.

The Cartan matrix can be used to work out the angle between two fundamental roots α_i and α_j as

$$\cos^2 \theta_{ij} = \frac{A_{ij} A_{ji}}{4} \tag{13}$$

where we do not sum over the indices.

The information in a Cartan matrix can further be encoded in a Dynkin diagram. The Dynkin diagram tells us what the lengths of fundamental roots relative to each other are and the angles between fundamental roots.

For each fundamental root there is a node in the Dynkin diagram. The quantity $k = A_{ij} A_{ji}$ and the relative lengths of roots α_i and α_j are computed for all pairs i, j. For semi-simple Lie algebras, k is an integer and can take the following values:

- $k = 0$. The roots are orthogonal. There is no line between the nodes.
- $k = 1$. The roots are separated by $2\pi/3$. Place a single line connecting the nodes.
- $k = 2$. The roots are separated by $3\pi/4$. Place a double line with an arrow pointing from the node for the long root to the node for the short root.
- $k = 3$. The roots are separated by $5\pi/6$. Place a triple line with an arrow pointing from the node for the long root to the node for the short root.

Definition 2.14 (Weight Space)**.** For a Cartan sub-algebra $\mathfrak{h}$ of semi-simple Lie algebra $\mathfrak{g}$ the weight space for a $\mathfrak{g}$-module V is

$$V_w = \{v \in V | H \cdot v = w(H)v, \forall H \in \mathfrak{h}\} \tag{14}$$

this allows the $\mathfrak{g}$-module for an irrep to be decomposed into weight spaces as

$$V = \bigoplus_w V_w. \tag{15}$$

Definition 2.15 (Fundamental Weight)**.** Given a set of fundamental roots $\{\alpha_1, \cdots, \alpha_r\}$ with coroots $\{\alpha_1^\vee \cdots, \alpha_r^\vee\}$, the fundamental weights obey

$$\langle w_i, \alpha_j^\vee \rangle = \delta_{ij} \tag{16}$$

The set of fundamental weights Γ are in a sense orthogonal to the coroots.

The fundamental weights and fundamental roots are related through the Cartan matrix as

$$\alpha_i = \sum_j w_j A_{ji}, \quad w_i = \sum_j \alpha_j \left(A^{-1}\right)_{ji} \tag{17}$$

Definition 2.16 (Dominant Integral Weight)**.** A dominant integral weight is a weight which is written in terms of the fundamental weights as

$$\lambda = \sum_i n_i w_i \tag{18}$$

where the n_i are non-negative integers.

Definition 2.17 (Dynkin Labels)**.** The non-negative integers n_i form the Dynkin label for a dominant integral weight as $[n_1, \cdots, n_r]$.

There is an ordering on the weights where we say a weight is "higher" if the difference of two weights is a positive integer amount of the fundamental roots.

Theorem 1 (Theorem of Highest Weight)**.** *For a dominant integral weight λ, there exists a unique finite dimensional irrep of $\mathfrak{g}$ with weight module V_λ which has λ as the highest weight.*

Recall that the module for a finite dimensional irrep of $\mathfrak{g}$ is the sum of weight modules. Each weight can be constructed from the highest weight by subtracting positive integer amounts of the simple roots. The allowed weights come in $\mathfrak{su}(2)$ modules for each fundamental root. So each $\mathfrak{g}$-module also decomposes in $\mathfrak{su}(2)$ modules. Thus the highest weight can be used to label a representation.

A neat way of working with irreps is to compute their *character* from the Weyl character formula. Since we can decompose a $\mathfrak{g}$-module into weight spaces. We can count the weight spaces in the module by grading each space with a monomial. Specifically for a rank r algebra the character for some $\mathfrak{g}$-module is given by

$$\chi(V)(x_1, \cdots, x_r) = \sum_{w \in \Gamma} (dimV_w) \prod_{i=1}^{r} x_i^{n_i}. \tag{19}$$

and if we are considering highest weight modules, V_λ, then if the Weyl group $\mathcal{W}$ is known then the Weyl character formula can take the form of

$$\chi(V_\lambda) = \frac{\sum_{s \in \mathcal{W}} (\det s) e(s(\lambda + \rho))}{\sum_{s \in \mathcal{W}} (\det s) e(s(\rho))} \tag{20}$$

where e is the monomial for an irrep with Dynkin labels $[n_1, \cdots, n_r], e([n_1, \cdots, n_r]) = \prod_{i=1}^{r} x_i^{n_i}$ and $\rho = \sum_i w_i$, we say $\det s = \pm 1$ for rotations and reflections respectively.

The convenience of characters is that they are simple to compute and manipulate. This is particularly evident when considering decomposition of representations and embeddings. For example, if we consider the direct sum of some representations with modules V_1 and V_2 we have that

$$\chi(V_1 \oplus V_2) = \chi(V_1) + \chi(V_2) \tag{21}$$

similarly for a tensor product of modules we have

$$\chi(V_1 \otimes V_2) = \chi(V_1) \times \chi(V_2). \tag{22}$$

The final useful property of characters comes from the Peter-Weyl theorem [32] which says that characters of irreps of a compact group are orthogonal under Weyl integration and form a complete basis. Suppose we have two characters $\chi([n_1, \cdots, n_r])$ and $\chi([m_1, \cdots, m_r])$ for some compact group G then these characters obey

$$\int_G d\mu_G \left(\chi([n_1, \cdots, n_r])\right)^* \chi([m_1, \cdots, m_r]) = \prod_{i=1}^{r} \delta_{n_i m_i} \tag{23}$$

where $d\mu_G$ is the *Haar measure* for G which is normalised s.t. $\int_G d\mu_G = 1$.

This can be explicitly be given for $G = SU(n)$ and is adapted from the formula given in [33] to one which requires only the positive roots,

$$\int_{SU(n)} d\mu_{SU(n)} = \frac{1}{(2\pi i)^{n-1}} \left(\prod_{l=1}^{n-1} \oint_{|y_l|=1} \frac{dy_l}{y_l} \right) \prod_{\alpha \in \Delta^+} \left(1 - \prod_{j=1}^{n-1} y_j^{\sum_{i=1}^{n-1} A_{ji} k_i} \right) \tag{24}$$

where a positive root is written in terms of the fundamental roots as $\alpha = \sum_{i=1}^{r} k_i \alpha_i$.

Another type of Lie algebra important for us later on are *affine* Lie algebras associated to our semi-simple Lie algebras. The Cartan matrix for the affine Lie algebras is defined as

Definition 2.18 (Affine Cartan Matrix)**.** Suppose A_{ij} is a Cartan matrix for a semi-simple Lie algebra $\mathfrak{g}$. The affine Cartan matrix is

$$\widetilde{A}_{i+1j+1} = \begin{pmatrix} A_{ij} & B_{ij+1} \\ -C_{i+1j} & 2 \end{pmatrix} \tag{25}$$

where C_{i+1j} are the Dynkin labels (as a row vector) for the adjoint representation of $\mathfrak{g}$ and B_{ij+1} is the transpose of Dynkin labels except under the mapping of non-zero entries to -1 (except for A_1 which has a mapping to -2 instead [34]).

The affine Cartan matrix appears to add an additional fundamental root, however the addition of the extra row and column actually means that the affine Cartan matrix has zero determinant and a zero eigenvalue. The rank of the algebra is still preserved as the additional root is really a linear combination of the others.

A final definition for this section are the Coxeter and dual Coxeter labels for an (affine) algebra [35].

Definition 2.19 (Coxeter Label)**.** Consider the highest root θ, and the fundamental roots $\alpha_i, i = 1, \cdots, r$ the Coxeter labels a_i are defined through

$$\theta =: \sum_{i=1}^{r} a_i \alpha_i. \tag{26}$$

Similarly we define the dual Coxeter labels.

Definition 2.20 (Dual Coxeter Label)**.** Consider the highest root θ of an algebra and the set of fundamental co-roots $\alpha_i^\vee, i = 1, \cdots, r$. The dual Coxeter labels are defined through

$$\frac{2}{\langle \theta, \theta \rangle} \theta =: \sum_{i=1}^{r} a_i^\vee \alpha_i^\vee. \tag{27}$$

A more convenient way of computing the (dual) Coxeter labels are by finding the (left) right null eigenvector of the Cartan or affine Cartan matrix for non-affine and affine Lie algebras respectively.

2.1.1 An Example - Affine G_2

Here we demonstrate the tools in action, we first compute the affine Cartan matrix for affine G_2, use this to compute the affine Dynkin diagram for G_2 and then finally show what the (dual) Coxeter labels for G_2 are. The Cartan matrix for G_2 is

$$A_{ij}^{G_2} = \begin{pmatrix} 2 & -3 \\ -1 & 2 \end{pmatrix}, \tag{28}$$

the Dynkin labels for the adjoint representation of G_2[1] is $[0, 1]$ and so $C_{3j} = (0, -1)$ and $B_{i3} = (0, -1)^T$ and the affine Cartan matrix for G_2 is

$$\widetilde{A}_{ij}^{G_2} = \left(\begin{array}{cc|c} 2 & -3 & 0 \\ -1 & 2 & -1 \\ \hline 0 & -1 & 2 \end{array}\right) \tag{29}$$

we can use these to work out the angle between the roots $\alpha_{1,2,3}$ from the formula

$$\cos^2\theta_{ij} = \frac{1}{4}\widetilde{A}_{ij}\widetilde{A}_{ji} \tag{30}$$

and compute

$$\theta_{12} = 5\pi/6, \quad \theta_{13} = \pi/2, \quad \theta_{23} = 2\pi/3, \tag{31}$$

so we know, using the rules for constructing Dynkin diagrams, that α_1 and α_2 are connected by a non-simply laced edge of multiplicity three, α_1 and α_3 are not connected by an edge and that α_2 and α_3 are connected by a simply-laved edge of multiplicity one. The relative lengths of the roots can be computed using

$$\frac{\langle\alpha_i, \alpha_i\rangle}{\langle\alpha_j, \alpha_j\rangle} = \frac{\widetilde{A}_{ji}}{\widetilde{A}_{ij}} \tag{32}$$

and we find

$$\langle\alpha_2, \alpha_2\rangle = 3\langle\alpha_1, \alpha_1\rangle, \quad \langle\alpha_2, \alpha_2\rangle = \langle\alpha_3, \alpha_3\rangle, \tag{33}$$

so α_2 and α_3 are the long roots (of equal length) and α_1 is the short root. This is all we need to construct the affine Dynkin diagram of G_2 given in Figure 1. Finally, we can see that the column vector, $(3, 2, 1)^T$ and row vector, $(1, 2, 1)$, are right and left null eigenvectors of the

[1] Here we will follow the `LieArt`[36] convention for labelling the adjoint of G_2.

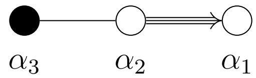

Figure 1: The Dynkin diagram for affine G_2 where the additional affine node is filled in black.

affine Cartan matrix and so the Coxeter labels for affine G_2 are $a_i = (3, 2, 1)$ and the dual Coxeter labels for affine G_2 are $a_i^\vee = (1, 2, 1)$.

This exercise can be repeated in a similar fashion for all semi-simple (and affine) Lie algebras.

2.1.2 Folding Lie algebras

We will state the main results on how a non-simply laced Lie algebra of type ADE can be folded following [37] where proofs of all the claims can also be found. Another review of folding Lie algebras using the Chevally-Serre basis is given in [26] with examples on how to explicitly construct the folding. Notably the latter also deals with cases where the starting Dynkin diagram is also non-simply laced e.g. the folding of B_3 into G_2.

Consider a simply laced root system Φ with a set of fundamental roots $\Delta = \{\alpha_i | i \in I\}$. Suppose that there is an automorphism σ on (Φ, Δ) which we can extend to an isometry on the vector space spanned by all of the roots. A very important condition that we can make is that all roots in the same σ-orbit are orthogonal. Let $I^\sigma = \{B_1, \cdots, B_l\}$ be the set of all σ-orbits. Then one can construct a vector

$$\beta_j = \sum_{i \in B_j} \alpha_i \tag{34}$$

for each σ-orbit.

The claims are that the set $\Delta^\sigma := \{\beta_1, \cdots, \beta_l\}$ are the set of roots for a (non-simply laced) root system Φ^σ. Not only that, but any root of Φ^σ must be of the form given in (34).

The final claim is that any algebra with a non-simply laced Dynkin diagram with root system $(\Phi^\sigma, \Delta^\sigma)$ may be thought of as the folding of a simply laced root system (Φ, Δ) by some autmorphism σ on the Dynkin diagram.

2.2 Elements of Algebraic Geometry

The definitions given here follow [38].

Definition 2.21 (Affine n Space)**.** An affine n space over an algebraically closed field F, denoted A^n, is the set of all n-tuples of elements of F.

We can also construct the polynomial ring in n variables over F, $A[x_1, \cdots, x_n]$. We wish to think of the elements of the polynomial ring as being functions from A^n into F.

Let us consider $f \in A$ where f is a polynomial. Then the set of zeroes of f is $Z(f) = \{P \in A^n | f(P) = 0\}$. This idea can be extended to any subset $T \subset A$ as

$$Z(T) = \{P \in A^n | f(P) = 0, \forall f \in T\} \tag{35}$$

Definition 2.22 (Algebraic Set)**.** A subset Y of A^n is an algebraic set if $\exists\ T \subseteq A$ s.t. $Y = Z(T)$.

The union and intersections of algebraic sets are also algebraic sets, we will not prove this.

Definition 2.23 (Zariski Topology)**.** The topology, where the sets are the complements of algebraic sets of A^n is the Zariski topology of A^n.

Definition 2.24 (Irreducible Subset of a Topology)**.** A non-empy subset X of a topology, is one which cannot be expressed as the union of two proper subsets, both closed in X.

The empty set is not considered irreducible.

Definition 2.25 (Affine Algebraic Variety)**.** An irreducible closed subset of A^n is an algebraic variety.

Now we are ready to define the key object that we will use in this work [39].

Definition 2.26 (Hilbert Series)**.** For an algebraic variety χ in $\mathbb{C}[x_1, \cdots, x_n]$ the Hilbert series is

$$HS_\chi(t) = \sum_{i=0}^{\infty} dim_{\mathbb{C}}(\chi_i) t^i \tag{36}$$

where χ_i is the i^{th} graded piece of the polynomial ring.

The interpretation is that the Hilbert series counts the number of independent graded monomials at each order.

The Hilbert series can be expressed as a quotient of two polynomials

$$HS(t) = \frac{P(t)}{Q(t)} \tag{37}$$

we say that an algebraic variety is *freely generated* if $P(t) = 1$ and $Q(t) = \prod_{i=1}^{\infty}(1-t^{d_i})$where the d_i are positive integers. The algebraic variety is a *complete intersection* if $Q(t) = \prod_{i=1}^{\infty}(1-t^{d_i})$ and $P(t) = \prod_{i=1}^{\infty}(1-t^{d'_i})$. The Hilbert series is *palindromic* if $P(t)$ is palindromic.

The (complex) *dimension* of a moduli space can be found by the order of the pole of the Hilbert series at $t = 1$. The quaternionic dimension is half of the complex dimension, when thinking about physics later it will be useful to use the quaternionic dimension and we will do so for the rest of this work.

2.2.1 An Example - The Hilbert Series for $\mathbb{C}^2/\mathbb{Z}_2$

We can have two coordinates on $\mathbb{C}^2$ which we will call $z_{1,2}$. Now supposing that there is a $\mathbb{Z}_2$ action on these coordinates that is; the identity acting on each coordinate does nothing and the other element of $\mathbb{Z}_2$ returns the negative of the coordinate. The possible monomials that are invariant under this $\mathbb{Z}_2$ action must be of even degree. These must be generated by three generators of degree two, $z_1^2, z_2^2, z_1 z_2$. At each (even) degree m there are $m+1$ independent invariant monomials constructed from the generators. If we replace $m \to 2p$ then the Hilbert series (HS) is

$$HS_{\mathbb{C}^2/\mathbb{Z}_2} = \sum_{p=0}^{\infty}(2p+1)t^{2p} = \frac{1-t^4}{(1-t^2)^3}. \tag{38}$$

This is a complete intersection and the (quaternionic) dimension of the moduli space is 1.

2.3 Nilpotent Orbits

We will review nilpotent orbits, mainly following [30]. Only relevant aspects from these definitions will be taken here and not a full exposition. A sketch of the classification of the nilpotent orbits of $\mathfrak{sl}_\mathfrak{n}$ will be given, and mentioned for other algebras.

Recall the definition of the adjoint representation of a Lie algebra $\mathfrak{g}$,

Definition 2.27 (Adjoint Representation of a Lie Algebra)**.**

$$ad : \mathfrak{g} \to End(\mathfrak{g})$$
$$ad_X Y = [X, Y]$$

A Lie algebra is also a vector space. A nilpotent operator is defined as

Definition 2.28 (Nilpotent Operator)**.** An element $X \in \mathfrak{g}$ is nilpotent if ad_X is a nilpotent endomorphism of $\mathfrak{g}$.

A semi-simple operator is defined as

Definition 2.29 (Semi-simple Operator)**.** An element $X \in \mathfrak{g}$ is semisimple if every ad_X invariant subspace of $\mathfrak{g}$ has an ad_X invariant complement.

Definition 2.30 (Jordan Decomposition Theorem)**.** Let V be a finite dimensional complex vector space. Then there exists unique operators $X_s, X_n \in End(V)$ where X_s is semi-simple and X_n is nilpotent such that $X = X_s + X_n$ where X is an endomorphism of V. We also have that X_s and X_n commute.

One can apply the Jordan decomposition to the adjoint operator. That is if $X = X_s + X_n$ for $X \in End(V)$ then we have $ad_X = (ad_X)_s + (ad_X)_n$ for $ad_X \in End(\mathfrak{gl}(V))$, see [30] for a proof.

The classification of conjugacy classes of nilpotent and semi-simple elements of a Lie algebra $\mathfrak{g}$ is done using the adjoint group G_{ad}. This is defined as

Definition 2.31 (Adjoint Group)**.** To a complex Lie algebra $\mathfrak{g}$ the adjoint group G_{ad} is the connected subgroup of $GL(\mathfrak{g})$ with Lie algebra $ad_{\mathfrak{g}}$.

For a semi-simple Lie algebra $\mathfrak{g}$ associated to some simply connected group G the adjoint group G_{ad} can be defined as $G/Z(G)$ where $Z(G)$ is the center of G.

We can define the orbit through X as

Definition 2.32 (Orbit)**.** $\mathcal{O}_X := \{\phi(X) | \phi \in G_{ad}\}$.

It is important to remember that the action of the adjoint group on a nilpotent element X is through conjugation. So the orbit is really a conjugacy class of a nilpotent element X of $\mathfrak{g}$, where the conjugating elements are in G_{ad}. Clearly the nilpotency of X is preserved under this conjugation.

Now we can construct the nilpotent orbits of A_n from the Dynkin-Kostant classification.

Definition 2.33 (Partition)**.** A partition of an integer n is a tuple of positive integers $[d_1, \cdots, d_k]$ s.t.

$$d_1 \geq d_2 \geq \cdots \geq d_k > 0, \quad \sum_{i=1}^{k} d_i = n.$$

A common notation we will use is if integer d_i appears p times in the partition we will write d_i^p as a short-hand. For example, $\{2^2, 1\}$ is a partition of 5.

Definition 2.34 (Elementary Jordan Block)**.** An elementary Jordan block of type r is an $r \times r$ matrix

$$J_r = \begin{pmatrix} 0 & 1 & 0 & \cdots & 0 & 0 \\ 0 & 0 & 1 & \cdots & 0 & 0 \\ \vdots & \vdots & \vdots & \ddots & \vdots & \vdots \\ 0 & 0 & 0 & \cdots & 0 & 1 \\ 0 & 0 & 0 & \cdots & 0 & 0 \end{pmatrix}, \tag{39}$$

this Jordan block is clearly a nilpotent matrix and so defines an nilpotent endomorphism of $\mathbb{C}^r$ (any complex r-component vector will go to zero under repeated actions of J_r). Consider $\mathbb{C}^n$ and a partition $[d_1, \cdots, d_k]$ of n, then

$$X_{[d_1 \cdots, d_k]} = \begin{pmatrix} J_{d_1} & 0 & 0 & \cdots & 0 \\ 0 & J_{d_2} & 0 & \cdots & 0 \\ \vdots & \vdots & \vdots & \ddots & \vdots \\ 0 & 0 & 0 & \cdots & J_{d_k} \end{pmatrix} \tag{40}$$

is clearly a nilpotent endomorphism of $\mathbb{C}^n$. The nilpotent orbit associated to a partition is then found by the action of the adjoint group G_{ad} of $\mathfrak{sl}_n$ which is PSL_n on the nilpotent element $X_{[d_1 \cdots d_k]}$.

It turns out that the nilpotent orbits of $\mathfrak{sl}_n$ are in one-to-one correspondence with partitions of n.

For the other classical orbits, $\mathfrak{so}_{2n}, \mathfrak{so}_{2n+1}, \mathfrak{usp}_{2n}, \mathfrak{usp}_{2n+1}$, the nilpotent orbits are labelled also by partitions of $2n$ and $2n+1$ respectively, but with the additional caveats on the types of partitions allowed for each algebra.

2.3.1 An Example - Nilpotent orbits of $\mathfrak{sl}_2$

This is a very simple example which has been covered before in [27] but nevertheless illuminating.

The partitions of 2 are $\{\{2\}, \{1^2\}\}$. Starting with $\{1^2\}$ the nilpotent element in $\mathbb{C}^2$ is

$$X_{\{1^2\}} = \begin{pmatrix} 0 & 0 \\ 0 & 0 \end{pmatrix}, \tag{41}$$

so it is clear that any action of the adjoint group on this nilpotent element is trivial. In fact $X_{\{1^2\}}$ is the only element of this orbit and so the orbit is trivial.

For the second case, the element of the orbit we are considering is

$$X_{\{2\}} = \begin{pmatrix} 0 & 1 \\ 0 & 0 \end{pmatrix}, \tag{42}$$

G_{ad} for $\mathfrak{sl}_2$ is $PSL_2 = SL(2)/\{\mathbf{1}_2, -\mathbf{1}_2\}$, however we note that conjugation of any element of $SL(2)$ by an element of PSL_2 gives the same conjugacy classes as if we did conjugation under $SL(2)$. This means we can construct the nilpotent orbit using the elements of $SL(2)$ (this is the key reason why integer partitions can label nilpotent orbits for $\mathfrak{sl}_n$ in a one-to-one way and not for other algebras). Given a generic element of $SL(2)$,

$$M = \begin{pmatrix} a & b \\ c & d \end{pmatrix}, \quad \det M = 1 \tag{43}$$

then the nilpotent orbit is defined as

$$\mathcal{O}_{\{2\}} = \{MX_{\{2\}}X^{-1}, \forall M \in SL(2)\} \tag{44}$$

and a generic element of the nilpotent orbit is

$$MX_{\{2\}}X^{-1} = \begin{pmatrix} -ac & a^2 \\ -c^2 & ac \end{pmatrix}. \tag{45}$$

We cannot include the trivial orbit in $\mathcal{O}_{\{2\}}$ because this would mean $a = c = 0$ and this means we cannot have M with unit determinant.

The notion of a *closure* of the orbit $\mathcal{O}_{\{2\}}$ defined as

$$\overline{\mathcal{O}}_{\{2\}} = \mathcal{O}_{\{2\}} \cup \mathcal{O}_{\{1^2\}} \tag{46}$$

now means the trivial orbit is included.

This notion of closure extends to other nilpotent orbits where the union of lower dimensional orbits are taken.

Now recall the algebraic variety $\mathbb{C}^2/\mathbb{Z}_2$ is generated by three generators $z_1^2, z_2^2, z_1 z_2$. For this nilpotent orbit $\bar{\mathcal{O}}_{\{2\}}$ of $\mathfrak{sl}_2$ there are two complex coordinates a, c and clearly three generators a^2, c^2, ac which is exactly the same as the $\mathbb{C}^2/\mathbb{Z}_2$ with the identification of $z_{1,2} \leftrightarrow$

a, c. The HS for the closure of the minimal nilpotent orbit of $\mathfrak{sl}_2$ is the same as for $\mathbb{C}^2/\mathbb{Z}_2$ and in fact the varieties are the same.

A property of an nilpotent orbit we will refer to later is the height [40].

Definition 2.35 (Height)**.** The height of an nilpotent orbit $\mathcal{O}$ is defined as

$$ht(\mathcal{O}) = max\{n \in \mathbb{N} | (ad_X)^n \neq 0, X \in \mathcal{O}\}. \tag{47}$$

Although we have covered the nilpotent orbits of $\mathfrak{sl}_2$ using matrices, there is a more general way of classifying nilpotent orbits which we outline and do not provide proofs.

Definition 2.36 (Standard Triple)**.** A standard triple of a semi-simple Lie algebra $\mathfrak{g}$ with a subalgebra isomorphic to $\mathfrak{sl}_2$ is the triple of non-zero elements in $\mathfrak{g}$, $\{H, X, Y\}$ that satisfy

$$[H, X] = 2X, \quad [H, Y] = -2Y, \quad [X, Y] = H. \tag{48}$$

the elements H, X, Y are called the *neutral*, *nilpositive*, and *nilnegative* elements of the triple respectively.

There is a theorem of Jacobson-Morozov [41, 42] which says that each nilpotent element X of some Lie algebra $\mathfrak{g}$ falls into some standard triple $\{H, X, Y\}$ for some $\mathfrak{sl}_2 \subset \mathfrak{g}$.

There is a theorem of Kostant which says that there is an injection of a standard triple $\{H, X, Y\}$ into X upto conjugacy of X.

Together, the Jacobson-Morozov theorem and Kostant's theorem imply that there is a bijection between nilpotent orbits (and hence their closures) and the conjugacy classes of a nilpotent element. There is also hence a bijection between the standard triple and (closures of) nilpotent orbits.

The standard triple is defined by a subalgebra $\mathfrak{sl}_2$ of $\mathfrak{g}$. Thus there is a homorphism (really an embedding) of $SU(2)$ into G. So there is a bijection between these homomorphisms and the distinct nilpotent orbits. To find the (distinct) nilpotent orbits one only needs to consider the possible embeddings of $SU(2)$ into G. This was done by Dynkin in [43].

The use of characters is very convenient when thinking about decompositions and embeddings of subgroups. The $SU(2)$ embedding into G which is given by the map ρ can be written from the viewpoint of characters by defining the mapping of character variables (we will call them fugacities later) so we say

$$\rho : \{x_1, \cdots, x_r\} \to \{x^{w_1}, \cdots, x^{w_r}\} \tag{49}$$

where the collection of exponents $[w_1, \cdots, w_r]$ is the *weight map*.

Another valid choice is to consider the simple root coordinates (called a topological fugacity later) which are related to the character variables through the Cartan matrix in the following way,

$$z_i = \prod_j x_j^{A_{ij}} \tag{50}$$

the homomorphism can also be defined using the simple root coordinates as

$$\rho : \{z_1, \cdots, z_r\} \to \{z^{q_1/2}, \cdots, z^{q_r/2}\} \tag{51}$$

the collection $\{q_1, \cdots, q_r\}$ is called the *root map*.

There is a very simple conversion of the root map and weight map. If one uses the expressions to convert between simple root coordinates and character coordinates, and the mapping of the homomorphism, the conversion between the weight map and root map is found to be

$$q_i = \sum_j A_{ij} w_j. \tag{52}$$

Finally, we introduce some terminology for the different types of nilpotent orbits we may encounter:

- The trivial orbit.
- The minimal nilpotent orbit is the non-trivial orbit of lowest dimension.
- The next to minimal nilpotent orbit is the non-trivial orbit of second lowest dimension.
- The maximal nilpotent orbit is the orbit of largest dimension.
- The sub-regular orbit is the orbit of the second largest dimension.

Note that some of these terms may coincide, for example, the minimal and maximal nilpotent orbit of $SU(2)$ are the same orbit!

It is worth mentioning that the partition type and $SU(2)$ embedding type classifications are indeed related as there is a homomorphism defined by the partition which takes the standard triple of $\mathfrak{sl}_2$ into a triple of the resultant algebra. This construction will not be made explicit here but mentioned to satisfy that both classifications are equivalent. Further details may be found in [30].

The simplest way of labelling orbits is to use the terminology in the bullet points above. In text, the next to minimal nilpotent orbit of F_4 may be written as $n.min.F_4$ and the closure of the next to minimal nilpotent orbit of F_4 may be written as $\overline{n.min.F_4}$. From this point on we will refer to the closure of a nilpotent orbit as a "nilpotent orbit" (omitting closure of) but will keep the line over the text. For orbits which are near to the minimal orbits further "next to"s can be added to the name. However, this can be quite excessive for some orbits and thus more appropriate names would be the partition, root maps, or the dimension of the HS (if there is only one orbit of that dimension). Consistency in the naming will be attempted, however a mixture of these naming conventions will be used as appropriate.

2.4 Hyper-Kähler Geometry

To define hyper-Kähler manifolds we need some definitions first, for which we will follow [44, 45]. We will assume basic knowledge of differential geometry.

To begin we will consider a complex manifold $\mathcal{M}$ of complex dimension m. The tangent space of $\mathcal{M}$ is spanned by $2m$ vectors which we call $\frac{\partial}{\partial x_\mu}$ and $\frac{\partial}{\partial y_\mu}$ where $1 \leq \mu \leq m$. A basis of $\mathcal{M}$ can be defined using these as

$$\frac{\partial}{\partial z_\mu} = \frac{1}{2}\left(\frac{\partial}{\partial x_\mu} - i\frac{\partial}{\partial y_\mu}\right) \tag{53}$$

$$\frac{\partial}{\partial \bar{z}_\mu} = \frac{1}{2}\left(\frac{\partial}{\partial x_\mu} + i\frac{\partial}{\partial y_\mu}\right) \tag{54}$$

a similar basis construction can be done for the cotangent space of $\mathcal{M}$ where instead we have $dz^\mu = dx + idy^\mu$ and $d\bar{z}^\mu = dx - idy^\mu$.

There is a map that can be defined on $\mathcal{M}$ which exchanges the real basis vectors (up to a sign). The map is $J_p : T_p\mathcal{M} \to T_p\mathcal{M}$

$$J_p\left(\frac{\partial}{\partial x^\mu}\right) = \frac{\partial}{\partial y^\mu} \qquad J_p\left(\frac{\partial}{\partial y^\mu}\right) = -\frac{\partial}{\partial x^\mu} \tag{55}$$

Definition 2.37 (Hermitian Metric)**.** A Hermitian metric g of a complex Riemannian manifold $\mathcal{M}$ satisfies

$$g_p(J_pX, J_pY) = g_p(X, Y) \tag{56}$$

at each $p \in \mathcal{M}$ for any $X, Y \in T_p(\mathcal{M})$

Definition 2.38 (Hermitian Manifold)**.** The pair $(\mathcal{M}, g)$, where $\mathcal{M}$ is a complex Riemannian manifold and g is a Hermitian metric, is a Hermitian manifold.

Definition 2.39 (Kähler Form)**.** The Kähler form Ω is defined as a tensor field on a Hermitian manifold as

$$\Omega_p(X,Y) = g_p(J_pX,Y) \tag{57}$$

for some $p \in \mathcal{M}$ for $X, Y \in T_p\mathcal{M}$. One can see, based off the action of J_p and the symmetry of the Hermitian metric that Ω is anti-symmetric and hence defines a two-form.

Definition 2.40 (Kähler Manifold)**.** A Kähler manifold is a Hermitian manifold whose Kähler form is closed.

It should be noted that the Kähler manifold is also a symplectic manifold as the Kähler form is also symplectic.

There is a clear analogy of Kähler manifolds with the complex number system. For example, both have two sets of real coordinates. Another similarity is that the almost complex structure maps one of these real basis vectors into the other basis, and for complex numbers multiplication by i rotates a real number into an imaginary number and vice versa. Just like the complex numbers can be extended to the quaterionic number system, the Kähler manifold can also be extended to the hyper-Kähler manifold.

Definition 2.41 (Hyper-Kähler Manifold)**.** A hyper-Kähler manifold is a Riemannian hypercomplex manifold ($\mathcal{M}$,g) with three almost complex structures I, J, K which obey

$$I_p^2 = J_p^2 = K_p^2 = I_pJ_pK_p = -id_{T_p\mathcal{M}} \tag{58}$$

where also g is Hermitian in all three almost complex structures. There are three Kähler forms for each complex structure and these are all closed for hyper-Kähler manifolds.

Hyper-Kähler manifolds are also symplectic manifolds as symplectic forms can be constructed from linear combinations of the Kähler forms.

The action of a Lie group can also be considered on Kähler manifolds. Consider a Lie group G with Lie algebra $\mathfrak{g}$ and its dual $\mathfrak{g}^*$. For any $\xi \in g^*$ there is a vector field V_ξ on $\mathcal{M}$ which is generated by ξ,

$$V_\xi(x) = \frac{d}{dt}e^{t\xi}x\bigg|_{t=0}. \tag{59}$$

Definition 2.42 (Moment Map)**.** For a Kähler manifold (or more generally for a symplectic manifold) the moment map is a G-equivariant map $\mu : \mathcal{M} \to g^*$ such that for all $\xi \in \mathfrak{g}$ $\nabla(\mu(\xi)) = J(V_\xi)$.

Definition 2.43 (Hamiltonian Group Action)**.** A G-action is Hamiltonian if a smooth moment map exists.

Definition 2.44 (Kähler Quotient)**.** If a $\zeta \in Z \subset \mathfrak{g}^*$, where Z is the dual of the center of $\mathfrak{g}$ is chosen. The quotient space

$$\mathcal{M}//_\zeta G := \mu^{-1}(\zeta)/\mathcal{M} \tag{60}$$

is a Kähler quotient of a Kähler manifold $\mathcal{M}$.

The extension of the Kähler quotient to the hyper-Kähler quotient was first done by Hitchin et al. [46].

Definition 2.45 (Hyper-Kähler Quotient)**.** Suppose that a Lie group G acts freely on a hyper-Kähler manifold and also preserves all three complex structures. Then the corresponding Kähler forms are preserved and thus three moment maps μ_1, μ_2, μ_3 can be defined. These may be collected into a single moment map

$$\vec{\mu} = (\mu_1, \mu_2, \mu_3) : \mathcal{M} \to \mathfrak{g}^* \times \mathbb{R}^3, \tag{61}$$

if $\vec{\zeta} = (\zeta_1, \zeta_2, \zeta_2)$ are chosen where each $\zeta_i \in Z$ then the hyper-Kähler quotient is defined as

$$\mathcal{M}//_{\vec{\zeta}} G := \vec{\mu}^{-1}(\vec{\zeta})/G. \tag{62}$$

Finally, given a moment map $\vec{\mu}$ and a particular complex structure is chosen, suppose it is I, then the real moment map $\mu_{\mathbb{R}} = \mu_I$ and the complex moment map $\mu_{\mathbb{C}} = \mu_J + i\mu_K$ can be defined for this particular choice. We will see shortly why this "repackaging" of the moment maps are useful when thinking about $3d$ $\mathcal{N} = 4$ gauge theories.

Nilpotent orbits are also hyper-Kähler quotients [47] and are singular spaces. A nilpotent orbit is said to be *normal* if it contains only rational Gorenstein singularities [48], in more common physics language the above statement is synonymous with saying the nilpotent orbit is Calabi-Yau [33], whereas an orbit that is not restricted in this way is said to be non-normal. Although this is a formal viewpoint, for our purposes, Stanley's theorem [49] tells us that the HS for a normal orbit is palindromic. One can do a *normalisation* of a non-normal orbit which is to take another moduli space with palindromic HS of the same dimension which forms a covering of the original space [50]. Of course a normal orbit is normalised to itself, but a non-normal orbit when normalised may often contain elements outside of the maximal orbit.

3 A Review of $3d$ $\mathcal{N} = 4$ Supersymmetry

Here we review $3d$ $\mathcal{N} = 4$ supersymmetry mainly following the lecture series on $3d$ $\mathcal{N} = 4$ given by Matthew Bullimore [51] but also [11, 52, 53] although these mainly focus on $4d$ $\mathcal{N} = 1$ supersymmetry. Details of results will not be presented in favour of presenting the relevant concepts for later calculations, however familiarity with supersymmetry will be assumed.

3.1 Supersymmetry Algebra

Our starting point is the supersymetry (SUSY) algebra. We will be concerned with $3d$ $\mathcal{N} = 4$ supersymmetry on $\mathbb{R}^3$ with Minkowski metric using the $(-++)$ convention. The spin group we consider is $SU(2)$ and fermions ψ^α transform in the fundamental of the spin group. The raising and lowering of the spin indices is done with the $SU(2)$ invariant tensors $\epsilon^{\alpha\beta}$ and $\epsilon_{\alpha\beta}$ respectively as usual.

Supersymmetry is an extension to the usual Poincaré algebra, which is generated by the four momentum P_μ and angular momentum J^μ_ν. The SUSY algebra introduces further fermionic generators $Q^{\mathcal{I}}_\alpha$ for $\mathcal{I} = 1, \cdots, \mathcal{N}$ which obey

$$\{Q^{\mathcal{I}}_\alpha, Q^{\mathcal{J}}_\beta\} = \delta^{\mathcal{I}J}(\sigma^\mu)_{\alpha\beta}P_\mu, \tag{63}$$

where $(\sigma^\mu)_{\alpha\beta}$ are the Pauli matrices. This is the extension of the Poincaré algebra to the super-Poincaré algebra.

3.2 R-Symmetry

We see that there is an $O(\mathcal{N})$ symmetry which rotates the supercharges amongst themselves. The connected subgroup $SO(\mathcal{N})$ of $O(\mathcal{N})$ forms the R-symmetry of the theory. This is a global symmetry which acts on the supercharges.

For our case of $\mathcal{N} = 4$, the R-symmetry is $SO(4)$, however we can use the fact that $SO(4) \equiv SU(2)_H \times SU(2)_C$, where the meaning of the subscripts H and C will become apparent later, to replace the $SO(4)$ index $\mathcal{I}$ with a pair of indices $A\dot{A}$ where A is an index for $SU(2)_H$ and $\dot{A}$ is an index for $SU(2)_C$ which both run up to two.

We can also rewrite (63) [2] using our new notation as

$$\{Q_\alpha^{A\dot{A}}, Q_\beta^{B\dot{B}}\} = \epsilon^{AB}\epsilon^{\dot{A}\dot{B}}(\sigma^\mu)_{\alpha\beta}P_\mu. \tag{64}$$

3.3 Vector and Hypermultiplets

Now that we have our SUSY algebra we want to compute massless multiplets from them. One can first consider $4d\,\mathcal{N}=2$ multiplets and dimensionally reduce them to $3d\,\mathcal{N}=4$ multiplets as was done first in [54]. An alternative approach is to consider $3d\,\mathcal{N}=4$ multiplets as a sum of $3d\,\mathcal{N}=2$ multiplets which can be constructed through the dimensional reduction of $4d\,\mathcal{N}=1$ multiplets.

We will consider the chiral and vector multiplets of $4d\,\mathcal{N}=1$ which can be obtained via the action of ladder operators, from the supersymmetry algebra taken on-shell for a massless particle, acting on a Clifford vacuum of lowest helicity. The multiplet is completed once one adds the CPT conjugate. Only the on-shell dof will be considered so we will neglect any auxiliary fields. Then the field content of our multiplets are [11]:

- $Cplet_{4d,\mathcal{N}=1}$ - 1 Weyl fermion + 2 real scalar
- $Vplet_{4d,\mathcal{N}=1}$ - 1 gauge field + 1 Weyl fermion

then one may dimensionally reduce to $3d\,\mathcal{N}=2$ by demanding that fields are dependent on only three of the dimensions and independent of the last. We can also use representation theory to find the branching rules of $\mathfrak{so}(4)_\mathbb{C} \simeq \mathfrak{su}(2)_\mathbb{C} \times \mathfrak{su}(2)_\mathbb{C}$ to $\mathfrak{so}(3)_\mathbb{C} \simeq \mathfrak{su}(2)_\mathbb{C}$. The usual branching rules [55] are

$$\begin{aligned}
&[1,1]_{\mathfrak{so}(4)_\mathbb{C}} \to [2]_{\mathfrak{so}(3)_\mathbb{C}} \oplus [0]_{\mathfrak{so}(3)_\mathbb{C}} \\
&[1,0]_{\mathfrak{so}(4)_\mathbb{C}} \to [1]_{\mathfrak{so}(3)_\mathbb{C}} \\
&[0,1]_{\mathfrak{so}(4)_\mathbb{C}} \to [1]_{\mathfrak{so}(3)_\mathbb{C}} \\
&[0,0]_{\mathfrak{so}(4)_\mathbb{C}} \to [0]_{\mathfrak{so}(3)_\mathbb{C}},
\end{aligned}$$

this tells us that the vector in $4d$ decomposes into a vector in $3d$ and a scalar, this is sensible as the dimensional reduction suppresses one direction of the original vector. The spinors in $4d$ decompose into spinors in $3d$ and the scalar in $4d$ decomposes into a scalar in $3d$ where we work with real dof. The dimensional reduction procedure is summarised below [56]:

[2] Here we have not included the central charges and will introduce them in a later subsection

- $Cplet_{3d,\mathcal{N}=2}$ - 1 Weyl fermion +2 real scalars
- $Vplet_{3d,\mathcal{N}=2}$ - 1 (three) vector + 2 gauginos + 1 real scalar.

Finally, the $3d\,\mathcal{N}=4$ multiplets can be constructed by the sums

$$Hplet_{3d,\mathcal{N}=4} = \bar{C}plet_{3d,\mathcal{N}=2} \oplus Cplet_{3d,\mathcal{N}=2}$$
$$Vplet_{3d,\mathcal{N}=4} = Vplet_{3d,\mathcal{N}=2} \oplus Cplet_{3d,\mathcal{N}=2}$$

where the bar denotes a conjugate Cplet. In terms of dynamical fields we have:

- $Hplet_{3d,\mathcal{N}=4}$ - 4 real scalars + 2 Weyl fermions
- $Vplet_{3d,\mathcal{N}=4}$ - 1 vector + 3 real scalars + 2 gauginos +1 Weyl fermion

The $3d\,\mathcal{N}=4$ vectormultiplet (Vplet) has a scalar field which transforms in the adjoint of $SU(2)_C$. The hypermultiplet (Hplet) has a scalar field which transforms in the fundamental of $SU(2)_H$ [57].

3.4 Flavour Symmetry

Flavour symmetry is a symmetry which commutes with the supercharges, these flavour symmetries take the form of $G_H \times G_C$.

Local operators charged under the G_H flavour symmetry are built from the Hplet scalar fields. In the UV we can only see an abelian subgroup T_C of the symmetry G_C. This abelian subgroup is called the topological symmetry.

3.5 Masses and FI Parameters

The SUSY algebra also admits central extensions, so we introduce further generators which commute with the supercharges, momentum and angular momentum generators. To be consistent with the symmetries of the indices, the form of the central extension is

$$\{Q_\alpha^{A\dot{A}}, Q_\beta^{B\dot{B}}\} = \epsilon^{AB}\epsilon^{\dot{A}\dot{B}}(\sigma^\mu)_{\alpha\beta}P_\mu + \epsilon_{\alpha\beta}\epsilon^{AB}Z^{\dot{A}\dot{B}} + \epsilon_{\alpha\beta}\epsilon^{\dot{A}\dot{B}}Z^{AB} + (\sigma^\mu)_{\alpha\beta}Z_\mu^{AB,\dot{A}\dot{B}}, \tag{65}$$

where we have the pair of indices on the scalar central charges Z^{AB} and $Z^{\dot{A}\dot{B}}$ to be symmetric. We see that these central charges transform in the adjoint of $SU(2)_H$ and $SU(2)_C$

respectively. The 1-form central charge $Z_\mu^{AB,\dot{A}\dot{B}}$ transform in the product of the adjoint representations of both $SU(2)_H$ and $SU(2)_C$. The 1-form central charge is associated to domain walls.

As the scalar central charges necessarily commute with the super-Poincaré generators a natural form is to have them proportional to the flavour symmetry generators. We assert that

$$Z^{AB} = \zeta^{AB} J_C, \quad Z^{\dot{A}\dot{B}} = m^{\dot{A}\dot{B}} J_H, \tag{66}$$

where ζ^{AB} are the FI parameters which are valued in the Cartan subalgebra of the flavour symmetry G_C and the $m^{\dot{A}\dot{B}}$ are the mass parameters which are valued in the Cartan subalgebra of the flavour symmetry G_H. The symmetrisation of the indices tell us that the FI and mass parameters transform in the adjoint of the $SU(2)_H$ and $SU(2)_C$ respectively.

3.6 Topological Symmetry

Topological or hidden symmetries are an interesting feature of $3d$ theories. Let us consider $U(1)$ gauge theory in $3d$, then there is a field strength 2-form F which satisfies

$$dF = 0, \quad d * F = 0, \tag{67}$$

which are closure and the Bianchi identity respectively. The special case about $d = 3$ is that the Hodge dual of F is a $3 - 2 = 1$-form current $J = *F$. The Bianchi identity immediately implies

$$dJ = 0 \tag{68}$$

thus the current J is conserved and means that there is some symmetry associated to that current. This symmetry cannot be seen from the Lagrangian and hence explains the name *hidden*, note that this could only be done in three dimensions so this symmetry also bears the name *topological*.

Since we are on $\mathbb{R}^3$ the Poincaré lemma states that all closed forms are exact. Thus we can write $J = d\gamma$ for some 0-form γ. The current conservation equation is automatically satisfied by the nilpotency of the exterior derivative. The equation of motion for the 0-form γ is $d * d\gamma = 0$. This 0-form γ is often called the dual photon since in $3d$ there is only one polarisation of the gauge field and so the action can be expressed in terms of a single scalar field [58]. In fact this scalar field is periodic as for a 0-form gauge field (the dual photon) the form of the gauge transformation is a linear shift. The dual photon is a compact scalar and is circle valued.

3.7 Monopole Operators

The idea of topological symmetry can also be extended to non-abelian gauge symmetries which contain at least one abelian $U(1)$ and for each $U(1)$ we have a conserved current [55].

The corresponding conserved current for a non-abelian gauge theory is

$$J = *TrF \tag{69}$$

It was then proposed that these topological symmetries could be studied as monopole operators [59], in $3d$ the monopole operators used are 't Hooft monpole operators [60].

Monopole operators are local disorder operators which can be inserted into the path integral [61] and integrated over gauge field configurations. These operators are defined by the Dirac monopole singularity that they introduce. There is an insertion of a monopole operator at a point and we excise a 2-sphere around this point. The singularity takes the form

$$A_{N/S}(\vec{r}) = \frac{m}{2}(\pm 1 - \cos\theta)d\varphi \tag{70}$$

where we work in spherical polar coordinates and m is a magnetic charge. There are two patches of a 2-sphere and so the singularity is different on the Northern and Southern patches. However, to ensure that the transition function is smooth between patches there is a Dirac quantisation condition [62] which forces m to Lie in the weight lattice of the Langlands dual group of the gauge symmetry. Importantly, monopole operators are charged under the topological symmetry.

3.8 Moduli Space of Vacua

The moduli space of a SUSY gauge theory is the space of vacuum expectation values (vev) a theory can have. Only scalars can acquire a non-trivial vev due to Lorentz symmetry. There are scalars in the Hplets and Vplets all of which can acquire non-trivial vevs. This leads to the notion of a branch, where if the scalars in the Vplet are zero then the non-zero vevs of the Hplet parameterise the Higgs branch $\mathcal{M}_H$ and vice versa for the Coulomb branch $\mathcal{M}_C$. There is a possibility that both Hplet and Vplet vevs are non-zero, this is called a mixed branch. Finally, when both Hplet and Vplet vevs are zero this is the point where the Higgs branch and Coulomb branch intersect. This point is the IR fixed point of the theory.

The moduli space for a $3d$ $\mathcal{N}=4$ theory is then the union of all of the branches

$$\mathcal{M} = \mathcal{M}_C \cup \mathcal{M}_H \cup_i \mathcal{M}_i \tag{71}$$

where $\mathcal{M}_i$ denotes some mixed branches.

We will not be concerned with mixed branches in this work and will consider the Coulomb branches of theories. However, due to $3d$ mirror symmetry [21] (discussed soon) which relates Higgs and Coulomb branches, Higgs branches will also be discussed.

Although we will not show in detail the solutions to the vacuum equations, the general idea will be presented. In the Higgs phase the mass parameters are switched off by definition. The Hplet has four real scalars, so for a theory with k Hplets we may naively expect a moduli space of $\mathbb{R}^{4k}$, which at this point should hint at a possible hyper-Kähler moduli space. The Hplets must also transform under some linear quaternionic representation of the gauge group (we will see later, in practise, we only need to specify unitary representations of the gauge group). Indeed, the F and D-terms respectively, for generic FI parameters, are interpreted as real and complex moment maps, which should be understood as being associated to the Kähler and holomorphic symplectic forms respectively. These forms are constructed from the Hplet scalars. Recall that to define a hyper-Kähler quotient a set of parameters must be chosen, these are the FI parameters. So the geometry of the Higgs branch is that of a hyper-Kähler quotient. A non-renormalisation theorem tells us that the Higgs branch is protected from quantum corrections, except possibly at strong coupling. If the FI paramaters are also taken to be zero, the Higgs branch also has a conical singularity.

In the Coulomb phase, the FI parameters are necessarily switched off. In the IR, the vacuum equations force the three scalars to lie in the Cartan subalgebra of the gauge symmetry [63]. The Cartan subalgebra of the gauge symmetry is the maximal torus and so the gauge symmetry is broken to this maximal torus. In the classical case the three real scalars in the Vplet and the periodic dual photon (from the dualisation of the IR abelian gauge fields) would suggest that the classical Coulomb branch in 3d theories is [64]

$$\mathcal{M}_C^{class.} = (\mathbb{R}^3 \times S^1)^{rnk(G)}/\mathcal{W}_G. \tag{72}$$

However, the Coulomb branch receives quantum corrections, both perturbative and non-perturbative [54, 65]. In the end the Coulomb branch is also a hyper-Kähler quotient. If the masses are taken to be zero, then the Coulomb branch also acquires a conical singularity.

3.9 $3d$ Mirror Symmetry

A duality between two $3d$ $\mathcal{N} = 4$ theories was found by Intriligator and Seiberg [21] when thinking of these theories in type IIB string theory.

The geometry of the Higgs branch of one theory is the same as the geometry of the Coulomb branch of its $3d$ mirror dual and vice versa. The global symmetries of the Higgs branch of one theory and the global symmetry of the Coulomb branch can also be exchanged in this way and vice versa. Similarly the masses and FI parameters of one theory can be exchanged with the FI parameters and masses of the $3d$ mirror dual theory. This is a remarkable relationship between some theories and a very useful one at that. If for example, the tools for working with the Higgs branch of a theory are inefficient, there may be better luck if the Coulomb branch of the $3d$ mirror theory was studied instead.

The acquisition of a $3d$ mirror theory can be done using brane systems as in [18], however this point is for illustration and will not be used in this work.

4 Techniques in Quiver Gauge Theories

Here, we describe the main techniques we will use in computations. Simple examples will also be given.

4.1 Quivers

A quiver is a diagram which tells us the gauge symmetries, flavour symmetries and how Hplets and Vplets transform under those symmetries [17] for some supersymmetric gauge theory. We will focus on $3d$ $\mathcal{N} = 4$ quiver gauge theories in this work and so we give an example of such a quiver in Figure 2, where the circle node is a gauge symmetry and the square node is a flavour symmetry. The line tells us that we have N_f Hplets transforming in the fundamental representation of the $U(N_c)$ gauge group. There are Vplets which transform in the adjoint of the corresponding gauge group. We can also include adjoint Hplets by drawing a line from a gauge group node to itself.

The quiver tells us about a unitary representation of the gauge group and not a quaternionic one. This is because of the isomorphism $Sp(k) \simeq USp(2k, \mathbb{C}) := Sp(2k, \mathbb{C}) \cap U(k, k)$. So the $k \times k$ quaternionic symplectic matrices forming the quaternionic representations can simply be replaced by unitary complex symplectic $2k \times 2k$ matrices. Furthermore, we can restrict to a cotangent type quaternionic representation. This allows us to simply define a unitary representation $\rho : G \to U(k)$ which acts on $\mathbb{C}^k$. The cotangent type quaternionic representations mean that the space which these quaternionic representations act on decompose as $Q \simeq \mathbb{C}^k \oplus \mathbb{C}^{k^*}$ [51].

We can also have multiple gauge nodes in our quiver. The gauge symmetry of the theory is the product of the groups associated to the gauge nodes. Lines connecting two gauge nodes tell us that there is a Hplet that transforms in the bifundamental representation of the gauge groups connected by the line. In a quiver with only gauge nodes, a $U(1)$ subgroup can be *ungauged* as the action of this $U(1)$ is a trivial action. If the quiver has gauge nodes of $U(n_i), i = 1, \cdots, N$ connected in a chain, the gauge symmetry is $S(\prod_{i=1}^{N} U(n_i))$. If there is already a flavour group in the quiver we cannot ungauge an overall $U(1)$. The latter type of quiver is called a *framed* quiver.

As we will deal with Coulomb branches when performing computations, the quivers we consider are called *magnetic* quivers. The definition of a magnetic quiver Q for some gauge theory $\mathcal{T}$ in some dimension d is [66]

$$\mathcal{H}^d(\mathcal{T}) = \mathcal{C}^{3d}(Q) \tag{73}$$

where the theory $\mathcal{T}$ can live in any dimension but the magnetic quiver must be for a three dimensional theory.

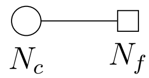

Figure 2: The $3d$ $\mathcal{N}=4$ quiver for $U(N_c)$ gauge theory with $SU(N_f)$ flavour symmetry.

4.2 The Monopole Formula

The monopole formula gives the Hilbert series of the Coulomb branch of a $3d$ $\mathcal{N}=4$ quiver gauge theory. We present the formula below and then give a brief explanation of the various parts following the discoverers of the formula [67],

$$HS_G(t,z) = \sum_{m \in \Gamma^*_{\hat{G}}/\mathcal{W}_{\hat{G}}} z^{J(m)} t^{2\Delta(m)} P_G(t^2, m). \tag{74}$$

Recall that the monopole operators are labelled by a magnetic flux m that takes values in the weight lattice of the Langlands dual group, $\hat{G}$ to the gauge group G, to satisfy the Dirac quantisation condition. Further, the Coulomb branch should be parameterised by the gauge invariant monopole operators and so should be labelled by fluxes in the weight lattice of the Langlands dual group modulo Weyl transformations.

For the Hilbert series we grade the monopole operators by the charges they have under the global symmetries of the Coulomb branch. These symmetries are the R-symmetry and the topological symmetry. The R-charge is given by the formula below,

$$\Delta(m) = -\sum_{\alpha \in \Delta^+} |\alpha(m)| + \frac{1}{2}\sum_{i=1}^{n} \sum_{\rho_i \in \mathcal{R}_i} |\rho_i(m)|. \tag{75}$$

where Δ^+ is the set of positive roots of our gauge symmetry and ρ_i are the weights of the matter-field representations $\mathcal{R}_i$.

The counting variable t^2 is called a fugacity (we will explain the naming sense later). The normalisation of t^2 is often taken due to the factors of $1/2$ in the R-charge. Recall the reason is that irreps of $SU(2)_C$ are labelled by half-integers.

We introduce a counting variable z for the topological symmetry and this is graded by the total magnetic flux $J(m)$.

Finally, we have gauge invariant operators of the residual symmetry group H_m when a flux m breaks G. This is given by

$$P_G(t^2, m) = \prod_{i}^{rnk(G)} \frac{1}{1 - t^{d_i(m)}} \tag{76}$$

where d_i are the degrees of the Casimirs of H_m.

Once the HS has been computed, we will find that it will often admit an infinite power series expansion as well as a closed form expression. If thinking about the power series expansion, the HS and the coefficients of the series are conjugate in the sense of a Legendre transformation. For this reason, if one considers the coefficient of the variable t^2 as a conserved charge, then $\log t$ is a chemical potential and hence t is called a fugacity [27]. We can similarly give the counting variable z the name of *topological fugacity*.

4.2.1 The Monopole Formula for unitary nodes

The monopole formula as presented above appears quite abstract. As we are concerned with unitary quivers, that is quivers with only unitary or special unitary nodes, we give more explicit expressions for the monopole formula.

Case 1 - $U(k_1)$ gauge node connected to $U(k_2)$ gauge node with multiplicity a

For this case, unitary groups are Langlands self-dual [68]. Thus we need the weight lattice of $U(k_1) = SU(k_1) \times U(1)$ modulo the Weyl group of $U(k_1)$. This is simply $-\infty \leq m_1 \leq \cdots \leq m_{k_1} \leq \infty$ for integers m_i which are the components of the magnetic flux.

The dressing factor for a unitary gauge group is given by [67]

$$P_{U(k)} = \prod_{i=1}^{k} \frac{1}{(1 - t^{2i})^{\tilde{\lambda}_i(\vec{m})}} \tag{77}$$

where $\tilde{\lambda}_i(\vec{m})$ is the length of the i^{th} row of the dual Young tableau associated to a flux $\vec{m}$. For example, the associated Young tableau for the flux $\vec{m} = (7, 7, 7, 4, 4, 3, 3, -2)$ is 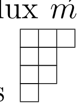 .

The dual Young tableau is 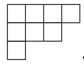, and so the dressing factor is

$$P_{U(8)}(t,7,7,7,4,4,3,3,-2) = \frac{1}{(1-t^2)^4\,(1-t^4)^3(1-t^6)}. \tag{78}$$

Now we need to compute the R-charge. Given that $U(k_1) \simeq SU(k_1) \times U(1)$, the root system of $U(k_1)$ is the direct sum of the root systems of $SU(k_1)$ and $U(1)$, $U(1)$ is abelian and so its root system is trivial, thus $SU(k_1)$ and $U(k_1)$ have the same root system, which we know well.

Finally, to deal with the non-simply laced edge which points from the $U(k_1)$ node to the $U(k_2)$ node with multiplicity a, all we do is put a factor a in front of all of the flux components associated to $U(k_2)$ in the Hplet contribution. So supposing, $U(k_1)$ has a flux $\vec{m}$ and $U(k_2)$ has a flux $\vec{n}$, the R-charge is given by

$$\Delta(\vec{m},\vec{n}) = -\sum_{1\le i<j\le k_1} |m_i - m_j| - \sum_{1\le u<j\le k_2} |n_i - n_j| + \frac{1}{2}\sum_{i=1}^{k_1}\sum_{j=1}^{k_2} |m_i - a n_j| \tag{79}$$

$U(k_1)$ single edge to $U(k_2)$ flavour node

Here we only consider the contribution from the Hplets, since the vector multiplet contribution is discussed above.

The $U(k_2)$ flavour symmetry means that we have k_2 Hplets in the fundamental of $U(k_1)$. There is no flux associated to the flavour symmetry and so the Hplet contribution is

$$\Delta_{hyper}(\vec{m}) = \frac{k_2}{2}\sum_{i=1}^{k_1} |m_i|. \tag{80}$$

4.2.2 $U(1)$ with n flavours

We put together the moving parts in a simple example, $U(1)$ with n flavours (which is commonly known as SQED with n flavours). We draw the quiver in Figure 3. We start with the computation of the R-charge. The magnetic flux associated to the $U(1)$ gauge node is a

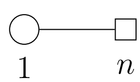

Figure 3: The quiver for $U(1)$ with n flavours.

single integer m which takes values in the range $-\infty \le m \le \infty$. The group $U(1)$ is abelian so it has no root system and thus no contribution from the vector multiplets. The remaining contribution is from the Hplets whose form is given above so

$$\Delta(m) = \frac{n}{2}|m|. \tag{81}$$

As the flux is labelled by only a single integer, there is only one Young tableau associated to it, $\Box$. The classical dressing factor takes the form,

$$P_{U(1)}(m) = \frac{1}{1-t^2}. \tag{82}$$

The total magnetic charge is simply $J(m) = m$, so putting this into the monopole formula we have

$$HS(t,z) = \frac{1}{1-t^2} \sum_{-\infty \leq m \leq \infty} z^m t^{n|m|} \tag{83}$$

$$= \frac{1-t^{2n}}{(1-t^2)\,(1-zt^n)(1-z^{-1}t^n)}. \tag{84}$$

4.3 Highest Weight Generating Functions and Plethystics

The plethystics program [69] gives us a systematic way to count the gauge invariant operators (GIOs) that parameterise the moduli spaces we study. Given a set of "basic" GIOs, we can consider the representations of the global symmetry these transform in and construct symmetric products of these using the plethystic exponential (PE). We choose symmetric products in order to satisfy the Pauli statistics. This can be seen for the Higgs branch of SQCD theories by considering the irreps that the gauge invariant mesons and baryons transform in, and constructing higher order invariants by symmetrisation, for example [70]. The expression for the PE of a function $f(t, x_i)$ is

$$PE[f(t,x_i)] = \exp\left(\sum_{k=1}^{\infty} \frac{f(t^k, x_i^k) - f(0,0)}{k}\right), \tag{85}$$

from this formula it is very simple to check that

$$PE[f(t)+g(t)] = PE[f(t)]PE[g(t)], \tag{86}$$

which is a useful identity.

We also have the inverse of the plethystic exponential, which is aptly named the plethystic logarithm (PL). This is given by

$$PL[f(t,x_i)] = \sum_{k=1}^{\infty} \frac{\mu(k) \log f(t^k, x_i^k)}{k}, \tag{87}$$

where $\mu(k)$ is the Möbius function [71] and is defined for positive integer k as

$$\mu(k) = \begin{cases} +1 & k \quad \text{is square-free with an even number of prime factors} \\ -1 & k \quad \text{is square-free with an odd number of prime factors} \\ 0 & k \quad \text{has a squared prime factor.} \end{cases} \tag{88}$$

Exact Hilbert series' are often unwieldy expressions, and so it is convenient to package them as a PE. This is very simply done by taking the PL of the HS one computes. There is a further convenience if one computes the highest weight generating function. Instead of using characters of irreps, one uses a *highest weight fugacity*. Recall that any irrep can be labelled by a highest weight which itself is labelled by Dykin labels. Then one introduces the fugacities μ_i as

$$[n_1, \cdots, n_r] \leftrightarrow \mu_1^{n_1} \cdots \mu_r^{n_r}. \tag{89}$$

Thus for a given refined HS one computes the HWG for some compact group with rank r as [70, 72],

$$HWG(t, \mu_1 \cdots, \mu_r) = \sum_{k_1=0}^{\infty} \cdots \sum_{k_r=0}^{\infty} \int_G d\mu_G \chi([\mu_1^{k_1}, \cdots \mu_r^{k_r}])^* HS(t, x_1, \cdots x_r) \mu_1^{k_1} \cdots \mu_r^{k_r}. \tag{90}$$

To explain the above formula, the Peter-Weyl theorem [32] says that characters of irreps of some compact group are orthogonal under Weyl integration. A refined Hilbert series can be written exactly as an infinite series in t^2, the coefficients are characters. So we use the orthogonality of characters to pick up only the highest weight fugacities associated to the character(s) that appear in the HS. This is the highest weight generating function. Finally, one may re-express this as a PE by taking the PL.

Often the integration required to get the HWG can be computationally expensive. It is very common to guess the HWG by looking first at the t^2 term of the refined HS to identify the irrep for that term. Then taking the PE of the corresponding highest weight fugacity and adding a term by hand to the HWG to match the HS at order t^4, then repeating the process of taking PEs and adding new terms. If this is done to a sufficiently high order, one can be confident on the form of the HWG.

4.3.1 An Example - $\mathbb{C}^2/\mathbb{Z}_2$

The unrefined Hilbert series for $\mathbb{C}^2/\mathbb{Z}_2$ is calculated to be

$$HS_{\mathbb{C}_2/\mathbb{Z}_2} = \frac{1-t^4}{\left(1-t^2\right)^3} \tag{91}$$

we can take the PL of this and find

$$PL[HS_{\mathbb{C}_2/\mathbb{Z}_2}] = 3t^2 - t^4, \tag{92}$$

this tells us explicitly that we have three generators of second degree,$z_1^2, z_2^2, z_1 z_2$, and one relation at degree four, $(z_1)^2(z_2)^2 = (z_1 z_2)^2$. The PL of the HS has made this explicit. Note that relations appear in the PE as a negative term, this is then manifested in the HS as a term roughly of the form $(1-t^d)$ in the numerator. For this reason, a freely generated moduli space is named such, as it has no relations constraining the coordinates and hence the numerator is one.

We can go further by refining the HS. All the $\mathbb{Z}_2$ invariant monomials are of the form $z_1^a z_2^b$ where $a+b$ is even. We assign a fugacity of t_1 for z_1 and t_2 for z_2, the refined HS is then

$$HS(t_1, t_2) = \sum_{\substack{a,b=0 \\ a+b even}}^{\infty} t_1^a t_2^b = \frac{1+t_1 t_2}{(1-t_1)^2(1-t_2^2)} = \frac{1-t_1^2 t_2^2}{(1-t_1^2)(1-t_1 t_2)(1-t_2^2)}, \tag{93}$$

finally we can make a fugacity map $t_1 \to tx$ and $t_2 \to t/x$ to find

$$HS(t,x) = \frac{1-t^4}{\left(1-t^2x^2\right)\left(1-t^2\right)\left(1-t^2/x^2\right)}. \tag{94}$$

If this is expanded in powers of t we see that the coefficients of t form characters of $SU(2)$. Indeed we find

$$HS(t,x) = \sum_{p=0}^{\infty} \chi([2p]) t^{2p}. \tag{95}$$

Taking the PL of this we find

$$PL[HS(t,x)] = \chi([2])t^2 - \chi([0])t^4 \tag{96}$$

which again tells us that we have three generators transforming in the adjoint representation of $SU(2)$ with a relation transforming in the singlet of $SU(2)$.

Now we can compute the HWG of the HS by remembering to take $[2p] \to \mu^{2p}$, then

$$HWG(t,\mu) = \sum_{k=0}^{\infty} \int_{SU(2)} d\mu_{SU(2)} \chi([\mu^k])^* \left(\sum_{p=0}^{\infty} \chi[\mu^{2p}] t^{2p} \right) \mu^k \tag{97}$$

which upon evaluating gives

$$HWG(t,\mu) = \sum_{p=0}^{\infty} \mu^{2p} t^{2p} = \frac{1}{1-\mu^2 t^2} \implies PL[HWG[t,\mu]] = \mu^2 t^2. \tag{98}$$

Note that there is no term at order t^4 in the HWG, the HWG is simply a generating function for the HS after the corresponding highest weight fugacities have been converted into the appropriate characters. If one wants to find the generators and relations for the variety, the HS should be used. Nevertheless, the HWG is an incredibly useful tool as we will see later when discussing discrete quotients of moduli spaces.

4.4 Namikawa's Theorem

Before moving on to computing the HS of more complicated quivers, it is important that we are able to identify the moduli spaces we get from the Hilbert series.

In some cases this can be easily done by considering the invariant monomials. For others, this may be more difficult. Fortunately, there is a theorem due to Namikawa [73] when "translated into physics" says that if all the generators of some hyper-Kähler singularity has R-charge one, then the moduli space is a nilpotent orbit of the global symmetry of the moduli space [27]. It turns out that many of the Coulomb branches we compute will be nilpotent orbits.

More directly, if the series expansion of the unrefined series is taken, the coefficient of the t^2 term is the dimension of the adjoint representation of the isometry group of the hyper-Kähler variety. This will give an indication of what the global symmetry will be for computing the HWG from the refined HS. The resulting variety should also be thought of as being a nilpotent orbit or a cover or a deformation of one.

4.5 Construction of Magnetic Quivers for Nilpotent Orbits and their Normalisations

It was shown that one could construct a balanced unitary magnetic quiver for a nilpotent orbit of height two or less by the affine Dynkin diagram of the algebra, first for simply laced groups in [67], and then for non-simply laced groups in [74]. The latter introduced the construction of magnetic quivers from root maps and weight maps. The introduction of non-simply laced edges meaning to include a multiplicity in the R-charge was also introduced here. However, theories with non-simply laced edges do not have a Lagrangian description, nevertheless they have valid Coulomb branches.

This was further extended in [34] to work for all orbits of height 2 or less. To construct a magnetic quiver for one of these orbits, four pieces of data are required; the group G, the dual Coxeter labels for that group, the root map, and weight map for the $SU(2)$ embedding.

The construction is as follows:

- Check the height of the orbit. Take the usual vector dot product of the dual Coxeter labels and the root map for the given orbit. If the height is 2 or less then proceed, if not, there is no known algorithmic way of constructing magnetic quivers for these orbits.
- Take the affine Dynkin diagram for G and use a labelling of the nodes from $1, \cdots, rnk(G)$ following [75].
- The gauge nodes, in order, are given by the entries of the weight map for the orbit.
- The flavour nodes, in order, are given by the root map entries of the orbit.

For orbits of height three or greater this construction sometimes produces a $\mathbb{Z}_2$ cover of the orbit and sometimes something else entirely. This construction also fails if the orbit is of non-normal type, though a normalisation of these orbits could be constructed using the Nilpotent Orbit Normalisation (NON) formula [76]. The starting point is the localisation formula for generalised Hall-Littlewood functions. Special cases for $SU(n)$ were used to construct the Hilbert series of Higgs and Coulomb branches of $T^{\sigma}_{\rho}(SU(N))$ theories [77].

The formula for any Lie group G is

$$HS^{G}\left(x_{1,\cdots,r},t,[n_1,\cdots,n_r]\right)=\sum_{w\in W_{G/H}} w\cdot\left(x^{[n_1,\cdots,n_r]}\prod_{\alpha\in\widetilde{\Delta}_{G/H}}\frac{1}{1-z^{\alpha}t^2}\prod_{\beta\in\Delta^+_{G/H}}\frac{1}{1-z^{-\beta}}\right), \tag{99}$$

where the x_i are the character fugacities and the z_i are topological fugacities. The notation of z^{α} is analogous to the conversion between character and topological fugacities. Although the NON formula is from group theoretic considerations and not physical ones, we decide to stick with the name *topological fugacity* since this is consistent with the use of the monopole formula on a magnetic quiver which gives the same (normalisation of a) nilpotent orbit. The original work refers to these as *simple root fugacities*. The subgroup $H \subset G$ is semi-simple and regular with a positive root space Δ^+_H. This group is chosen so that the quotient group G/H has positive roots $\Delta^+_{G/H} = \Delta^+_G \ominus \Delta^+_H$. Another piece of data is $\widetilde{\Delta}^+_{G/H}$ which is a subset of $\Delta^+_{G/H}$ and chosen depending on what is to be calculated. The sum is over representatives w of the cosets $W_{G/H}$. This action is directly on the x_i as $x \to w\cdot x$ and implicitly on z through its action on the x_i. We recall that the topological fugacities and the character fugacities are related through the Cartan matrix.

In [76], (99) was adapted by making the following choices: set all Dynkin labels to zero, choose H to be the stability group of the highest root, which is called G_0, and choose the subset $\widetilde{\Delta}^+_{G/G_0} = \Delta^+_G \ominus \Delta^{[1]}_G$, where $\Delta^{[1]}_G$ is the set of positive roots of G with characteristic height 1. The height of a root $\alpha = \sum_i a_i\alpha_i$ is computed as $h = \sum_i a_i q_i$. Where the q_i are the root map for the highest root. Each subset of positive roots is specified by an embedding of $SU(2)$ into G so this formula is really specified by each embedding. After some rearrangements, the formula for the normalisation of nilpotent orbits is given by

$$HS^{G(\rho)}_{NON}(z_1,\cdots,z_r,t)=\sum_{w\in W_G} w\cdot\left(\prod_{\alpha\in\widetilde{\Delta}_{G/G_0}}\frac{1}{1-z^{\alpha}t^2}\prod_{\beta\in\Delta^+_G}\frac{1}{1-z^{-\beta}}\right) \tag{100}$$

For normal orbits, the normalisation formula simply reproduces the Hilbert series of the orbit.

All of the root maps and weight maps for the $SU(2)$ homomorphisms into classical ABCD-type groups can be found in Appendix B of [78] and for exceptional groups in Appendix D of [76]. Not only this, but the orbits corresponding to these data can also be found. All identification of orbits in this work are consistent with the above papers.

4.6 Quiver Balance

The R-charge has positive contributions with a factor half from the Hplets and negative contributions from Vplets. A negative R-charge may result in an uncomputable Hilbert series. This then places some constraints on the number of Hplets and Vplets associated to each node for a valid Hilbert series.

This idea was studied in [79] for simply laced quivers. There are three types of quiver that one could have:

- Good Quivers. All monopole operators have an R-charge whose absolute value is greater than 1.
- Ugly Quivers. Monopole operators have an R-charge of 1/2.
- Bad Quivers. Monopole operators have R-charge less than or equal to zero.

More directly, we can determine from a given quiver whether it is "good", "bad", or "ugly" following the prescription for simply laced quivers given in [79] and extended to non-simply laced quivers in [78] for affine Dynkin type quivers using the Cartan matrix for affine Dynkin diagrams. To do this, we first need to compute a quantity called the *excess* for a gauge node with group $U(n)$. If this gauge node has a set of neighbouring nodes (which can be flavour or gauge nodes) $\{U(m_i)\}$ for $i = 1, \cdots N$, with a non-simply laced edge of multiplicity λ_i from $U(n)$ to $U(m_i)$, the excess of n is defined as

$$e_n = \sum_{i=1}^{N} \lambda_i m_i - 2n. \tag{101}$$

This formula is adapted from the equation for the balance of the node using the Cartan matrix as in [76]. However, the formula presented above is often quicker to use in practise.

If a quiver has nodes with a single adjoint Hplet and these nodes are connected to only one other gauge node, the following procedure as given in [80] is used:

- If a node of $U(k)$ has an adjoint Hplet on it, replace the adjoint Hplet with a non-simply laced edge of k such that the original node is short.
- The node of $U(k)$ is then set to $U(1)$.
- Apply the usual formula for computing balance with this new quiver.

A quiver is "good" if all gauge nodes have a positive excess, "ugly" if some gauge nodes have an excess of -1 and "bad" if any gauge node has an excess $e < -1$. A quiver is balanced if all gauge nodes have an excess of zero.

It is worth saying that the "good", "bad" and "ugly" classification of quivers does not mean that they are necessarily invalid gauge theories. For our purposes, this classification tells us about the computability of the Hilbert series of the Coulomb branch.

4.7 Gluing

The monopole formula is a direct way of computing the Hilbert series of the Coulomb branch of a quiver. However, for longer quivers it is often inefficient to compute. If we suppose our quiver has multiple legs attached to a common gauge node, we can consider the HS of each individual leg, but assuming the common node is a flavour symmetry instead. The HS of the Coulomb branch of each of these is computed with background fluxes associated to that flavour symmetry and can then be glued together in the following way,

$$HS(t^2) = \sum_{\vec{m} \in \Gamma^*_{\hat{G}} / \mathcal{W}_{\hat{G}}} t^{2\Delta_{vec}(G)} P_G(\vec{m}, t^2) \prod_{i=1}^{l} HS_G^{(i)}(\vec{m}, t^2), \tag{102}$$

where we have suppressed character fugacities and assumed we have l legs with Hilbert series $HS_G^{(i)}(\vec{m}, t^2)$ which is a function of the magnetic flux $\vec{m}$ associated to the common flavour symmetry G.

4.7.1 An Example - Magnetic Quiver for $\overline{min.E_6}$

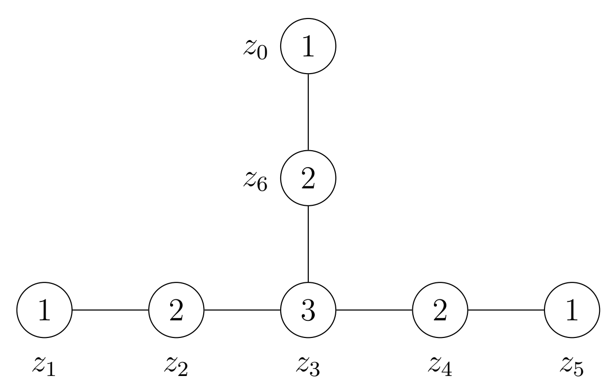

Figure 4: Magnetic quiver for $\overline{min.E_6}$. The label inside node is the n of $U(n)$, the z_i are the topological fugacities.

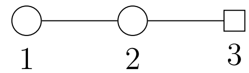

Figure 5: A leg of affine E_6. Topological fugacities have been suppressed.

The quiver whose Coulomb branch we wish to compute is given in Figure 4 where we have included the standard labelling of topological fugacities as in [75]. The balanced subset of nodes forms the Dynkin diagram for affine E_6. We note that there are three identical legs attached to the central node of three which is shown in Figure 5. We compute the Hilbert series of each leg with the background magnetic flux associated to the flavour node of three. Appropriate topological charges must be chosen for each leg. As the affine E_6 quiver consists of only gauge nodes there is an overall $U(1)$ symmetry which we are allowed to ungauge. Further, this quiver is simply laced and so one can ungauge this $U(1)$ on any node. We choose the common node of three as this will speed up computation. The ungauging of the $U(1)$ corresponds to a shift in one of the magnetic fluxes in the magnetic flux $\vec{m} = (m_1, m_2, m_3)$ associated to the central node of three. The ungauging in the monopole formula is implemented by setting one of the three fluxes to zero. This is not as ideal as ungauging a node of one, as there is only a single flux, so a node of one gets ungauged to a flavour node. If a node of rank higher than one is ungauged this is typically represented by a squircle [81].

Finally, we note that in Figure 4 there is an additional topological charge z_0 as we choose to ungauge a $U(1)$ from the node of three, instead of a node of one. We can eliminate this using the gauge fixing condition [81]

$$\prod_{i=1}^{N} z_i^{r_i} = 1 \tag{103}$$

and explicitly we have $z_0 = (z_1 z_2^2 z_3^3 z_4^2 z_5 z_6^2)^{-1}$. The whole quiver is fully balanced and forms the Dynkin diagram of affine E_6 and so we expect the global symmetry of the Coulomb branch to be E_6. We can compute the unrefined Hilbert series as,

$$HS(t^2) = \frac{(1+t^2)\begin{pmatrix}1 + 55t^2 + 890t^4 + 5886t^6 + 17929t^8 + 26060t^{10} \\ + 17929t^{12} + 5886t^{14} + 890t^{16} + 55t^{18} + t^{20}\end{pmatrix}}{(1-t^2)^{22}} \tag{104}$$

$$\begin{aligned} PL[HS] = {} & 78t^2 - 651t^4 + 12376t^6 - 296946t^8 + 7755189t^{10} - 212057222t^{12} + 5975677162t^{14} \\ & - 172018163850t^{16} + 5031500238596t^{18} - 149021032678947t^{20} + O\left(t^{21}\right). \end{aligned} \tag{105}$$

The coefficient of t^2 is 78, which is the dimension of the adjoint representation of E_6 and so the Coulomb branch does indeed have an E_6 global symmetry. The refined Hilbert series can also be computed and from this the HWG can be computed as

$$HWG = PE[\nu_6 t^2], \tag{106}$$

where ν_6 is a highest weight fugacity for E_6. We also identify the moduli space as the minimal nilpotent orbit of E_6 [76].

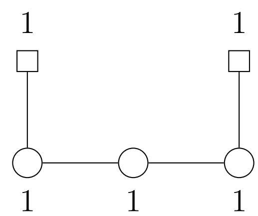

Figure 6: Magnetic quiver for $\overline{min.A_3}$.

5 Discrete Gauging and Folding

Here we give some examples of discrete gauging and folding magnetic quivers.

5.1 Folding

The folding of simply laced Dynkin diagrams can give a non-simply laced Dynkin diagram. A magnetic quiver whose balanced subset of gauge nodes that forms a Dynkin diagram of G will have G as the isometry group of the Coulomb branch. If a magnetic quiver is folded in such a way that the balanced subset of gauge nodes form a new Dynkin diagram of G' then it is expected that the isometry of the Coulomb branch of the folded quiver is G'. However, we know also that non-simply laced edges in a magnetic quiver correspond to an additional multiplicity in the R-charge and these theories do not have a Lagrangian description. Perhaps some non-simply laced quivers have an interpretation as folded quivers of simply laced quivers. This is checked with some computations.

To perform a folding of a magnetic quiver, a common node to which identical legs are connected is first identified. If k legs are folded, then these legs are replaced with just one of the identical legs. However, a non-simply laced edge of multiplicity k is introduced with the central node as long. Examples below will illustrate this.

In terms of the Coulomb branch, the folded Coulomb branch corresponds to the fixed points of the original Coulomb branch under the action of whatever the quiver automorphism group is. For this reason we expect that the dimension of the Coulomb branch is not preserved under folding.

5.1.1 Folding $\overline{min.A_3}$

The magnetic quiver for $\overline{minA_3}$ is shown in Figure 6. The Hilbert series can be computed

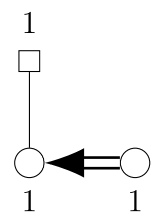

Figure 7: Magnetic quiver for $\overline{min.C_2}$.

from the monopole formula. The unrefined series is

$$HS\left(t^2\right) = \frac{\left(1+t^2\right)\left(1+8t^2+t^4\right)}{\left(1-t^2\right)^6} \tag{107}$$

$$PL[HS] = 15t^2 - 36t^4 + 160t^6 - 945t^8 + 6048t^{10} - 39760t^{12} + 267840t^{14} - 1844640t^{16} + 12912480t^{18} - 91497168t^{20} + O\left(t^{21}\right), \tag{108}$$

the HWG may be computed in terms of the highest weight fugacities for A_3 as

$$HWG = PE[\nu_1\nu_3 t^2]. \tag{109}$$

The folding of this quiver results in the magnetic quiver for $\overline{min.C_2}$ shown in Figure 7, the Hilbert series can be computed as

$$HS\left(t^2\right) = \frac{1+6t^2+t^4}{\left(1-t^2\right)^4} \tag{110}$$

$$PL[HS] = 10t^2 - 20t^4 + 64t^6 - 280t^8 + 1344t^{10} - 6560t^{12} + 32640t^{14} - 166320t^{16} + 862400t^{18} - 4524576t^{20} + O\left(t^{21}\right), \tag{111}$$

using the refined series the HWG can be computed as

$$HWG = PE[\mu_1^2 t^2]. \tag{112}$$

We computed the HWG of the minimal nilpotent of A_3 as $PE[\nu_1\nu_3 t^2]$, and found that the HWG for the folded quiver is $PE[\mu_1^2 t^2]$. It is as if we had mapped $\nu_1, \nu_3 \to \mu_1$ and $\nu_2 \to \mu_2$. This is indeed the automorphism map on the Dynkin diagram of A_3 and we recover the folding of A_3 into C_2.

5.1.2 Folding $\overline{min.E_6}$

The magnetic quiver for the minimal nilpotent orbit of E_6, its HS and HWG were computed in Section 4.7.1.

The folding gives the quiver shown in Figure 8. The balanced subset of nodes form the Dynkin diagram of F_4 and so we expect an F_4 global symmetry. The HS is computed using the monopole formula and we find

$$HS\left(t^2\right) = \frac{1+36t^2+341t^4+1208t^6+1820t^8+1208t^{10}+341t^{12}+36t^{14}+t^{16}}{\left(1-t^2\right)^{16}} \tag{113}$$

$$\begin{aligned} PL[HS] = {} & 52t^2 - 325t^4 + 4472t^6 - 77623t^8 + 1458976t^{10} - 28619435t^{12} \\ & + 577976256t^{14} - 11920099464t^{16} + 249764800064t^{18} - 5298923856304t^{20} + O\left(t^{21}\right) \end{aligned} \tag{114}$$

the HWG is computed from the refined HS (not shown here) to be

$$HWG = PE[\mu_1 t^2]. \tag{115}$$

The Coulomb branch is the $\overline{min.F_4}$.

The folding of the Dynkin diagram of E_6 maps the node labelled "6" to the node labelled "1" in the Dynkin diagram of F_4[3]. If the mapping of the highest weight fugacities $\nu_6 \to \mu_1$ is made, we recover the HWG for the minimal nilpotent orbit of F_4 from the minimal nilpotent orbit of E_6.

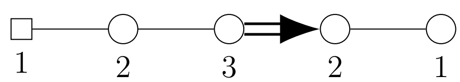

Figure 8: Magnetic quiver for $\overline{min.F_4}$.

[3]This is the opposite convention as Fig 5 of [26] but agrees with [75].

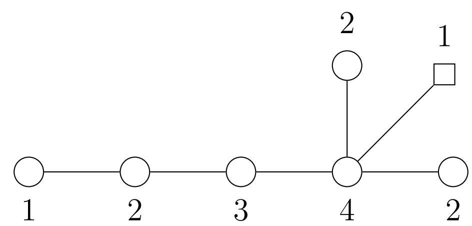

Figure 9: Magnetic quiver for $\overline{n.n.min.D_6}$

5.1.3 Folding $\overline{n.n.minD_6}$

The magnetic quiver for $\overline{n.n.minD_6}$ is given in Figure 9. The unrefined HS is computed to be

$$HS\left(t^2\right) = \frac{\left(1+t^2\right)^2 \begin{pmatrix} 1+36t^2+590t^4+4853t^6+21516t^8+52933t^{10}+71802t^{12} \\ +52933t^{14}+21516t^{16}+4853t^{18}+590t^{20}+36t^{22}+t^{24} \end{pmatrix}}{\left(1-t^2\right)^{28}} \tag{116}$$

$$PL[HS] = 66t^2 - 78t^4 - 847t^6 + 17523t^8 - 197637t^{10} + 1244671t^{12} + 4640647t^{14} - 268125726t^{16} + 4396067885t^{18} - 42966905025t^{20} + O\left(t^{21}\right). \tag{117}$$

The HWG is computed to be

$$HWG = PE[\nu_2 t^2 + \nu_4 t^4]. \tag{118}$$

The magnetic quiver for $\overline{n.n.minD_6}$ can be folded to give the magnetic quiver for $\overline{n.n.minB_5}$ shown in Figure 10. The unrefined HS is computed to be

$$HS\left(t^2\right) = \frac{\begin{pmatrix} 1+31t^2+430t^4+3013t^6+11508t^8+25288t^{10}+32802t^{12} \\ +25288t^{14}+11508t^{16}+3013t^{18}+430t^{20}+31t^{22}+t^{24} \end{pmatrix}}{\left(1-t^2\right)^{24}} \tag{119}$$

$$PL[HS] = 55t^2 - 66t^4 - 397t^6 + 8030t^8 - 83963t^{10} + 552783t^{12} - 525746t^{14} - 47910115t^{16} + 837259280t^{18} - 8626751474t^{20} + O\left(t^{21}\right) \tag{120}$$

and the HWG is computed to be

$$HWG = PE[\mu_2 t^2 + \mu_4 t^4], \tag{121}$$

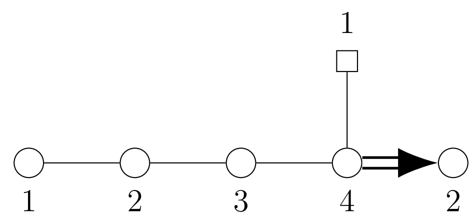

Figure 10: Magnetic quiver for $\overline{n.n.min.B_5}$.

the $\mathbb{Z}_2$ graph automorphism on the magnetic quiver for $\overline{n.n.minD_6}$ is also apparent here. The nodes labelled "5" and "6" of the D_6 Dynkin diagram are mapped to each other but the other nodes are invariant. As the HWG for $\overline{n.n.minD_6}$ did not involve $\nu_{5,6}$, the HWG of $\overline{n.n.min.B_5}$ is of the same form, but of course the highest weight fugacities $\mu_{2,4}$ are for B_5 and not D_6.

5.2 Discrete Gauging

We introduce the notion of a *bouquet* of gauge nodes, which is the attachment of multiple nodes with one bond to a common node. We consider *complete bouquets* which means that the nodes in the bouquet are all gauge nodes of $U(1)$. An example of a complete bouquet of n nodes of one attached to a node of k is given in Figure 13. It was conjectured in [82] that the Coulomb branch of a quiver, with a complete bouquet of n nodes of $U(1)$ attached to a node of k (assuming k is large enough that the node is good or ugly) called $Q_{\{1^n\}}$ is related to a quiver with a gauge node of n with an adjoint Hplet $Q_{\{n\}}$ by

$$\mathcal{C}(Q_{\{n\}}) = \mathcal{C}(Q_{\{1^n\}})/S_n. \tag{122}$$

This is because there is a S_n permutation symmetry between the $U(1)$ nodes in the bouquet which becomes an S_n global symmetry on the Coulomb branch. This discrete global symmetry can be gauged and is the Coulomb branch of $Q_{\{n\}}$ which can be checked using the monopole formula.

For quivers whose Coulomb branches are complete intersections, the Hilbert series can be written as the PE of a finite polynomial. Thus, one may use the Burnside lemma [83, 84], which gives us the number of orbits of a set under the action of a discrete finite group. In [26] it is shown how to compute the HWG of a discretely gauged Coulomb branch from the HWG of the original Coulomb branch. We start with a HWG that is a complete intersection and so the HWG can be written in the form

$$HWG[\mathcal{C}] = \frac{\prod_{k'=1}^{K'}(1 - M'_{k'})}{\prod_{k=1}^{K}(1 - M_k)} \tag{123}$$

where the $\{M_k\}$ is the set of all monomials (in terms of highest weight fugacities and t^2) that appear in the PE with positive coefficient (which is why they appear in the denominator) and the $\{M'_{k'}\}$ are the set of monomials which appear in the PE with negative coefficients (which is why they appear in the numerator). It was conjectured in [26] that the HWG of the Coulomb branch discretely gauged by Γ is

$$HWG(\mathcal{C}/\Gamma) = \frac{1}{|\Gamma|}\sum_{j=1}^{n} c_j \times \frac{\prod_{k'=1}^{K'}(1 - \lambda_{R',j}^{k'} M'_{k'})}{\prod_{k=1}^{K}(1 - \lambda_{R,j}^{k} M_k)} \tag{124}$$

where c_j is the number of elements in the j^{th} conjugacy class of Γ and $\lambda_{R,j}^k$ is a list of eigenvalues of the matrices forming the irrep R of Γ associated to the the conjugacy class j.

The idea behind discrete gauging is to take some HWG for a Coulomb branch with a global symmetry G and branch it to some subgroup G' of G and assign irreps of some discrete group to the terms in the branched HWG. The Burnside lemma formula, (124), computes the invariants under this discrete group. This discretely gauges the Coulomb branch. However, this procedure is dependent on the choice of subgroup G' and the discrete group Γ. For quivers with complete bouquets, the conjectured discretely gauged quiver's HS can be computed to see the resultant G' and the discrete group is clearly S_n for however many $U(1)$ in the bouquet were collected into the node with adjoint matter. We can also discretely gauge subgroups of the global symmetry for magnetic quivers without bouquets. If the moduli space of the Coulomb branch is known, the mathematics literature may provide inspiration for what to choose for the discrete gauging.

The Burnside lemma also gives another reason as to why HWGs are so useful, as the highest weight fugacities commute with the "charges" in finite groups. In general, the character fugacities do not commute with the "charges" and hence one must work with the HWG to discretely gauge the Coulomb branches here.

Kostant and Brylinski provided a classification of discretely gauged nilpotent orbits producing other nilpotent orbits [24]. Given the HWG for some nilpotent orbit, the Burnside lemma can be used to perform a discrete quotient and the resulting nilpotent can be identified. Then a quiver for the result can also be found. This was originally done in [26], where the notion of a *wreathed* quiver was introduced. Wreathing is an analogous procedure to folding where an automorphism on the quiver introduces a wreathed product of the legs under identification (whereas for folding a non-simply laced edge was introduced). A modification of the monopole formula was made for wreathed quivers which allowed for computations of the Coulomb branch HS.

A shortcoming of using the Burnside lemma is that the assignment of irreps of the discrete group is often guesswork and no algorithmic treatment exists. Nevertheless, it is often obvious how to assign the irreps and there are often very few possibilities to consider.

As we will deal with nilpotent orbits in this work, the HWG for the Coulomb branch are known and the resulting nilpotent orbits usually have known magnetic quivers. The approach with the Burnside lemma will be taken here instead of using wreathed quivers.

Finally, the action on the Coulomb branch under discrete gauging is to identify points in the moduli space under the discrete group. Unlike folding, points in the moduli space are not being excluded and so the dimension of the moduli space is preserved.

5.2.1 Discrete Gauging $\overline{min.A_3}$ by $\mathbb{Z}_2$

The third result of [24] says that

$$\overline{n.minC_2} = \overline{min.A_3}/\mathbb{Z}_2. \tag{125}$$

To apply the Burnside lemma, the branching rules of $A_3 \to C_2$ which can be implemented by the projection matrix [4]in [85],

$$P_{ij} = \begin{pmatrix} 1 & 0 \\ 0 & 1 \\ 1 & 0 \end{pmatrix} \tag{126}$$

is used to find the character fugacity map using

$$x'_i = \prod_{j=1}^{2} x_j^{\left(P^T\right)_{ji}} \tag{127}$$

as

$$x'_1 \to x_1, \quad x'_2 \to x_2, \quad x'_3 \to x_1 \tag{128}$$

[4]The projection matrix here gives a map between the character fugacities. This is different from the projection matrices in [75] which are used to decompose weight vectors of a representation of some algebra into weight vectors of some maximal subalgebra(s). The decompositions both give are the same, however.

from this the HWG in terms of C_2 highest weight fugacities is written as

$$HWG = PE[(\mu_1^2 + \mu_2)t^2]. \tag{129}$$

Using this we now identify each term in (124), $\Gamma = \mathbb{Z}_2$ so $|\Gamma| = 2$. The character table for $\mathbb{Z}_2$ is given in Table 1 so there are two conjugacy classes $\mathbf{1}$ and ε both of order one. The branched HWG has no terms in the numerator so the set $M'_{k'}$ is empty and the set $M_k = \{\mu_1^2 t^2, \mu_2 t^2\}$. Since $\mathbb{Z}_2$ is abelian it only has one dimensional representations and so the character table provides the eigenvalues of the elements of a characteristic for each conjugacy class for each irrep so $\lambda_1 = (1,1)$ and $\lambda_2 = (1,-1)$.

$\mathbb{Z}_2$	e	a
$\mathbf{1}$	1	1
ε	1	-1

Table 1: Character table for $\mathbb{Z}_2$

We can assign $\mathbb{Z}_2$ irreps as

$$\begin{aligned} PE[\mathbf{1}\mu_1^2 t^2 + \varepsilon \mu_2 t^2] \to & \frac{1}{2}\left(\frac{1}{1-\mu_1^2 t^2}\frac{1}{1-\mu_2 t^2} + \frac{1}{1-\mu_1^2 t^2}\frac{1}{1+\mu_2 t^2}\right) \\ &= \frac{1}{(1-\mu_1^2 t^2)(1-\mu_2^2 t^4)} \qquad (130) \\ &= PE[\mu_1^2 t^2 + \mu_2^2 t^4] \qquad (131) \end{aligned}$$

which we recognise as the HWG for $\overline{n.min.C_2}$. This agrees with the third result of [24].

5.2.2 Discrete Gauging $\overline{min.E_6}$ by $\mathbb{Z}_2$

We give an example of performing the discrete gauging, which agrees with the fourth result of [24],

$$\overline{n.minF_4} = \overline{minE_6}/\mathbb{Z}_2. \tag{132}$$

Recall the HWG for $\overline{min.E_6}$ is computed as (106). Now we need to write this HWG in terms of highest weight fugacities for F_4, to do this we must implement the branching rule from E_6 into F_4, this is done at the level of the Hilbert series through a fugacity map of the CSA

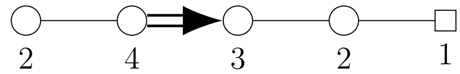

Figure 11: Magnetic quiver for $\overline{n.min.F_4}$.

coordinates. The projection matrix P ,

$$P_{ij} = \begin{pmatrix} 0 & 0 & 0 & 1 \\ 0 & 0 & 1 & 0 \\ 0 & 1 & 0 & 0 \\ 0 & 0 & 1 & 0 \\ 0 & 0 & 0 & 1 \\ 1 & 0 & 0 & 0 \end{pmatrix} \tag{133}$$

for this branching rule determines the fugacity map. The application of this map allows for the HWG for $\overline{min.E_6}$ to be branched to

$$PE[\nu_1 t^2] \rightarrow PE[(\mu_1 + \mu_4)t^2] \tag{134}$$

where the μ_i are highest weight fugacities for F_4. The irreps are assigned as

$$PE[\mathbf{1}\mu_1 t^2 + \varepsilon\mu_4 t^2] \rightarrow PE[\mu_1 t^2 + \mu_4^2 t^4], \tag{135}$$

which is recognised as the HWG for $\overline{n.min.F_4}$.

The quiver whose Coulomb branch gives the next to minimal nilpotent orbit of F_4 is given in Figure 11.

5.2.3 Discrete Gauging $\overline{n.n.minD_6}$ by $\mathbb{Z}_2$

The second result of [24] says

$$\overline{n.min.B_5} = \overline{min.D_6}/\mathbb{Z}_2, \tag{136}$$

this time we will not recover the result but use it as inspiration for performing another discrete gauging.

The HWG for the Coulomb branch of $\overline{n.n.min.D_6}$ is computed to be $PE[\nu_2 t^2 + \nu_4 t^4]$.

The branching rule of $D_6 \to B_5$ can be implemented using the fugacity map

$$y_{1,2,3,4} \to x_{1,2,3,4}, \quad y_{5,6} \to x_5, \tag{137}$$

which can be found using the projection matrix in [85]. The resultant HWG is

$$HWG = PE[(\mu_1 + \mu_2)\, t^2 + (\mu_3 + \mu_4)\, t^4]. \tag{138}$$

Finally, the $\mathbb{Z}_2$ irreps can be assigned as

$$PE[(\varepsilon\mu_1 + \mathbf{1}\mu_2)\, t^2 + (\varepsilon\mu_3 + \mathbf{1}\mu_4)\, t^4] \to PE[\mu_2 t^2 + \left(\mu_1^2 + \mu_4\right) t^4 + \mu_1\mu_3 t^6 + \mu_3^2 t^8 - \mu_1^2\mu_3^2 t^{12}] \tag{139}$$

this is the HWG for the orbit of B_5 with partition $\{3, 2^2, 1^4\}$. This orbit is of height 3 and so a magnetic quiver is not known.

5.2.4 Discrete Gauging $\overline{n.minF_4}$ by $\mathbb{Z}_2^2$

The eighth result of [24] says

$$\overline{\mathcal{O}}^{D_4}_{\{3,2^2,1\}} = \overline{min.F_4}/\mathbb{Z}_2^2. \tag{140}$$

The minimal nilpotent orbit of F_4 has $HWG = PE[\nu_1 t^2]$, then one may rewrite this in terms of D_4 highest weight fugacities through the branching rules $F_4 \to B_4 \to D_4$. Then we have

$$PE[\nu_1 t^2] \to PE[(\mu_1 + \mu_2 + \mu_3 + \mu_4)t^2] \tag{141}$$

in terms of D_4 highest weight fugacities.

Finally, to compute the discrete quotient we identify charges of $\mathbb{Z}_2 \times \mathbb{Z}_2$ as

$$PE[(\varepsilon\varepsilon'\mu_1 + \mathbf{1}\mathbf{1}'\mu_2 + \mathbf{1}\varepsilon'\mu_3 + \varepsilon\mathbf{1}'\mu_4)\, t^2] \to \frac{1}{4}\sum_{c=\pm 1}\sum_{d=\pm 1} \frac{1}{(1-cd\mu_1 t^2)(1-\mu_2 t^2)(1-d\mu_3 t^2)(1-c\mu_4 t^2)} \tag{142}$$

$$= \frac{1+\mu_1\mu_3\mu_4 t^6}{(1-\mu_1^2 t^4)(1-\mu_2 t^2)(1-\mu_3^2 t^4)(1-\mu_4^2 t^4)} \tag{143}$$

$$= \frac{1-\mu_1^2\mu_3^2\mu_4^2 t^{12}}{(1-\mu_1^2 t^4)(1-\mu_2 t^2)(1-\mu_3^2 t^4)(1-\mu_4^2 t^4)(1-\mu_1\mu_3\mu_4 t^6)} \tag{144}$$

$$= PE[\mu_2 t^2 + (\mu_1^2+\mu_3^2+\mu_4^2)t^4 + \mu_1\mu_3\mu_4 t^6 - \mu_1^2\mu_3^2\mu_4^2 t^{12}] \tag{145}$$

this is the HWG of the nilpotent orbit of D_4 with partition $\{3, 2^2, 1\}$.

This orbit is of height 3 and no magnetic quiver is known.

5.2.5 Discrete Gauging $\overline{min.D_4}$ by S_4

The magnetic quiver for the $\overline{min.D_4}$ is shown in Figure 14a. Using the monopole formula we compute the HS for the Coulomb branch, giving first the unrefined HS, then the highest weight generating function,

$$HS\left(t^2\right) = \frac{(1+t^2)\left(1+17t^2+48t^4+17t^6+t^8\right)}{(1-t^2)^{10}} \tag{146}$$

$$\begin{aligned} PL[HS] = {} & 28t^2 - 106t^4 + 833t^6 - 8400t^8 + 91392t^{10} - 1031905t^{12} + 11978880t^{14} \\ & - 142013760t^{16} + 1710477440t^{18} - 20858793984t^{20} + O\left(t^{21}\right) \end{aligned} \tag{147}$$

and finally we have the highest weight generating function

$$HWG = PE[\nu_2 t^2], \tag{148}$$

where ν_2 is a highest weight fugacity for D_4.

The conjectured quiver whose Coulomb branch is that of the previous but discretely gauged by S_4 is shown in Figure 14b. We cannot read off the global symmetry directly as this would give us two nodes connected by a quadruple bond, which is not of Dynkin type. Thus, we must compute the unrefined HS to give us a clue as to what the global symmetry

Irrep	()	(12)	(12)(34)	(123)	(1234)
$\mathbf{1}$	1	1	1	1	1
ε	1	-1	1	1	-1
$\mathbf{2}$	$\{1,1\}$	$\{1,-1\}$	$\{1,1\}$	$\{-\omega,-\omega^{-1}\}$	$\{1,-1\}$
$\mathbf{3}$	$\{1,1,1\}$	$\{1,1,-1\}$	$\{1,-1,-1\}$	$\{1,-\omega,-\omega^{-1}\}$	$\{-1,i,-i\}$
$\bar{3}$	$\{1,1,1\}$	$\{1,-1,-1\}$	$\{1,-1,-1\}$	$\{1,-\omega,-\omega^{-1}\}$	$\{1,i,-i\}$

Figure 12: Character table for S_4 with eigenvalues of matrix representations. We use notation $\omega = e^{i\pi/3}$.

of the Coulomb branch is. Doing this we find that the unrefined Hilbert series is

$$HS\left(t^2\right) = \frac{1+3t^2+13t^4+25t^6+46t^8+48t^{10}+46t^{12}+25t^{14}+13t^{16}+3t^{18}+t^{20}}{\left(1-t^2\right)^{10}\left(1+t^2\right)^5} \tag{149}$$

$$PL[HS] = 8t^2+12t^4-6t^6-21t^8+14t^{10}+63t^{12}-71t^{14}-266t^{16}+412t^{18}+1211t^{20}+O\left(t^{21}\right) \tag{150}$$

the perturbative expansion has a coefficient of 8 for the t^2, this is the dimension of the adjoint of A_2 and so tells us that the Coulomb branch has an A_2 global symmetry.

So we now rewrite the HWG for the Coulomb branch of the affine D_4 quiver in terms of A_2 highest weight fugacities which is given by

$$HWG = PE[(3\mu_1+3\mu_2+\mu_1\mu_2+2)t^2-2\mu_1\mu_2t^4] \tag{151}$$

and now proceed with the discrete gauging formula. We assign the irreps of S_4 to the various terms in the HWG and charge the terms appropriately using the eigenvalues of the matrices in each conjugacy class for the assigned irrep. The eigenvalues are given in Table 12, with the assignment of the charges as

$$PE[(\mathbf{3}\mu_1+\mathbf{3}\mu_2+\mathbf{2}+\mathbf{1}\mu_1\mu_2)t^2-\mathbf{2}\mu_1\mu_2t^4] \tag{152}$$

$$\hookrightarrow PE[\mu_1\mu_2t^2+\left(\mu_1^2+\mu_1\mu_2+\mu_2^2+1\right)t^4+\left(\mu_1^3+\mu_1^2\mu_2+\mu_1^2+\mu_1\mu_2^2+\mu_2^3+\mu_2^2+1\right)t^6$$
$$+\left(\mu_1^4+\mu_1^2\mu_2+\mu_1^2+\mu_1\mu_2^2+\mu_2^4+\mu_2^2\right)t^8+\left(\mu_1^4-\mu_1^3\mu_2^2-\mu_1^2\mu_2^3+\mu_1^2\mu_2+\mu_1\mu_2^2+\mu_2^4\right)t^{10}+O\left(t^{11}\right)] \tag{153}$$

where we do not present the closed form HWG for brevity.

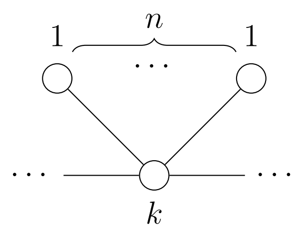

Figure 13: An example of a complete bouquet attached to a node of k on a quiver.

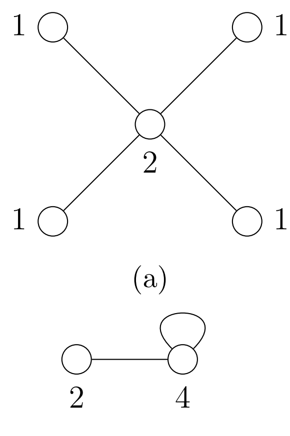

Figure 14: (a) Magnetic quiver for $\overline{min.D_4}$. (b) The quiver whose Coulomb branch is that of the nilpotent orbit of D_4 discretely gauged by S_4.

5.3 Quiver Subtraction

The Kraft-Procesi transition and transverse slices had already been studied in the context of type IIB string theory [27], quiver subtraction [19] is a natural procedure done on quivers to make this apparent. The process of quiver subtraction for unitary quivers is rather simple. The original paper [19] describes this process only when the quiver being subtracted has the same number of gauge nodes as the original. The quivers considered there could be framed. However, a more general subtraction process for unframed quivers is detailed in Appendix A of [80]. Furthermore, we will perform quiver subtraction only once at a time on an unframed quiver in later sections, which simplifies the algorithm for our purposes, which we present.

Consider two quivers Q and Q' such that the gauge nodes of Q' forms a connected subgraph of Q. Then choose an alignment of Q' against Q, this is to determine where the subtraction of Q' will occur on Q. Ensure that the ranks of the gauge groups in Q' are less than or equal to the corresponding gauge node in Q and similarly ensure that flavour nodes are aligned (if present) and that the rank of the flavour node of Q is greater than that of Q'. Then the quiver subtraction process is:

- Subtract the rank of the gauge nodes of Q' from Q in the corresponding positions of the chosen alignment. Then do the same for the flavour nodes.
- If a node in Q has changed its balance, restore this balance by adding the appropriate number of flavours to that node.

Examples of this will be given in Section 6.

6 Hyper-Kähler Quotients

Another option for taking quotients of moduli spaces is to use continuous groups. There are a great deal of possible moduli spaces with various global symmetries each with many different subgroups. The number of possible quotients one can study are clearly large. A sensible restriction we can make is to start with nilpotent orbits and take quotients by $SU(n)$ starting with $n = 2$ and going up. Another restriction we make is to consider only the moduli spaces which are also nilpotent orbits upon doing the quotient. There is a general result which says the nilpotent orbits are hyper-Kähler quotients (HKQ) of some other space. Some examples for low-dimensional groups also have nilpotent orbits that are HKQs of other nilpotent orbits [47]. These low rank results will not be studied here, instead we look at nilpotent orbits of exceptional algebras.

Now we detail how to construct a HKQ. Firstly, we may compute the HS for the starting moduli space from the monopole formula or from the nilpotent orbit normalisation formula (if the starting orbit is normal). Since we have restricted to looking for HKQs that give nilpotent orbits, given the global symmetry G of the original moduli space, we must look for embeddings of the form $G' \times SU(n) \subset G$ which can be found in [75]. The branching rule is then applied to the HS. The HKQ then proceeds as the Molien-Weyl integral

$$HS_{G/SU(n)} = \int_{SU(n)} d\mu_{SU(n)} \frac{HS_G}{PE[\chi([1, 0, \cdots, 0, 1])t^2]} \tag{154}$$

where we integrate over the character fugacities of the adjoint of $SU(n)$ [78]. Scalars in the adjoint of $SU(n)$ are being projected out in this process which is exactly what is desired in the HKQ.

As seen in the formula for the HKQ, the resulting moduli space will be of lower quaternionic dimension by the dimension of the adjoint representation of $SU(n)$ than we started with. This imposes a selection of the starting moduli space for a given HKQ, as the dimension of the result will be known.

6.1 $SU(2)$ Hyper-Kähler Quotients

We make explicit the form of (154) for the case of HK quotienting by $SU(2)$. The character for the adjoint representation of $SU(2)$ can be computed from the Weyl character formula and gives $\chi([2]) = y^2 + 1 + y^{-2}$. Thus, we have

$$PE[\chi\left([2]\right) t^2] = \frac{1}{\left(1-y^2t^2\right)\left(1-t^2\right)\left(1-t^2/y^2\right)}. \tag{155}$$

The final part is the Haar measure for which we use (24), $SU(2)$ has only one positive root and the Cartan matrix is $A_{SU(2)} = (2)$ and so the form of the Haar measure is

$$\int_{SU(2)} d\mu_{SU(2)} = \oint_{|y|} \frac{dy}{2\pi i} \frac{1-y^2}{y}, \tag{156}$$

putting this together, the explicit form of the HK quotient is

$$HS_{G/SU(2)}(t, x_i) = \oint_{|y|=1} \frac{dy}{2\pi i} \frac{1-y^2}{y} \left(1-y^2t^2\right)\left(1-t^2\right)\left(1-t^2/y^2\right) HS_G(t, x_i, y) \tag{157}$$

6.1.1 F_4

The magnetic quiver for $\overline{min.F_4}$ is given in Figure 8. The unrefined HS is again given by

$$HS\left(t^2\right) = \frac{1+36t^2+341t^4+1208t^6+1820t^8+1208t^{10}+341t^{12}+36t^{14}+t^{16}}{\left(1-t^2\right)^{16}} \tag{158}$$

the HWG in terms of the highest weight fugacities for F_4 is

$$HWG = PE[\mu_1 t^2]. \tag{159}$$

The minimal nilpotent of F_4 has dimension 8 and so we must look for subalgebras of F_4 which have nilpotent orbits of dimension 5. There are three such cases which are summarised in Table 2 [5].

The next to minimal nilpotent orbit of F_4 has dimension 11 and so we look for subalgebras which have nilpotent orbits of dimension 8. There is only one such case $A_1 \times C_3 \subset F_4$ however this computation fails.

The higher dimensional orbits have too high of a dimension to give a nilpotent orbit of some subalgebra after performing the $SU(2)$ HK quotient and so we stop.

[5] The HKQ using the embedding of $C_3 \times A_1$ was first computed by Rudolph Kalveks, Imperial College London.

Subgroup	26_{F_4}	HWG	Moduli Space
$A_3 \times A_1$	$(4,2)+(4',2)+(6,1)+(1,3)+(1,1)$	$PE[\mu_1\mu_3 t^2 + (\mu_2^2+\mu_1\mu_3)t^4 + \mu_2(\mu_1^2+\mu_3^2)t^6 - \mu_1^2\mu_2^2\mu_3^2 t^{12}]$	$\overline{sub.reg.A_3}$
$C_3 \times A_1$	$(6,2)+(14,1)$	$PE[\mu_1 t^2 + \mu_2^2 t^4]$	$\overline{n.minC_3}$
$G_2 \times A_1$	$(7,3)+(1,5)$	$PE[\mu_1 t^2 + \mu_2^2 t^4 + \mu_2^3 t^6 + \mu_1^2 t^8 + \mu_1\mu_2^3 t^{10} - \mu_1^2\mu_2^6 t^{20}]$	$\overline{sub.reg.G_2}$

Unrefined Series	Magnetic Quiver	Height
$\frac{(1+t^2)(1+4t^2+10t^4+4t^6+t^8)}{(1-t^2)^{10}}$	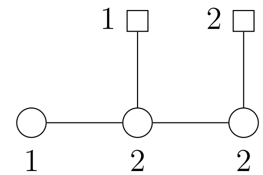	4
$\frac{(1+t^2)(1+10t^2+41t^4+10t^6+t^8)}{(1-t^2)^{10}}$	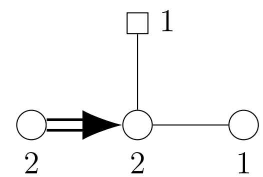	1
$\frac{(1+t^2)(1+3t^2+6t^4+3t^6+t^8)}{(1-t^2)^{10}}$	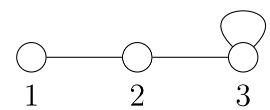	4

Table 2: Table of the embeddings of the **26** of F_4 into the respective subgroups. The HWG once the $SU(2)$ HKQ is done is shown as well as the resulting moduli space, unrefined HS, height of the orbit, and magnetic quiver.

6.1.2 E_6

We repeat the above analysis for the minimal nilpotent orbit of E_6. The quiver whose Coulomb branch gives the minimal nilpotent orbit of E_6 is given in Figure 4. The unrefined HS is given by

$$HS\left(t^2\right) = \frac{(1+t^2)\begin{pmatrix}1+55t^2+890t^4+5886t^6+17929t^8+26060t^{10}\\ +17929t^{12}+5886t^{14}+890t^{16}+55t^{18}+t^{20}\end{pmatrix}}{(1-t^2)^{22}}. \tag{160}$$

The HWG in terms of the highest weight fugacities for E_6 is

$$HWG = PE[\mu_6 t^2]. \tag{161}$$

The minimal nilpotent orbit of E_6 is of dimension 11 and so we look for subalgebras with nilpotent orbits of dimension 8. There are two cases to consider $A_1 \times A_5$ and $A_1 \times C_3 \subset E_6$. It turns out that only the embedding of A_5 gives a unique nilpotent orbit. As $C_3 \subset A_5$ the embedding of C_3 recovers the result of the embedding with A_5, except with the branching rule of $A_5 \to C_3$. The results are shown in Table 3.

The next to minimal nilpotent orbit of E_6 is of dimension 16 and so the only relevant embedding is of $A_1 \times A_5 \subset E_6$, however this fails.

No other higher dimension orbit of E_6 will give a nilpotent orbit after $SU(2)$ hyper-Kähler quotient.

Subgroup	27_{E_6}	HWG	Moduli Space
$A_5 \times A_1$	$(15,1)+(\bar{6},2)$	$PE[\mu_1\mu_5 t^2 + \mu_2\mu_4 t^4]$	$\overline{n.minA_5}$

Unrefined Series	Magnetic Quiver	Height
$\frac{(1+t^2)^2(1+17t^2+119t^4+251t^6+119t^8+17t^{10}+t^{12})}{(1-t^2)^{16}}$	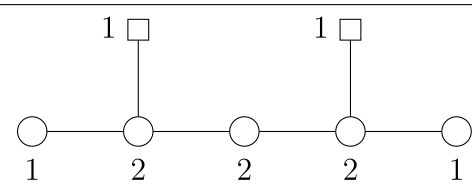	2

Table 3: Table of the embeddings of the **27** of E_6 into the respective subgroups. The HWG once the $SU(2)$ HKQ is done is shown as well as the resulting moduli space, unrefined HS, height of the orbit, and magnetic quiver.

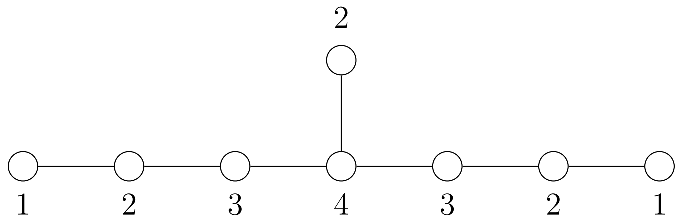

Figure 15: Magnetic quiver for $\overline{min.E_7}$.

6.1.3 E_7

The quiver whose Coulomb branch gives the nilpotent orbit of E_7 is given in Figure 15. The unrefined HS is given by

$$HS\left(t^2\right) = \frac{(1+t^2)\begin{pmatrix}1+98t^2+3312t^4+53305t^6+468612t^8+2421286t^{10}+7664780t^{12}\\ +15203076t^{14}+19086400t^{16}+15203076t^{18}+7664780t^{20}+2421286t^{22}\\ +468612t^{24}+53305t^{26}+3312t^{28}+98t^{30}+t^{32}\end{pmatrix}}{\left(1-t^2\right)^{34}} \tag{162}$$

$$\begin{aligned}PL[HS] = {} & 133t^2 - 1540t^4 + 42427t^6 - 1489961t^8 + 57501752t^{10} - 2335315080t^{12} + 97950208356t^{14} \\ & - 4200649168099t^{16} + 183122659795824t^{18} - 8084865388756002t^{20} + O\left(t^{21}\right)\end{aligned} \tag{163}$$

The HWG is given by

$$HWG = PE[\mu_1 t^2]. \tag{164}$$

The minimal nilpotent orbit of E_7 is of dimension 17 and so the relevant algebras must have a nilpotent orbit of dimension 14. The relevant embeddings are $A_1 \times D_6$, $A_1 \times A_5$, $A_1 \times F_4$, $A_1 \times B_5$. However, the embedding of A_5 fails, and since $B_5 \subset D_6$, we just recover the result for D_6 with the branching rule of $D_6 \to B_5$ which importantly is applied before the HKQ. If the $D_6 \to B_5$ embedding is applied after the HKQ, one could perform an $\mathbb{Z}_2$ quotient or folding as is done in Section 5. These are summarised in Table 4.

It is possible that these embeddings can be used to get nilpotent orbits from higher dimensional orbits of E_7. However, these all fail.

Subgroup	56_{E_7}	HWG	Moduli Space	Height
$D_6 \times A_1$	$(12,2)+(\bar{32},1)$	$PE[\mu_2 t^2 + \mu_4 t^4]$	$\overline{n.n.minD_6}$	2
$F_4 \times A_1$	$(26,2)+(1,4)$	$PE[\mu_1 t^2 + \mu_4^2 t^4 + \mu_2 t^6 + \mu_3^2 t^8]$	$\overline{n.n.minF_4}$	3

Unrefined HS	Magnetic Quiver
$\frac{\left(1+t^2\right)^2 \begin{pmatrix} 1+36t^2+590t^4+4853t^6+21516t^8 \\ +52933t^{10}+71802t^{12}+52933t^{14}+21516t^{16} \\ +4853t^{18}+590t^{20}+36t^{22}+t^{24} \end{pmatrix}}{\left(1-t^2\right)^{28}}$	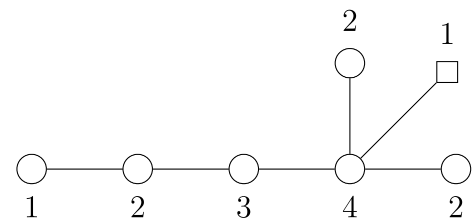
$\frac{\left(1+t^2\right)^2 \begin{pmatrix} 1+22t^2+254t^4+1773t^6+7171t^8 \\ +16619t^{10}+22030t^{12}+16619t^{14}+7171t^{16} \\ +1773t^{18}+254t^{20}+22t^{22}+t^{24} \end{pmatrix}}{\left(1-t^2\right)^{28}}$	Not known

Table 4: Table of the embeddings of the **56** of E_7 into the respective subgroups. The HWG once the $SU(2)$ HKQ is done is shown as well as the resulting moduli space, unrefined HS, height of the orbit, and magnetic quiver (if known).

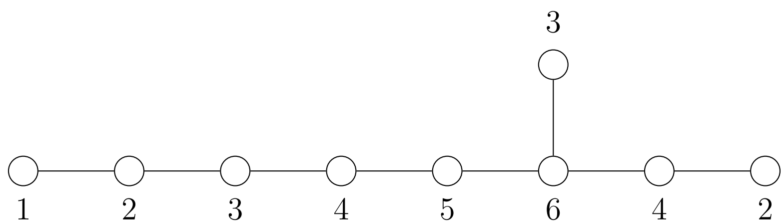

Figure 16: Magnetic quiver for $\overline{min.E_8}$.

6.1.4 E_8

The quiver whose Coulomb branch gives the nilpotent orbit of E_8 is given in Figure 16. The unrefined HS is given by

$$HS\left(t^2\right) = \frac{(1+t^2)\begin{pmatrix}1+189t^2+14080t^4+562133t^6+13722599t^8+220731150t^{10}\\ +2454952400t^{12}+19517762786t^{14}+113608689871t^{16}\\ +492718282457t^{18}+1612836871168t^{20}+4022154098447t^{22}\\ +7692605013883t^{24}+11332578013712t^{26}\\ +12891341012848t^{28}+11332578013712t^{30}+7692605013883t^{32}\\ +4022154098447t^{34}+1612836871168t^{36}+492718282457t^{38}\\ +113608689871t^{40}+19517762786t^{42}+2454952400t^{44}\\ +220731150t^{46}+13722599t^{48}+562133t^{50}+14080t^{52}+189t^{54}+t^{56}\end{pmatrix}}{(1-t^2)^{58}} \tag{165}$$

$$\begin{aligned}PL[HS] = {} & 248t^2 - 3876t^4 + 151373t^6 - 7687628t^8 + 435398224t^{10} - 26165259499t^{12}\\ & + 1630958592252t^{14} - 104187415680490t^{16} + 6773833458472024t^{18}\\ & - 446310851509994404t^{20} + O\left(t^{21}\right)\end{aligned} \tag{166}$$

The HWG is given by

$$HWG = PE[\mu_1 t^2]. \tag{167}$$

The minimal nilpotent orbit of E_8 is of dimension 29 and so the embeddings we consider are $A_1 \times E_7, A_1 \times B_6, A_1 \times E_6 \subset E_8$ which have orbits of dimension 26. These results have been verified at the level of the unrefined HS and so the HWG in Table 5 is a conjecture at this point. The magnetic quiver is also a conjecture, however the unrefined series of the Coulomb branch of this quiver matches that which is found.

Subgroup	248_{E_7}	HWG	Moduli Space	Height
$E_7 \times A_1$	$(56,2)+(133,1)+(1,3)$	$PE[\mu_2 t^2 + \mu_4 t^4]$	$\overline{n.minE_7}$	2

Unrefined HS
$\frac{\left(1+t^2\right)^2 \left(\begin{array}{l} 1+79t^2+3161t^4+75291t^6+1158376t^8+12099785t^{10}+88650725t^{12}+465895118t^{14} \\ +1783653576t^{16}+5026645901t^{18}+10497603729t^{20}+16309233956t^{22}+18885794304t^{24} \\ +16309233956t^{26}+10497603729t^{28}+5026645901t^{30}+1783653576t^{32}+465895118t^{34} \\ +88650725t^{36}+12099785t^{38}+1158376t^{40}+75291t^{42}+3161t^{44}+79t^{46}+t^{48} \end{array}\right)}{\left(1-t^2\right)^{52}}$

Magnetic Quiver
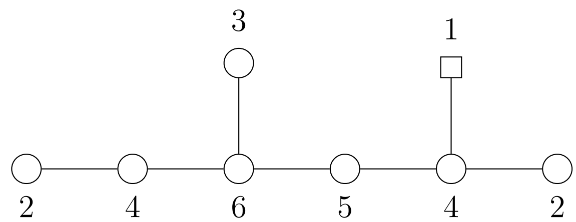

Table 5: Table of the embeddings of the **248** of E_8 into the respective subgroups. The HWG once the $SU(2)$ HKQ is done is shown as well as the resulting moduli space, unrefined HS, height of the orbit, and magnetic quiver.

6.1.5 G_2

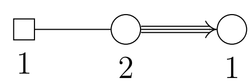

Figure 17: Magnetic quiver for $\overline{min.G_2}$.

The HK quotients of the orbits of G_2 is presented last as there is an unexpected result which does not follow the general pattern. The quiver whose Coulomb branch is the minimal nilpotent orbit of G_2 is given in Figure 17. The unrefined HS for the minimal nilpotent orbit of G_2 is

$$HS\left(t^2\right) = \frac{\left(1+t^2\right)\left(1+7t^2+t^4\right)}{\left(1-t^2\right)^6} \tag{168}$$

$$PL[HS] = 14t^2 - 28t^4 + 105t^6 - 540t^8 + 3024t^{10} - 17325t^{12} + 101520t^{14} - 608580t^{16} + 3709440t^{18} - 22884120t^{20} + O\left(t^{21}\right), \tag{169}$$

the HWG for the minimal nilpotent orbit of G_2 (computed from the refined series is)

$$HWG = PE[\mu_1 t^2]. \tag{170}$$

We present the table of embeddings of $SU(2)$ into G_2 and the corresponding HK quotients in Table 6. To be clear, the table shows the result when the second $SU(2)$ has been quotiented out. The minimal nilpotent orbit of G_2 is of dimension three, the $SU(2)$ HK quotient should

Subgroup	7_{G_2}	HWG	Moduli Space	Unrefined Series	Magnetic Quiver	Height
$A_1 \times A_1$	$(2,2)+(1,3)$	$PE[\mu^2 t^2]$	$\overline{minA_1}$	$\frac{(1-t^4)}{(1-t^2)^3}$	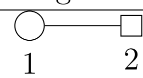	2

Table 6: Table of the embeddings of the **7** of G_2 into the respective subgroups. The HWG once the second $SU(2)$ HKQ is done is shown as well as the resulting moduli space, unrefined HS, height of the orbit, and magnetic quiver.

reduce the dimension by three to zero, however we find a moduli space of dimension one. This is highly unexpected!

If one quotients out by the first $SU(2)$ then indeed a zero dimensional moduli space is found, however this is not a nilpotent orbit.

6.1.6 Comments on $SU(2)$ HKQs

There is a very clear quiver subtraction one can make on the starting magnetic quivers to reproduce the magnetic quivers of the HK quotients in some cases.

First start with the magnetic quiver for the minimal nilpotent orbit of F_4 given in Figure 8. We will gauge the flavour node of one back into a gauge node. Then if the subtraction of $(1)-(2)-(1)$ is done on the long side, we find the $\overline{n.minC_3}$ as shown in Figure 18. Subtraction on the short side of $\overline{minF_4}$ can be done using $(1) => (2)-(1)$ to deal with the non-simply laced edge to produce the $\overline{n.minA_3}$ as shown in Figure 19. The other nilpotent orbits of exceptional algebras (except G_2) are all simply laced. Subtraction of $(1)-(2)-(1)$ from a leg with $(1)-(2)-\cdots$ will also produce the magnetic quiver for the result of the HKQ in some cases. Explicitly, this can be seen for $\overline{n.minA_5}$ from $\overline{min.E_6}$, $\overline{n.n.min.D_6}$ from $\overline{min.E_7}$ and $\overline{min.E_7}$ from $\overline{min.E_8}$.

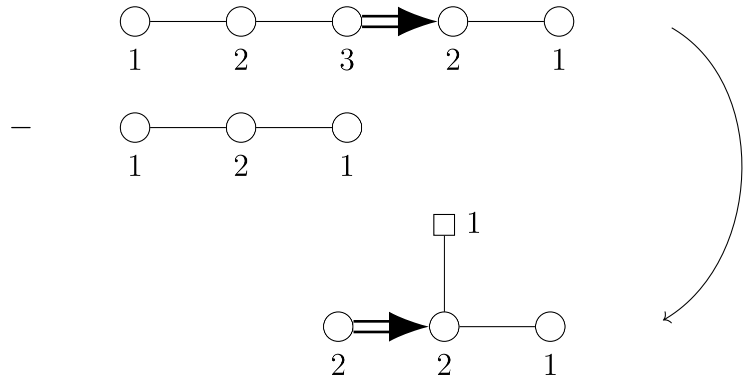

Figure 18: Quiver subtraction scheme shown on the magnetic quiver for $\overline{min.F_4}$ to produce the magnetic quiver for $\overline{n.minC_3}$.

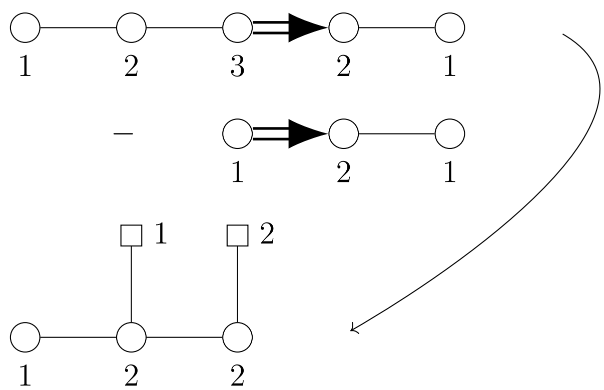

Figure 19: Quiver subtraction scheme shown on the magnetic quiver for $\overline{min.F_4}$ to produce the magnetic quiver for $\overline{n.minA_3}$.

6.2 $SU(3)$ Hyper-Kähler Quotients

To perform the $SU(3)$ HK quotients one may use (154) for $SU(3)$.

The character of the adjoint of $SU(3)$ is $\chi([1,1]) = 2 + y_1/y_2^2 + 1/y_1y_2 + y_1^2/y_2 + y_2/y_1^2 + y_1y_2 + y_2^2/y_1$ and so

$$PE[\chi([1,1])\, t^2] = \frac{1}{\begin{pmatrix} (1-t^2)^2 (1-y_1t^2/y_2^2)(1-t^2/y_1y_2)(1-y_1^2t^2/y_2) \\ \times (1-y_2t^2/y_1^2)(1-y_1y_2t^2)(1-y_2^2t^2/y_1) \end{pmatrix}}, \tag{171}$$

finally for the Haar measure we use (24). The Dynkin diagram of $SU(3)$ tells us that there are two fundamental roots $\alpha_{1,2}$ and Weyl reflections give us the full root space. From this, we see there are three positive roots of $SU(3)$ $\alpha_1, \alpha_2, \alpha_1 + \alpha_2$. The Cartan matrix of $SU(3)$ may also be found from the Dynkin diagram of $SU(3)$. Using this the Haar measure is found to be

$$\int_{SU(3)} d\mu_{SU(3)} = \oint_{|y_1|=1} \frac{dy_1}{2\pi i} \oint_{|y_2|=1} \frac{dy_2}{2\pi i} \left(1 - y_1^2/y_2\right)(1 - y_1y_2)\left(1 - y_2^2/y_1\right) \tag{172}$$

These can be put together to give the formula for the HKQ by $SU(3)$ which we will not present.

There are no valid embeddings of $SU(3)$ into G_2 and so we will not consider this. Although there are valid embeddings and orbits of $SU(3)$ into F_4 and E_6 these failed.

There are two cases we consider. The first is the minimal nilpotent orbit of E_8 and the second, more interesting case, is the minimal nilpotent orbit of E_7.

6.2.1 $\overline{min.E_8}//SU(3)$

The results, which have also recently appeared in [86], are summarised in Table 7. Furthermore there is also a valid quiver subtraction algorithm which reproduces the double cover of the 21 dimensional orbit of E_6 which is shown in Figure 20.

Subgroup	248_{E_8}	HWG	Moduli Space
$E_6 \times A_2$	$(78,1)+(27',3)+(27,\bar{3})+(1,8)$	$PE[\mu_6 t^2 + (\mu_1\mu_5 + \mu_6)t^4 + 2\mu_3 t^6 + \mu_2\mu_4 t^8]$	$\mathbb{Z}_2$ cover of 21 dim E_6

Unrefined HS	Magnetic Quiver	Height
$\frac{\left(1+t^2\right)^2(1+35t^2+708t^4+9121t^6+78994t^8+472618t^{10}+\cdots+24858218t^{20}+palindrome)}{(1-t^2)^{42}}$	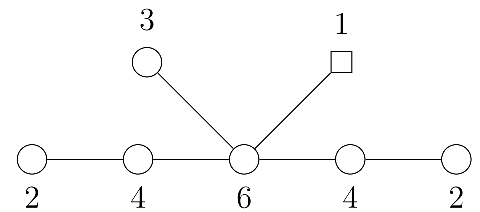	2

Table 7: Table of the embeddings of the **248** of E_8 into the respective subgroups. The HWG once the $SU(3)$ HKQ is done is shown as well as the resulting moduli space, unrefined HS, height of the orbit, and magnetic quiver.

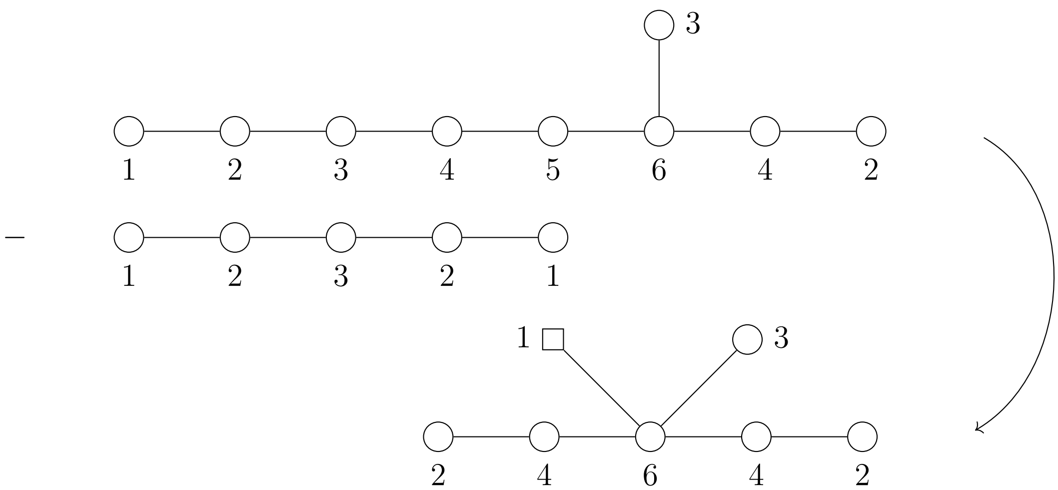

Figure 20: Quiver subtraction on the magnetic quiver of $\overline{minE_8}$ by $(1)-(2)-(3)-(2)-(1)$ to produce the magnetic quiver for $\overline{minE_7}$.

It is easily shown at the level of the unrefined series that the moduli space found is the double cover of the 21 dimensional nilpotent orbit of E_6. If one considers the assignment of the $\mathbb{Z}_2$ charges on the HWG for the 21 dimensional orbit of E_6,

$$PE[\mathbf{1}\mu_6 t^2 + (\mathbf{1}\mu_1\mu_5 + \varepsilon\mu_6)t^4 + \mathbf{1}\mu_3 t^6 + \varepsilon\mu_3 t^6 + \mathbf{1}\mu_2\mu_4 t^8] \to PE\begin{bmatrix}\mu_6 t^2 + \mu_1\mu_5 t^4 + \mu_3 t^6 + \left(\mu_2\mu_4 + \mu_6^2\right) t^8 \\ + \mu_3\mu_6 t^{10} + \mu_3^2 t^{12} - \mu_3\mu_6 t^{20}\end{bmatrix} \tag{173}$$

this HWG will produce the unrefined HS for the 21 dimensional orbit of E_6.

6.2.2 $\overline{min.E_7}//SU(3)$

This is a more interesting case, although results so far at the level of the unrefined HS. There is an embedding of $E_7 \to A_5 \times A_2$ which decomposes the adjoint of E_7 in the following way,

$$(133) \to (35, 1) + (15, \bar{3}) + (\bar{15}, 3) + (1, 8). \tag{174}$$

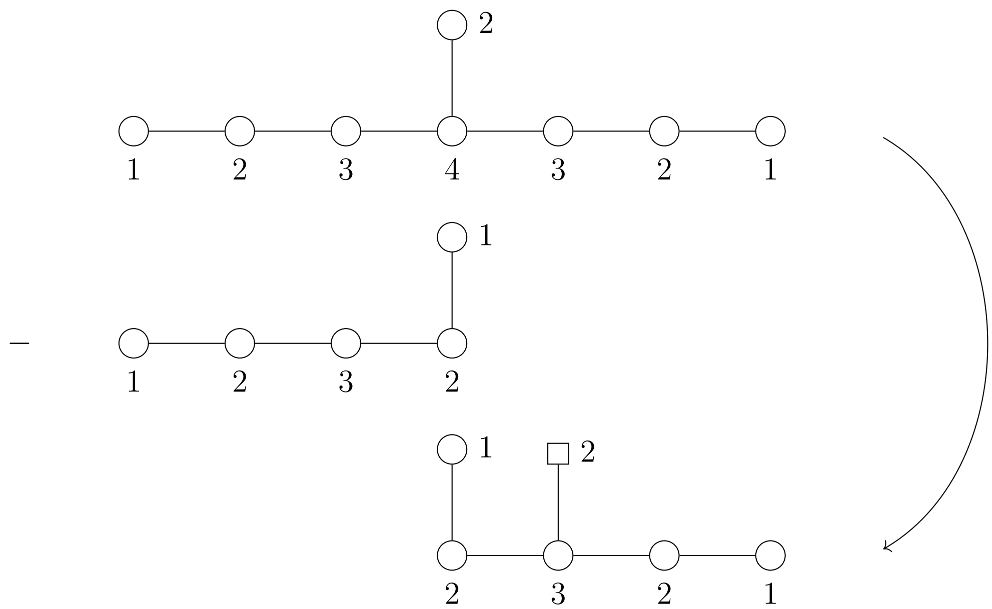

Figure 21: Quiver subtraction on the magnetic quiver for $\overline{min.E_7}$ to produce quiver Q_1.

The following calculations were computed at the level of the unrefined HS. Using the embedding the $SU(3)$ HKQ is computed and the unrefined series is found to be

$$HS_{HKQ} = \frac{1+17t^2+152t^4+727t^6+1861t^8+2211t^{10}+1062t^{12}+52t^{14}-83t^{16}-15t^{18}-t^{20}}{\left(1-t^2\right)^{18}} \tag{175}$$

$$PL[HS_{HKQ}] = 35t^2 - t^4 - 225t^6 + 994t^8 + 133t^{10} - 33055t^{12} + 221625t^{14} - 327110t^{16} - 6235566t^{18} + 58795900t^{20} + O\left(t^{21}\right). \tag{176}$$

We can see if quiver subtraction can tell us something. There are two possible alignments of $(1)-(2)-(3)-(2)-(1)$ to perform the subtraction from. The quivers they produce, Q_1 and Q_2, are shown in Figure 21 and Figure 22 respectively. The HS for the Coulomb branches of Q_1 and Q_2 can be computed using the monopole formula and we find

$$HS_{Q_1} = \frac{\left(1+t^2\right)^3\left(1+14t^2+72t^4+133t^6+72t^8+14t^{10}+t^{12}\right)}{\left(1-t^2\right)^{18}} \tag{177}$$

$$PL[HS_{Q_1}] = 35t^2 - 36t^4 + 35t^6 + 139t^8 - 1932t^{10} + 14405t^{12} - 84450t^{14} + 411705t^{16} - 1596805t^{18} + 3655596t^{20} + O\left(t^{21}\right). \tag{178}$$

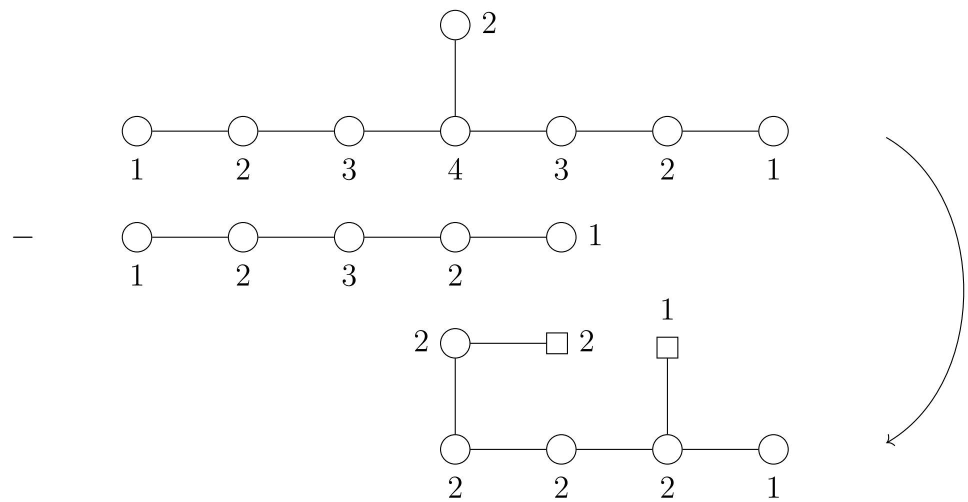

Figure 22: Quiver subtraction on the magnetic quiver for $\overline{min.E_7}$ to produce quiver Q_2.

and

$$HS_{Q_2} = \frac{1 + 17t^2 + 152t^4 + 552t^6 + 1042t^8 + 1042t^{10} + 552t^{12} + 152t^{14} + 17t^{16} + t^{18}}{(1-t^2)^{18}} \tag{179}$$

$$\begin{aligned} PL[HS_{Q_2}] = {} & 35t^2 - t^4 - 400t^6 + 3150t^8 - 11088t^{10} - 58520t^{12} + 1236960t^{14} - 9373770t^{16} \\ & + 22024464t^{18} + 366536520t^{20} + O\left(t^{21}\right). \end{aligned} \tag{180}$$

What we find is that Q_1 is the magnetic quiver for the 9-dimensional nilpotent orbit of $SU(6)$ with partition $\{2^3\}$ and that Q_2 is the magnetic quiver for the 9-dimensional nilpotent orbit of $SU(6)$ with partition $\{3, 1^3\}$.

A conjecture as to what moduli space the HKQ is, is that it is either the union or intersection of the Coulomb branches of Q_1 and Q_2. Before computation, we suspect that the HKQ is not the intersection as these moduli spaces tend to be of lower dimension than either Q_1 or Q_2's Coulomb branch. It is more likely that the HKQ is the union of the two Coulomb branches.

From basic set theory we have

$$\mathcal{C}\left(Q_1 \cup Q_2\right) = \mathcal{C}\left(Q_1\right) + \mathcal{C}\left(Q_2\right) - \mathcal{C}\left(Q_1 \cap Q_2\right), \tag{181}$$

this extends to the HS of the Coulomb branch also. What remains is to find what the magnetic quiver for $Q_1 \cap Q_2$ is. Let us consider the subtraction of $(1) - [2]$ from Q_1 and Q_2

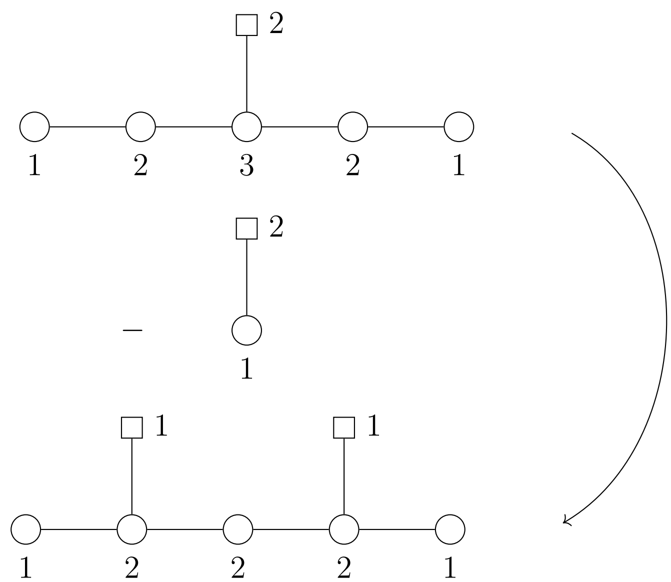

Figure 23: Quiver subtraction on the Q_1 by (1)-[2] to find the intersection with Q_2.

as shown in Figure 23 and Figure 24, we find that the result of the subtraction in both cases are the same. This quiver is the intersection of Q_1 and Q_2.

The HS of $Q_1 \cap Q_2$ can be computed to be

$$HS_{Q_1 \cap Q_2} = \frac{\left(1+t^2\right)^2\left(1+17t^2+119t^4+251t^6+119t^8+17t^{10}+t^{12}\right)}{\left(1-t^2\right)^{16}} \tag{182}$$

$$\begin{aligned} PL[HS_{Q_1 \cap Q_2}] = {} & 35t^2 - 36t^4 - 140t^6 + 2295t^8 - 19278t^{10} + 109900t^{12} - 282285t^{14} + 2714985t^{16} \\ & + 50016330t^{18} - 464962869t^{20} + O\left(t^{21}\right). \end{aligned} \tag{183}$$

The moduli space is recognised as the $\overline{n.minA_5}$.

Finally, we can check the conjecture. Indeed we find, at the level of the unrefined series that

$$HS_{HKQ} = HS_{Q_1} + HS_{Q_2} - HS_{Q_1 \cap Q_2} \tag{184}$$

this allows us to conjecture following relationship between nilpotent orbits,

$$\overline{\mathcal{O}}^{E_7}_{min}//SU(3) = \overline{\mathcal{O}}^{A_5}_{\{2^3\}} \cup \overline{\mathcal{O}}^{A_5}_{\{3,1^3\}}. \tag{185}$$

where we have labelled the orbits of A_5 by their partition data[6].

[6] Affine Grassmannians were not mentioned in this work but for interest all three quivers Q_1, Q_2, Q_3 are slices in the affine Grassmanian for A_5 [87].

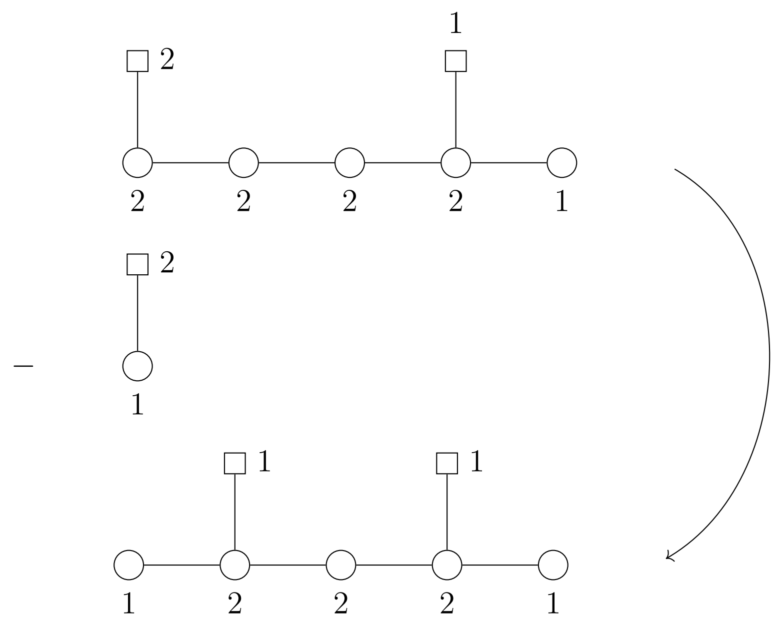

Figure 24: Quiver subtraction on the Q_2 by (1)-[2] to find the intersection with Q_1.

6.3 $SU(4)$ Hyper-Kähler Quotients

The form of the Haar measure is found using (24) and the character of the adjoint representation of $SU(4)$ is computed as

$$\chi\left([1,0,1]\right) = \frac{y_1^2}{y_2}+\frac{y_3y_1}{y_2^2}+y_3y_1+\frac{y_2y_1}{y_3}+\frac{y_1}{y_2y_3}+\frac{y_3^2}{y_2}+\frac{y_2}{y_1^2}+\frac{y_3}{y_1y_2}+\frac{y_2^2}{y_1y_3}+\frac{1}{y_1y_3}+\frac{y_2}{y_3^2}+\frac{y_2y_3}{y_1}+3. \quad (186)$$

Using these, the form of the HKQ formula can be found.

6.3.1 $\overline{min.E_8}//SU(4)$

There is a case for $SU(4)$ which is detailed below. Owing to the higher ranks of these groups, the following observations are made at the level of the unrefined HS. Nevertheless, they are interesting.

There is an embedding of $SU(4)$ into E_8 as $E_8 \to D_8 \to D_5 \times A_3$. The adjoint of E_8 is embedded in the following way.

$$(248) \to (45,1) + (16,\bar{4}) + (10,6) + (\bar{16},4) + (1,15) \quad (187)$$

The unrefined HS for the HKQ of $\overline{min.E_8}$ by $SU(4)$ is computed to be,

$$HS_{HKQ} = \frac{\begin{pmatrix} 1+31t^2+527t^4+6107t^6+52373t^8+345656t^{10}+1797971t^{12}+7492866t^{14} \\ +25334481t^{16}+70196782t^{18}+160666686t^{20}+305615401t^{22}+485171897t^{24} \\ +644267797t^{26}+715706822t^{28}+663498242t^{30}+510361507t^{32}+322272336t^{34} \\ +163913491t^{36}+64739862t^{38}+18219171t^{40}+2600856t^{42}-519889t^{44} \\ -458384t^{46}-154401t^{48}-32963t^{50}-4768t^{52}-464t^{54}-29t^{56}-t^{58} \end{pmatrix}}{(1-t^2)^{28}(1+t^2)^{14}} \tag{188}$$

$$PL[HS_{HKQ}] = 45t^2+45t^4-310t^6-265t^8+8097t^{10}-8926t^{12}-301433t^{14}+1402500t^{16} + 8289481t^{18}-94612783t^{20}+O\left(t^{21}\right) \tag{189}$$

As before, we find that the unrefined series is not palindromic. This moduli space is not a nilpotent orbit, it is something else[7].

Given the success of the previous example, we can try use quiver subtraction to see if the moduli space is the union of the possible options.

Let us perform the subtraction for the case of $SU(4)$. What we find is that we have two possible choices which are shown in Figure 25 and Figure 26 to produce quivers Q_1 and Q_2 respectively. It is clear to see that the balanced subset of gauge nodes have a D_5 symmetry. We shall compute the HS of the Coulomb branch of these quivers and find,

$$HS_{Q_1} = \frac{\begin{pmatrix} 1+31t^2+527t^4+5897t^6+47273t^8+285461t^{10}+1343916t^{12}+5055611t^{14} \\ +15479731t^{16}+39119978t^{18}+82470761t^{20}+146194456t^{22}+219190327t^{24} \\ +279054212t^{26}+302367936t^{28}+279054212t^{30}+219190327t^{32}+146194456t^{34} \\ +82470761t^{36}+39119978t^{38}+15479731t^{40}+5055611t^{42}+1343916t^{44} \\ +285461t^{46}+47273t^{48}+5897t^{50}+527t^{52}+31t^{54}+t^{56} \end{pmatrix}}{(1-t^2)^{28}(1+t^2)^{14}} \tag{190}$$

$$PL[HS_{Q_1}] = 45t^2+45t^4-520t^6+1145t^8+14862t^{10}-155241t^{12}+235187t^{14}+7488490t^{16} - 68324393t^{18}+28249826t^{20}+O\left(t^{21}\right) \tag{191}$$

[7] The appearance of the adjoint of D_5 appearing at order t^2 and t^4 in the PL is indicative that this moduli space is a slice in the affine Grassmannian. This is interesting as the moduli space is constructed from a HKQ and not in the usual way for slices in the affine Grassmanian.

and also

$$HS_{Q_2} = \frac{(1+t^2)^2 \begin{pmatrix} 1+15t^2+166t^4+1015t^6+3611t^8+7656t^{10}+9896t^{12} \\ +7656t^{16}+3611t^{18}+1015t^{20}+166t^{22}+15t^{24}+t^{26} \end{pmatrix}}{(1-t^2)^{28}} \tag{192}$$

$$PL[HS_{Q_2}] = 45t^2+44t^4-355t^6-725t^8+18338t^{10}-47845t^{12}-741460t^{14}+6195930t^{16} + 12246314t^{18}-423974775t^{20}+O\left(t^{21}\right). \tag{193}$$

The Coulomb branch of Q_1 does not appear to be a moduli space that is easily recognisable. It is certainly not a nilpotent orbit or a cover of it. However, the quiver Q_1 is the same as the magnetic quiver for the minimal nilpotent orbit of D_5 if all flavour and gauge node ranks are doubled. The PL of the HS again has the adjoint of D_5 appear at orders t^2 and t^4 so it appears to be a slice in the affine Grassmannian.

The Coulomb branch of Q_2 appears to be the normalisation of the 14-dimensional nilpotent orbit of D_5 labelled by the partition $\{3^2,2^2\}$.

The final issue is to consider what $Q_1 \cap Q_2$ is. Let us start with Q_1 and subtract (1)-[2] from it as in Figure 27. We find that it is the same result if we also subtract (1)-[2] from Q_2 as in Figure 28. So the magnetic quiver $Q_1 \cap Q_2$ is given as the result of these subtractions. We can again compute the unrefined series for it.

$$HS_{Q_1\cap Q_2} = \frac{(1+t^2) \begin{pmatrix} 1+18t^2+216t^4+1385t^6+5230t^8+11447t^{10}+14886t^{12} \\ +11447t^{14}+5230t^{16}+1385t^{18}+216t^{20}+18t^{22}+t^{24} \end{pmatrix}}{(1-t^2)^{26}} \tag{194}$$

$$PE[HS_{Q_1\cap Q_2}] = 45t^2+44t^4-565t^6+685t^8+24893t^{10}-202200t^{12}-231435t^{14}+15209045t^{16} - 90860835t^{18}-441415386t^{20}+O\left(t^{21}\right) \tag{195}$$

Finally, we can test the conjecture at the level of the unrefined HS, indeed we find that

$$HS_{HKQ} = HS_{Q_1\cup Q_2} = HS_{Q_1} + HS_{Q_2} - HS_{Q_1\cap Q_2}. \tag{196}$$

This appears to be further evidence of the conjecture that if multiple quiver subtractions are possible in the HKQ of a magnetic quiver, the HKQ gives the union of the possibilities[8].

[8] All three quivers are slices in the affine Grassmannian.

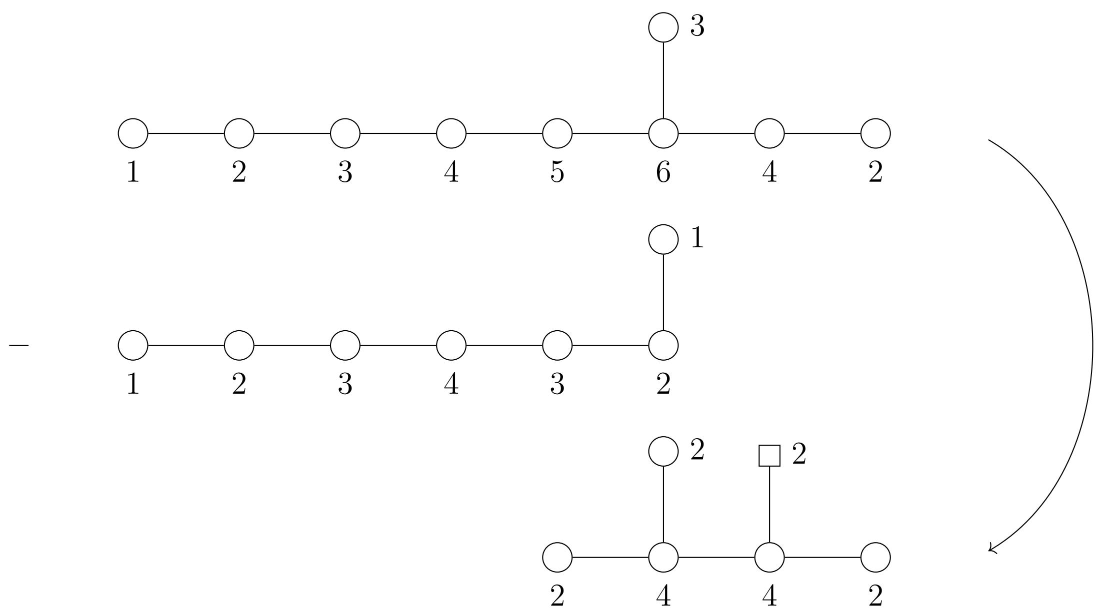

Figure 25: Quiver subtraction on the magnetic quiver for $\overline{min.E_8}$ to produce quiver Q_1.

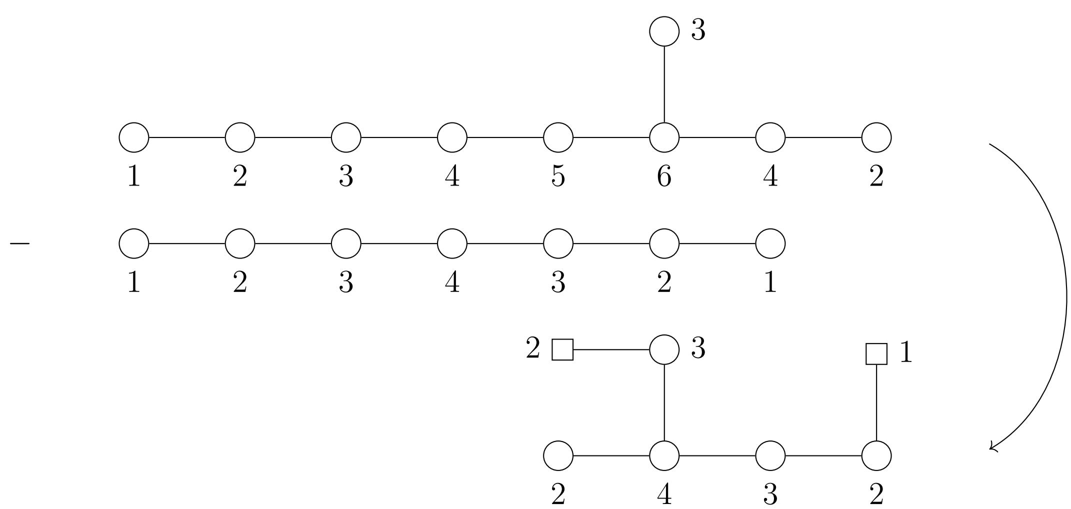

Figure 26: Quiver subtraction on the magnetic quiver for $\overline{min.E_8}$ to produce quiver Q_2.

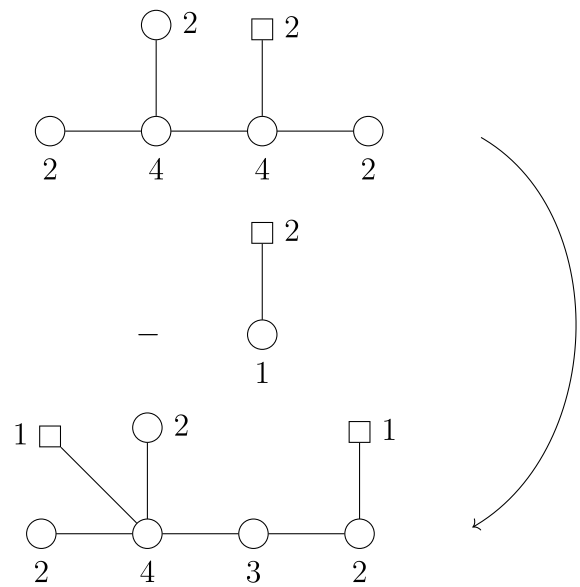

Figure 27: Quiver subtraction on the Q_1 by (1)-[2] to find the intersection with Q_2.

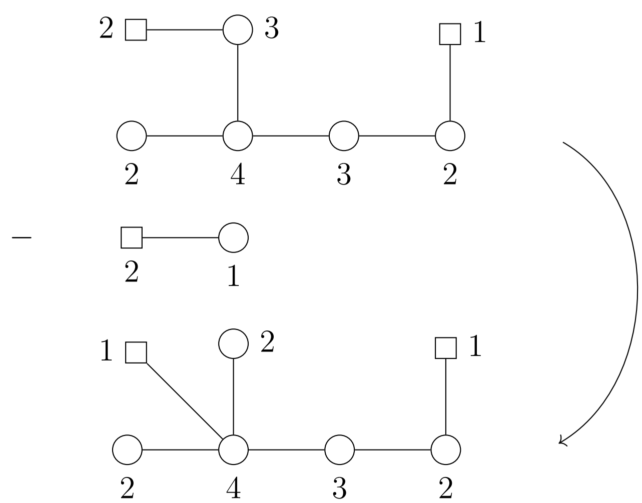

Figure 28: Quiver subtraction on the Q_2 by (1)-[2] to find the intersection with Q_1.

7 Conclusions and Future Work

We have studied the Coulomb branches of $3d$ $\mathcal{N} = 4$ quiver gauge theories through the Hilbert series. The magnetic quivers for nilpotent orbits could be folded and the action of the automorphism map on the Dynkin diagram is reflected in the HWG for the Coulomb branch of the folded quiver. This also gave an interpretation of non-simply laced edges in magnetic quivers analogous to non-simply laced edges in Dynkin diagrams. The discrete gauging of Coulomb branches which were nilpotent orbits were also studied. These were constructed from the HWG of the original Coulomb branch and then application of the Burnside lemma allowed the HWG of the discretely gauged Coulomb branch to be found and hence the resultant Coulomb branch could be identified as some other nilpotent orbit. The results of the discrete gauging were found to be consistent with the classification of Kostant and Brylinski [24].

This is contrasted with the study of hyper-Kähler quotients by $SU(n)$ groups of nilpotent orbits which we studied as the Coulomb branch of some magnetic theory. New results relating two magnetic theories via the hyper-Kähler quotient of one Coulomb branch into another were found in the case of the HKQ by $SU(2)$ of the minimal orbits of F_4, E_6 and E_7 and conjectured for E_8 where the limitation lies in computational ability. The latter has the expected unrefined Hilbert series and perturbative refined results seem promising, however a full refined computation is yet to be done. For some resulting orbits a quiver subtraction algorithm yielded the correct magnetic quiver. This is a similar for the $SU(3)$ HKQ of $\overline{minE_8}$ producing the double cover of the 21 dimensional orbit of E_6 respectively. There were cases where multiple alignments of the quiver subtraction were possible. Such as for the $\overline{min.E_7}//SU(3)$ and $\overline{min.E_8}//SU(4)$. The unrefined series indicated that the HKQ produces the unions of the Coulomb branches of the possible quivers. In particular, the unrefined HS suggested that $\overline{min.E_7}//SU(3)$ would be the union of the two 9-dimensional orbits of A_5 and that $\overline{min.E_8}//SU(4)$ would be the union of the normalisation of the 14-dimensional orbit of D_5 and another moduli space which is not a nilpotent orbit but a slice in the affine Grassmannian [87].

The results for $\overline{min.G_2}$ need some further explaining as it appears that the quotient fails the simple test of reducing dimension of the moduli space by three.

As mentioned at the beginning of Section 6, there are a great deal of moduli spaces to consider and to take HKQs of. A possible avenue is to look at other classes of moduli spaces such as the moduli space of instantons [74] using the embeddings above. Another route is to look at slices in the affine Grassmannian, there are infinite examples one can consider here and so it may be possible to learn about relationships between slices of the affine Grassmannian for different algebras.

A particularly interesting bit of future work is to realise the results we have in terms of a brane system. The double cover of the 21 dimesnional orbit of E_6 from the minimal nilpotent orbit of E_8 was not only calculated in [86] but also shown as a brane system in type IIA string theory. The introduction of quiver subtraction was in order to understand the Kraft-Procesi transitions as a brane system [19, 27, 28], so the ability to do quiver subtraction for some of the examples presented here means that it is encouraging that a brane system for some of the examples presented here exists.

Appendices

A $SU(2)$ Hyper-Kähler Quotients of min F_4

Here we present more (non-maximal) embeddings of $SU(2)$ into F_4. It should be noted that the recovered unrefined series is that of a result from a maximal embedding. The embeddings are given in Table 8, the unrefined HS and the HWG for the HKQ is given in Table 9 and the identification of the moduli space (if known) is given in Table 10.

The table supports the decision to look only at maximal embeddings of $SU(n)$ groups as what is recovered by non-maximal embeddings is usually a result from a maximal embedding.

Number	Subgroup	26_{F_4}
1	$C_3 \times A_1$	$(6,2)+(14,1)$
2	$A_3 \times A_1$	$(4,2)+(4',2)+(6,1)+(1,3)+(1,1)$
3	$G_2 \times A_1$	$(7,3)+(1,5)$
4	$A_2 \times A_1$	$(3,3)+(3',3)+(1,3)+(1,5)$
5	$A_2 \times A_1$	$(8,1)+(3,3)+(3',3)$
6	$A_1 \times A_1$	$2(3,3)+(1,3)+(1,5)$
7	$C_2 \times A_1 \times A_1$	$(1,1,1)+(4,1,2)+(1,2,2)+(4,2,1)+(5,1,1)$
8	$A_1 \times A_1 \times A_1$	$(1,5,1)+(2,3,2)+(1,3,3)$
9	$A_1 \times A_1 \times A_1 \times A_1$	$(1,1,1,1)-(1,3,1,1)+(1,5,1,1)+(1,1,1,3)+(2,1,2,1)-(1,1,2,2)+(1,3,2,2)-(2,1,1,2)+(2,3,1,2)$

Table 8: Table of the embeddings of the **26** of F_4 into the respective subgroups.

Number	Unrefined HS	HWG
1	$\frac{(1+t^2)(1+10t^2+41t^4+10t^6+t^8)}{(1-t^2)^{10}}$	$PE[\mu_1^2 t^2 + \mu_2^2 t^4]$
2	$\frac{(1+t^2)(1+4t^2+10t^4+4t^6+t^8)}{(1-t^2)^{10}}$	$PE[\mu_1\mu_3 t^2 + (\mu_2^2 + \mu_1\mu_3)t^4 + \mu_2(\mu_1^2 + \mu_3^2)t^6 - \mu_1^2\mu_2^2\mu_3^2 t^{12}]$
3	$\frac{(1+t^2)(1+3t^2+6t^4+3t^6+t^8)}{(1-t^2)^{10}}$	$PE[\mu_2 t^2 + \mu_1^2 t^4 + \mu_1^3 t^6 + \mu_2^2 t^8 + \mu_1^3\mu_2 t^{10} - \mu_1^6\mu_2^2 t^{20}]$
4	$\frac{(1+t^2)(1+3t^2+6t^4+3t^6+t^8)}{(1-t^2)^{10}}$	$PE[(\mu_1\mu_2 + \mu_1 + \mu_2)t^2 + (1 + \mu_1 + \mu_1^2) + \mu_2 + \mu_1\mu_2 + \mu_2^2)t^4 + O(t^6)]$
5	$\frac{\left(\begin{array}{l}1+3t^2+31t^4+55t^6+156t^8+132t^{10}\\ \quad +156t^{12}+55t^{14}+31t^{16}+3t^{18}+t^{20}\end{array}\right)}{(1-t^2)^{10}(1+t^2)^5}$	$PE[\mu_1\mu_2 t^2 + (1 + \mu_1^4 + \mu_1\mu_2 + \mu_2^4)t^4 + O(t^6)]$
6a	$\frac{\left(\begin{array}{l}1+3t^2+31t^4+55t^6+156t^8+132t^{10}\\ \quad +156t^{12}+55t^{14}+31t^{16}+3t^{18}+t^{20}\end{array}\right)}{(1-t^2)^{10}(1+t^2)^5}$	$PE[(\nu^2 + \nu^4)t^2 + (4 + \nu^2 + 4\nu^4 + 2\nu^8)t^4 + O(t^6)]$
6b	$\frac{(1+t^2)(1+3t^2+6t^4+3t^6+t^8)}{(1-t^2)^{10}}$	$PE[(3\omega^2 + \omega^4)t^2 + (6 + 6\omega^2 + 4\omega^4)t^4 O(t^6)]$
7a	$\frac{(1+t^2)(1+10t^2+41t^4+10t^6+t^8)}{(1-t^2)^{10}}$	$PE[(\omega^2 + \omega\mu_1 + \mu_1^2)t^2 + (1 + \mu_2 + \mu_2^2 + \omega\mu_1 + \omega\mu_1\mu_2)t^4 + O(t^6)]$
7b	$\frac{(1+t^2)(1+10t^2+41t^4+10t^6+t^8)}{(1-t^2)^{10}}$	$PE[(\nu^2 + \nu\mu_1 + \mu_1^2)t^2 + (1 + \mu_2 + \mu_2^2 + \nu\mu_1 + \nu\mu_1\mu_2)t^4 + O(t^6)]$
8a	$\frac{(1+t^2)(1+10t^2+41t^4+10t^6+t^8)}{(1-t^2)^{10}}$	$PE\left[\begin{array}{l}(\nu^2 + \omega^2 + \nu^4\omega^2)t^2\\ \quad + (2 + \nu^8 + \nu^2\omega^2 + \nu^6\omega^2 + \omega^4 + \nu^4(1 + \omega^2)^2)t^4 + O(t^6)\end{array}\right]$
8b	$\frac{(1+t^2)(1+3t^2+6t^4+3t^6+t^8)}{(1-t^2)^{10}}$	$PE[(\mu^2 + \omega^2 + \mu\omega^3)t^2 + (2 + \mu^2\omega^2 + \omega^4 + \mu\omega + 2\mu\omega^3)t^4 + O(t^6)]$
8c	$\frac{\left(\begin{array}{l}1+4t^2+35t^4+149t^6+438t^8+975t^{10}\\ \quad +1739t^{12}+2393t^{14}+2656t^{16}+palindrome\end{array}\right)}{(1-t^2)^{10}(1+t^2)^5(1-t+t^2)^3(1+t+t^2)^3}$	$PE[(\mu^2 + \nu^2)t^2 + (2 + \mu^2\nu^6 + \nu^8)t^4 + O(t^6)]$
9a	$\frac{(1+t^2)(1+10t^2+41t^4+10t^6+t^8)}{(1-t^2)^{10}}$	$PE[(1 + \nu^2 + (\mu^2 - 1)\nu\rho + (1 - \mu^2 + \mu^4)\rho^2)t^2 + O(t^4)]$
9b	$\frac{(1+t^2)(1+3t^2+6t^4+3t^6+t^8)}{(1-t^2)^{10}}$	$PE[(1 + \nu^2 + \rho^2 - \rho\omega + \omega^2 + \nu\rho(\rho\omega - 1))t^2 + O(t^4)]$
9c	$\frac{(1+t^2)(1+10t^2+41t^4+10t^6+t^8)}{(1-t^2)^{10}}$	$PE[(1 + (1 - \mu^2 + \mu^4)\rho^2 + (\mu^2 - 1)\rho\omega + \omega^2)t^2 + O(t^4)]$
9d	$\frac{(1+t^2)(1+4t^2+10t^4+4t^6+t^8)}{(1-t^2)^{10}}$	$PE[(1 + \nu^2 + \mu^2(\mu^2 - 1)\nu\omega + \omega^2)t^2 + O(t^4)]$

Table 9: Table of unrefined HS of $SU(2)$ quotients and of HWG for each embedding. Cases with multiple $SU(2)$ are labelled a,b,c,etc. where we quotient the A_1 from starting from the left. Each group in the embedding starting from the left has highest weight fugacity(ies) in the order $\mu_i, \nu_i, \rho_i, \omega_i$ where i is an appropriate integer label for groups of rank 2 or above.

Number	Moduli Space
1	$\overline{n.minC_3}$
2	$\overline{sub.reg.A_3}$
3	$\overline{sub.reg.G_2}$
4	$\overline{sub.reg.G_2}$
5	?
6a	?
6b	$\overline{sub.reg.G_2}$
7a	$\overline{n.minC_3}$
7b	$\overline{n.minC_3}$
8a	$\overline{n.minC_3}$
8b	$\overline{sub.reg.G_2}$
8c	?
9a	$\overline{n.minC_3}$
9b	$\overline{sub.reg.G_2}$
9c	$\overline{n.minC_3}$
9d	$\overline{sub.reg.A_3}$

Table 10: Table of the embeddings and the moduli space the $SU(2)$ hyper-Kähler quotients correspond to. Some moduli spaces have not been identified.

References

[1] Emmy Noether. “Invariante Variationsprobleme”. In: *Nachrichten von der Gesellschaft der Wissenschaften zu Göttingen, Mathematisch-Physikalische Klasse* 1918 (1918), pp. 235–257. URL: https://eudml.org/doc/59024.

[2] Steven Weinberg. “A Model of Leptons”. In: *Physical Review Letters* 19.21 (Nov. 1967), pp. 1264–1266. ISSN: 0031-9007. DOI: 10.1103/PhysRevLett.19.1264.

[3] Abdus Salam and J. C. Ward. “Weak and electromagnetic interactions”. In: *Il Nuovo Cimento* 11.4 (Feb. 1959), pp. 568–577. ISSN: 0029-6341. DOI: 10.1007/BF02726525.

[4] C. N. Yang and R. L. Mills. “Conservation of isotopic spin and isotopic gauge invariance”. In: *Selected Papers (1945-1980) Of Chen Ning Yang (With Commentary)* 7.1936 (2005), pp. 172–176.

[5] G. ’t Hooft and M. Veltman. “Regularization and renormalization of gauge fields”. In: *Nuclear Physics B* 44.1 (July 1972), pp. 189–213. ISSN: 05503213. DOI: 10.1016/0550-3213(72)90279-9. URL: https://linkinghub.elsevier.com/retrieve/pii/0550321372902799.

[6] Peter W. Higgs. “Broken Symmetries and the Masses of Gauge Bosons”. In: *Physical Review Letters* 13.16 (Oct. 1964), pp. 508–509. ISSN: 0031-9007. DOI: 10.1103/PhysRevLett.13.508.

[7] T. W. B. Kibble. “Symmetry Breaking in Non-Abelian Gauge Theories”. In: *Physical Review* 155.5 (Mar. 1967), pp. 1554–1561. ISSN: 0031-899X. DOI: 10.1103/PhysRev.155.1554.

[8] G. S. Guralnik, C. R. Hagen, and T. W. B. Kibble. “Global Conservation Laws and Massless Particles”. In: *Physical Review Letters* 13.20 (Nov. 1964), pp. 585–587. ISSN: 0031-9007. DOI: 10.1103/PhysRevLett.13.585.

[9] F. Englert and R. Brout. “Broken Symmetry and the Mass of Gauge Vector Mesons”. In: *Physical Review Letters* 13.9 (Aug. 1964), pp. 321–323. ISSN: 0031-9007. DOI: 10.1103/PhysRevLett.13.321.

[10] A. Einstein. “Die Grundlage der allgemeinen Relativitätstheorie”. In: *Annalen der Physik* 354.7 (1916), pp. 769–822. ISSN: 00033804. DOI: 10.1002/andp.19163540702. URL: https://onlinelibrary.wiley.com/doi/10.1002/andp.19163540702.

[11] Julius Wess and Jonathan Bagger. *Supersymmetry and Supergravity.* 2nd ed. Princeton University Press, 1992.

[12] Rudolf Haag, Jan T. Łopuszański, and Martin Sohnius. “All possible generators of supersymmetries of the S-matrix”. In: *Nuclear Physics B* 88.2 (Mar. 1975), pp. 257–274. ISSN: 05503213. DOI: 10.1016/0550-3213(75)90279-5. URL: https://linkinghub.elsevier.com/retrieve/pii/0550321375902795.

[13] Sidney Coleman and Jeffrey Mandula. “All Possible Symmetries of the S Matrix”. In: *Physical Review* 159.5 (July 1967), pp. 1251–1256. ISSN: 0031-899X. DOI: 10.1103/PhysRev.159.1251. URL: http://www.scholarpedia.org/article/Coleman-Mandula_theorem%20https://link.aps.org/doi/10.1103/PhysRev.159.1251.

[14] Richard E. Borcherds. “Monstrous moonshine and monstrous Lie superalgebras”. In: *Inventiones Mathematicae* 109.1 (Dec. 1992), pp. 405–444. ISSN: 0020-9910. DOI: 10.1007/BF01232032. URL: http://link.springer.com/10.1007/BF01232032.

[15] Wolfgang Lerche, Cumrun Vafa, and Nicholas P. Warner. “Chiral rings in N = 2 superconformal theories”. In: *Nuclear Physics B* 324.2 (Sept. 1989), pp. 427–474. ISSN: 05503213. DOI: 10.1016/0550-3213(89)90474-4. URL: https://linkinghub.elsevier.com/retrieve/pii/0550321389904744.

[16] Philip Candelas et al. “A pair of Calabi-Yau manifolds as an exactly soluble superconformal theory”. In: *Nuclear Physics B* 359.1 (July 1991), pp. 21–74. ISSN: 05503213. DOI: 10.1016/0550-3213(91)90292-6. URL: https://linkinghub.elsevier.com/retrieve/pii/0550321391902926.

[17] Michael R. Douglas and Gregory Moore. “D-branes, Quivers, and ALE Instantons”. In: (Mar. 1996). URL: http://arxiv.org/abs/hep-th/9603167.

[18] Amihay Hanany and Edward Witten. “Type IIB Superstrings, BPS Monopoles, And Three-Dimensional Gauge Dynamics”. In: (Nov. 1996). DOI: 10.1016/S0550-3213(97)00157-0.

[19] Santiago Cabrera and Amihay Hanany. “Quiver subtractions”. In: *Journal of High Energy Physics* 2018.9 (2018). ISSN: 10298479. DOI: 10.1007/JHEP09(2018)008.

[20] Juan Maldacena. “The Large-N Limit of Superconformal Field Theories and Supergravity”. In: *International Journal of Theoretical Physics* 38.4 (1999), pp. 1113–1133. ISSN: 00207748. DOI: 10.1023/A:1026654312961.

[21] K. Intriligator and N. Seiberg. “Mirror symmetry in three dimensional gauge theories”. In: *Physics Letters, Section B: Nuclear, Elementary Particle and High-Energy Physics* 387.3 (1996), pp. 513–519. ISSN: 03702693. DOI: 10.1016/0370-2693(96)01088-X.

[22] H.B.G. Casimir. “On the attraction between two perfectly conducting plates”. In: *Proc. K. Ned. Akad.* 360 (1948), pp. 793–795. URL: http://scholar.google.com/scholar?hl=en&btnG=Search&q=intitle:On+the+attraction+between+two+perfectly+conducting+plates#0.

[23] H. B. G. Casimir and D. Polder. “The Influence of Retardation on the London-van der Waals Forces”. In: *Physical Review* 73.4 (Feb. 1948), pp. 360–372. ISSN: 0031-899X. DOI: 10.1103/PhysRev.73.360. URL: https://link.aps.org/doi/10.1103/PhysRev.73.360.

[24] Ranee Brylinski and Bertram Kostant. “Nilpotent orbits, normality, and Hamiltonian group actions”. In: *Bulletin of the American Mathematical Society* 26.2 (1992), pp. 269–275. ISSN: 02730979. DOI: 10.1090/S0273-0979-1992-00271-9.

[25] Hanspeter Kraft and Claudio Procesi. “On the geometry of conjugacy classes in classical groups”. In: *Commentarii Mathematici Helvetici* 57.1 (Dec. 1982), pp. 539–602. ISSN: 0010-2571. DOI: 10.1007/BF02565876.

[26] Antoine Bourget, Amihay Hanany, and Dominik Miketa. "Quiver origami: discrete gauging and folding". In: *Journal of High Energy Physics* 2021.1 (2021). ISSN: 10298479. DOI: 10.1007/JHEP01(2021)086.

[27] Santiago Cabrera and Amihay Hanany. "Branes and the Kraft-Procesi Transition". In: (Sept. 2016). DOI: 10.1007/JHEP11(2016)175.

[28] Santiago Cabrera and Amihay Hanany. "Branes and the Kraft-Procesi transition: classical case". In: (Nov. 2017). DOI: 10.1007/JHEP04(2018)127.

[29] Giulia Ferlito and Amihay Hanany. "A tale of two cones: the Higgs Branch of Sp(n) theories with 2n flavours". In: (Sept. 2016). URL: http://arxiv.org/abs/1609.06724.

[30] David H. Collingwood and William M. McGovern. *Nilpotent Orbits in Semisimple Lie Algebras*. Ed. by Raoul H. Bott et al. 1993.

[31] William Fulton and Joe Harris. *Representation theory: a first course*. Springer-Verlag, 1991. ISBN: 0387975276.

[32] F. Peter and H. Weyl. "Die Vollständigkeit der primitiven Darstellungen einer geschlossenen kontinuierlichen Gruppe". In: *Mathematische Annalen* 97.1 (Dec. 1927), pp. 737–755. ISSN: 0025-5831. DOI: 10.1007/BF01447892.

[33] James Gray et al. "SQCD: A Geometric Apercu". In: (Mar. 2008). DOI: 10.1088/1126-6708/2008/05/099. URL: http://arxiv.org/abs/0803.4257%20http://dx.doi.org/10.1088/1126-6708/2008/05/099.

[34] Amihay Hanany and Rudolph Kalveks. "Construction and Deconstruction of Single Instanton Hilbert Series". In: (Sept. 2015). DOI: 10.1007/JHEP12(2015)118. URL: http://arxiv.org/abs/1509.01294%20http://dx.doi.org/10.1007/JHEP12(2015)118.

[35] Jurgen Fuchs and Christoph Schweigert. *Symmetries, Lie Algebras and Representations*. Ed. by P. V. Landshoff et al. 1st ed. Cambridge University Press, 2003. ISBN: 9780521541190.

[36] Robert Feger and Thomas W. Kephart. "LieART - A Mathematica application for Lie algebras and representation theory". In: *Computer Physics Communications* 192 (2015), pp. 166–195. ISSN: 00104655. DOI: 10.1016/j.cpc.2014.12.023.

[37] John. R. Stembridge. *Folding by Automorphisms*. Aug. 2008. URL: http://www.math.lsa.umich.edu/~jrs/papers/folding.pdf.

[38] Robin Hartshorne. *Algebraic Geometry*. Vol. 52. Graduate Texts in Mathematics. New York, NY: Springer New York, 1977. ISBN: 978-1-4419-2807-8. DOI: 10.1007/978-1-4757-3849-0. URL: http://link.springer.com/10.1007/978-1-4757-3849-0.

[39] Yan Xiao, Yang Hui He, and Cyril Matti. *Standard model plethystics*. Vol. 100. 7. 2019. ISBN: 0947241455148. DOI: 10.1103/PhysRevD.100.076001.

[40] Dmitri I. Panyushev. "On spherical nilpotent orbits and beyond". In: *Annales de l'institut Fourier* 49.5 (1999), pp. 1453–1476. ISSN: 0373-0956. DOI: 10.5802/aif.1726.

[41] Nathan Jacobson. "Completely Reducible Lie Algebras of Linear Transformations". In: *Proceedings of the American Mathematical Society* 2.1 (Feb. 1951), p. 105. ISSN: 00029939. DOI: 10.2307/2032629.

[42] V. V. Morozov. "On a nilpotent element in a semi-simple Lie algebra". In: *C. R. (Doklady) Acad. Sci. URSS (N.S.)* 36 (1942), pp. 83–86.

[43] E.B. Dynkin. "Semisimple subalgebras of semisimple Lie algebras". In: *Trans. Am. Math. Soc. Ser. 2* 6 (1957), pp. 111–244.

[44] Mikio Nakahara. *Geometry, Topology, and Physics*. Ed. by Douglas F. Brewer. 2nd ed. Taylor & Francis Group, 2003.

[45] P. B. Kronheimer. "The construction of ALE spaces as hyper-Kähler quotients". In: *Journal of Differential Geometry* 29.3 (1989), pp. 665–683. ISSN: 1945743X. DOI: 10.4310/jdg/1214443066.

[46] N. J. Hitchin et al. "Hyperkähler metrics and supersymmetry". In: *Communications in Mathematical Physics* 108.4 (Dec. 1987), pp. 535–589. ISSN: 0010-3616. DOI: 10.1007/BF01214418. URL: http://link.springer.com/10.1007/BF01214418.

[47] PIOTR Z. KOBAK and ANDREW SWANN. "CLASSICAL NILPOTENT ORBITS AS HYPERKÄHLER QUOTIENTS". In: *International Journal of Mathematics* 07.02 (Apr. 1996), pp. 193–210. ISSN: 0129-167X. DOI: 10.1142/S0129167X96000116.

[48] Y. Namikawa. "Extension of 2-forms and symplectic varieties". In: *Journal für die reine und angewandte Mathematik (Crelles Journal)* 2001.539 (Jan. 2001). ISSN: 0075-4102. DOI: 10.1515/crll.2001.070. URL: https://www.degruyter.com/document/doi/10.1515/crll.2001.070/html.

[49] Richard P Stanley. "Hilbert functions of graded algebras". In: *Advances in Mathematics* 28.1 (Apr. 1978), pp. 57–83. ISSN: 00018708. DOI: 10.1016/0001-8708(78)90045-2. URL: https://linkinghub.elsevier.com/retrieve/pii/0001870878900452.

[50] Rudolph J. K. Kalveks. “Group Symmetries and the Moduli Space Structures of SUSY Quiver Gauge Theories”. PhD thesis. Imperial College London, 2017.

[51] M. Bullimore. “A Mathematical Introduction to 3d N=4 Gauge Theories”. In: *Quantum Fields, Geometry and Representation Theory 2021*. Ed. by A. Balasubramaniyam et al. International Center for Theoretical Physics, 2021. URL: https://www.icts.res.in/program/qftgrt2021.

[52] P Argyres. *Introduction to Supersymetry*. 1996.

[53] David Tong. *Supsersymmetric Field Theory*. 2022. URL: https://www.damtp.cam.ac.uk/user/tong/susy/susy.pdf.

[54] Nathan Seiberg and Edward Witten. “Gauge Dynamics And Compactification To Three Dimensions”. In: (July 1996). URL: http://arxiv.org/abs/hep-th/9607163.

[55] Federico Carta. “Moduli Spaces of N = 4 , d = 3 Quiver Gauge Theories and Mirror Symmetry”. In: (2014).

[56] Cyril Closset and Heeyeon Kim. “Three-dimensional $\mathcal{N}=2$ supersymmetric gauge theories and partition functions on Seifert manifolds: A review”. In: (Aug. 2019). DOI: 10.1142/S0217751X19300114.

[57] Davide Gaiotto and Tadashi Okazaki. “Sphere correlation functions and Verma modules”. In: (Nov. 2019). DOI: 10.1007/JHEP02(2020)133.

[58] A.M. Polyakov. “Quark confinement and topology of gauge theories”. In: *Nuclear Physics B* 120.3 (Mar. 1977), pp. 429–458. ISSN: 05503213. DOI: 10.1016/0550-3213(77)90086-4.

[59] Denis Bashkirov and Anton Kapustin. “Supersymmetry enhancement by monopole operators”. In: (July 2010). DOI: 10.1007/JHEP05(2011)015.

[60] G. ’t Hooft. “On the phase transition towards permanent quark confinement”. In: *Nuclear Physics B* 138.1 (June 1978), pp. 1–25. ISSN: 05503213. DOI: 10.1016/0550-3213(78)90153-0.

[61] Stefano Cremonesi. “3d supersymmetric gauge theories and Hilbert series”. In: *arXiv* (2017), pp. 1–27. DOI: 10.1090/pspum/098/02.

[62] F. Englert and P. Windey. “Quantization condition for ’t Hooft monopoles in compact simple Lie groups”. In: *Physical Review D* 14.10 (Nov. 1976), pp. 2728–2731. ISSN: 0556-2821. DOI: 10.1103/PhysRevD.14.2728.

[63] Giulia Ferlito. “Mirror Symmetry in 3d supersymmetric gauge theories”. In: September (2013).

[64] Mathew Bullimore, Tudor Dimofte, and Davide Gaiotto. “The Coulomb Branch of 3d N=4 Theories”. In: (Mar. 2015). URL: http://arxiv.org/abs/1503.04817.

[65] Nathan Seiberg. “IR Dynamics on Branes and Space-Time Geometry”. In: (June 1996). DOI: 10.1016/0370-2693(96)00819-2.

[66] Santiago Cabrera, Amihay Hanany, and Marcus Sperling. “Magnetic quivers, Higgs branches and 6d N=(1,0) theories”. In: *Journal of High Energy Physics* 2019.6 (2019). ISSN: 10298479. DOI: 10.1007/JHEP06(2019)071.

[67] Stefano Cremonesi, Amihay Hanany, and Alberto Zaffaroni. “Monopole operators and Hilbert series of Coulomb branches of 3d N = 4 gauge theories”. In: *Journal of High Energy Physics* 2014.1 (2014). ISSN: 10298479. DOI: 10.1007/Jhep01(2014)005.

[68] Anton Kapustin and Edward Witten. “Electric-Magnetic Duality And The Geometric Langlands Program”. In: (Apr. 2006). URL: http://arxiv.org/abs/hep-th/0604151.

[69] Bo Feng, Amihay Hanany, and Yang-Hui He. “Counting Gauge Invariants: the Plethystic Program”. In: (Jan. 2007). DOI: 10.1088/1126-6708/2007/03/090.

[70] Amihay Hanany and Rudolph Kalveks. “Highest Weight Generating Functions for Hilbert Series”. In: (Aug. 2014). DOI: 10.1007/JHEP10(2014)152.

[71] A. F. Möbius. “Über eine besondere Art von Umkehrung der Reihen”. In: *Journal für die reine und angewandte Mathematik* 9 (1832).

[72] Julius Grimminger. *Real Mass Resolutions and Complex Mass Deformations of 3d N=4 Coulomb Branches*. Tech. rep. 2018.

[73] Yoshinori Namikawa. “A characterization of nilpotent orbit closures among symplectic singularities”. In: (Mar. 2016). DOI: 10.1007/s00208-017-1572-9.

[74] Stefano Cremonesi et al. “Coulomb branch and the moduli space of instantons”. In: *Journal of High Energy Physics* 2014.12 (2014). ISSN: 10298479. DOI: 10.1007/JHEP12(2014)103.

[75] Naoki Yamatsu. “Finite-Dimensional Lie Algebras and Their Representations for Unified Model Building”. In: (Nov. 2015). URL: http://arxiv.org/abs/1511.08771.

[76] Amihay Hanany and Rudolph Kalveks. "Quiver theories and formulae for nilpotent orbits of Exceptional algebras". In: *Journal of High Energy Physics* 2017.11 (Nov. 2017). ISSN: 10298479. DOI: 10.1007/JHEP11(2017)126.

[77] Stefano Cremonesi et al. "T ρ σ (G) theories and their Hilbert series". In: *Journal of High Energy Physics* 2015.1 (Jan. 2015), p. 150. ISSN: 1029-8479. DOI: 10.1007/JHEP01(2015)150. URL: http://link.springer.com/10.1007/JHEP01(2015)150.

[78] Amihay Hanany and Rudolph Kalveks. "Quiver Theories for Moduli Spaces of Classical Group Nilpotent Orbits". In: (Jan. 2016). DOI: 10.1007/JHEP06(2016)130. URL: http://arxiv.org/abs/1601.04020%20http://dx.doi.org/10.1007/JHEP06(2016)130.

[79] Davide Gaiotto and Edward Witten. "S-duality of boundary conditions in N = 4 super Yang-Mills theory". In: *Advances in Theoretical and Mathematical Physics* 13.3 (2009), pp. 721–896. ISSN: 10950753. DOI: 10.4310/ATMP.2009.v13.n3.a5.

[80] Kirsty Gledhill and Amihay Hanany. "Coulomb Branch Global Symmetry and Quiver Addition". In: (Sept. 2021). URL: http://arxiv.org/abs/2109.07237.

[81] Amihay Hanany and Anton Zajac. "Ungauging Schemes and Coulomb Branches of Non-simply Laced Quiver Theories". In: (Feb. 2020). DOI: 10.1007/JHEP09(2020)193. URL: http://arxiv.org/abs/2002.05716%20http://dx.doi.org/10.1007/JHEP09(2020)193.

[82] Amihay Hanany and Anton Zajac. "Discrete gauging in Coulomb branches of three dimensional N= 4 supersymmetric gauge theories". In: *Journal of High Energy Physics* 2018.8 (Aug. 2018). ISSN: 10298479. DOI: 10.1007/JHEP08(2018)158.

[83] William Burnside. *Theory of Groups of Finite Order*. 2012.

[84] Ferdinand Georg Frobenius. "Ueber die Congruenz nach einem aus zwei endlichen Gruppen gebildeten Doppelmodul". In: *Crelle's Journal* 101.4 (1887). DOI: 10.3931/e-rara-18804.

[85] Chang-Ho Kim et al. *Generalized projection matrices for nonsupersymmetric and supersymmetric grand unified theories*. Tech. rep. 1983, p. 15.

[86] Amihay Hanany and Marcus Sperling. "Magnetic quivers and negatively charged branes". In: (Aug. 2022). URL: http://arxiv.org/abs/2208.07270.

[87] Antoine Bourget et al. "Branes, Quivers, and the Affine Grassmannian". In: (Feb. 2021). URL: http://arxiv.org/abs/2102.06190.